

**Annual Report FY 2008**

**平成 20 年度活動報告**

**Institute for Geothermal Sciences**

Graduate School of Science

Kyoto University

**京都大学**

**大学院理学研究科**

**附属地球熱学研究施設**

Institute for Geothermal Sciences  
Graduate School of Science, Kyoto University

京都大学大学院理学研究科 附属地球熱学研究施設



Beppu Geothermal Research Laboratory  
Noguchibaru, Beppu, Oita 874-0903

Japan

Telephone: +81-977-22-0713

Facsimile: +81-977-22-0965

〒874-0903 大分県別府市野口原

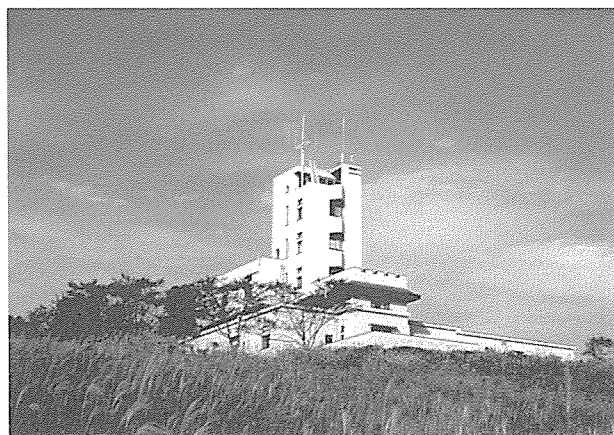
電話: 0977-22-0713

ファックス: 0977-22-0965

Homepage: <http://www.vgs.kyoto-u.ac.jp>

Aso Volcanological Laboratory  
Minamiaso, Kumamoto 869-1404, Japan  
Telephone: +81-9676-7-0022  
Facsimile: +81-9676-7-2153

阿蘇(火山研究センター)  
〒896-1404 熊本県阿蘇郡南阿蘇村河陽  
5280  
電話: 0967-67-0022  
ファックス: 0967-67-2153  
Homepage:  
<http://www.aso.vgs.kyoto-u.ac.jp/>



Front Cover Image:

A strombolian explosion in the 1<sup>st</sup> crater of Mt. Nakadake, Aso volcano in October 1979.

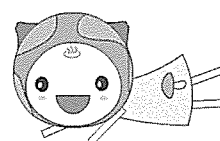
(Photo by M. Sako)

表紙の写真

1979 年 10 月の阿蘇中岳第一火口のストロンボリ噴火の様子(迫幹夫撮影)

Chinetu-chan designed by Miho Saito

Editorial compilation by T. Kawamoto, Printed by Primedia



## 序

地球熱学研究施設は、平成 9 年に火山研究施設（阿蘇）（昭和 3 年設立）と地球物理学研究施設（別府）（大正 13 年設立）が統合改組された理学研究科附属施設である。地球上で最大規模の火山・地熱温泉活動域のひとつである中部九州地域を巨大な実験装置とみなして、野外観測や室内実験などを中心に、造構運動・火山活動・地熱温泉活動など地球の熱的活動に関する地球熱学の学問体系の構築をめざしている。この基本理念に立脚して、専門分野の異なる研究者が弾力的に協力できるよう大部門制を採り、以下の 5 つの研究分野が置かれている。地熱流体論研究分野、地熱テクトニクス研究分野、火山構造論研究分野、火山活動論研究分野、地球熱学情報研究分野（外国人客員）である。平成 16 年度には京都大学が法人化され、研究教育の効率化さらには定員削減を余儀なくされる状況にある。法人化 5 年目に入り、2010 年度からはじまる第二期中期計画に向けて、施設運営のためには財政的に運営交付金に加えて競争的資金の確保が重要になっている。

平成 16 年度設置された施設運営協議会が平成 20 年度は 9 回開催され、理学研究科との連携が実質化されてきている。遠隔地の課題をみすえながら、阿蘇と別府の有機的な連携を強化する努力がより一層必要となっている。このような中で、学内での地球熱学研究施設の研究教育面での位置付けをより明確にすることが必要であり、平成 19 年 4 月からは、懸案であった京都勤務が、理学研究科附属施設の京都分室の形で認められ、院生・学生の教育や研究科内での役割分担の課題に取り組みはじめた。この実質化の拡充が平成 20 年度の重要な課題であった。平成 18 年度設置された TV 会議システムはセミナーや特別講演を中心に活用され、遠隔地からの情報発信に大きな役割をになっている。

人事面では平成 20 年 8 月に外国人客員の Singh 氏が離任、平成 21 年 3 月に陳中華氏が離任し、平成 21 年 4 月に Holloway 氏が着任した。研究員（研究機関）の石橋秀巳氏が、平成 20 年 6 月をもって退職し、東京大学地殻化学の研究員に採用された。後任としてマリ・ピトン氏が平成 20 年 10 月 1 日付けで別府に着任した。また、寺田暁彦氏が平成 21 年 4 月をもって退職し、東京工業大学の研究員となった。後任の三好雅也氏が 21 年 4 月に別府に着任した、別府の事務室で勤務された宮崎恵子氏が退職され、宮田美保氏が勤務を開始した。

21 世紀 COE が終了したが、研究施設の研究テーマが関係する重点課題 J2b や京都キャンパス・インドネシア ITB との共同研究（鍾乳洞プロジェクト）で成果をあげ、また、別府・阿蘇をフィールドとした多目的観測サイト活動を数多く実施した。これらの活動は、20 年度も地球惑星科学専攻や地球科学輻合部との協力で積極的に継続された。

平成 21 年 6 月

平成 20 年度地球熱学研究施設長

竹村恵二

## Preface

Institute for Geothermal Sciences was established in 1997 reorganized with Beppu Geophysical Research Laboratory (established in 1924) and Aso Volcanological Laboratory (established in 1930). We regard central Kyushu, one of the most active volcanic and geothermal fields in the world, as a natural experimental facility. The Institute for Geothermal Sciences is promoting a comprehensive research on thermal structure and the dynamics of the Earth's interior into volcanism, geothermics and tectonics by field work, laboratory experiments, and theory. Based on the fundamental scope of our research, a variety of research works can flexibly cooperate within this interdisciplinary geothermal science research system. We have the following five research units: geothermal fluids, geothermal tectonics, volcanic structure, volcano-dynamics and geothermal intelligence section with a visiting research scholar from abroad. In 2004 fiscal year, Kyoto University was reformed to juridical personalization of national universities. This puts us under pressure to do efficient education and research with limited staffs and funds. Total revenue has been decreased and we are forced to get other competitive fund associated since then.

Meetings of the steering committee set in 2004 were held nine times in Kyoto campus, and the cooperative relationship between our institute and Graduate School of Science was intensified. Taking into consideration on the subjects related to remote institutions from main campus, we need to make efforts to intensify cooperative work at Aso and Beppu. In 2007 fiscal year, the Kyoto Branch of our institute was established in Kyoto campus for more intensive education and sharing tasks for Graduate School. TV meeting systems connecting among Kyoto, Aso and Beppu were used constantly for seminars and special lectures.

In personal affairs, Dr. Singh from India worked at Aso during May to August, and Dr. Chen from Taiwan worked at Aso from October to end of March, and Prof. Holloway joined us in Beppu from April, 2009. As a postdoctoral associate, Dr. Hidemi ISHIBASHI left to University of Tokyo in July, 2008. Dr. Marie PYTHON was adopted in Beppu in October 2008. Dr. Akihiko TERADA left to Tokyo Institute of Technology in April, 2009. Dr. Masaya MIYOSHI joined in Beppu from April, 2009. Keiko MIYAZAKI as a secretary in Beppu left and Miho MIYATA joined us.

The activity of the KAGI 21 (Kyoto University Active Geosphere Investigations for the 21<sup>st</sup> Century Centers of Excellent program) program was finished, and our institute made a great contribution for scientific activity on water and material circulation at the active geosphere, stalagmite project and as a field station of the multi-purpose field site for education and research activity. These activities continue under the collaboration with Division of Earth and Planetary Sciences and Integrated Earth Science Hub.

Beppu, June 2009

Keiji TAKEMURA, Professor/Director



## 目次 Contents

構成員	Members	5
研究活動	Research Activities	6
機関内共同研究	Institution Colaboration	6
研究報告	Scientific Reports	21
公表論文	Publications	65
共同研究一覧	List of Collaboration	75
研究費	Funding	75
教育活動	Education	77
学位・授業	Academics	77
セミナー	Seminars	79
学会活動	Activities in Scientific Societies	82
社会活動	Public Relations	82
一般公開報告	Openhouse	84
来訪者	Visitors	91
定常観測	Routine Observations	94
装置, 設備	Instruments and Facilities	96

## 構 成 員 Members

教授	Professors	石橋秀巳	Hidemi Ishibashi
鍵山恒臣	Tsuneomi Kagiya	6月30日退職	東京大学地殻化学実験施設
竹村恵二(施設長)	Keiji Takemura (Director)	研究員へ	
准教授	Associate Professors	寺田暁彦	Akihiko Terada
大倉敬宏	Takahiro Ohkura	3月31日退職	東京工業大学 研究員へ
大沢信二	Shinji Ohsawa	ピトン マリー	Marie Python
古川善紹	Yoshitsugu Furukawa	10月1日着任	
		山田誠	Makoto Yamada
助教	Assistant Professors	研修員	Research Fellow
宇津木充	Mitsuru Utsugi	なし	
川本竜彦	Tatsuhiko Kawamoto		
柴田知之	Tomoyuki Shibata	研究生	Research Student
山本順司	Junji Yamamoto	三島壮智 (岡山理科大学・京都大学特別研究交流)	Taketoshi Mishima
外国人客員	Visiting Faculty		
Singh, Nagendra Pratap		大学院生	Graduate Student
5月7日着任、8月16日離任		小森省吾	Syogo Komori
陳 中華	Chang-Hwa Chen	安部祐希	Yuki Abe
10月1日着任、3月31日離任		岩部智沙	Chisa Iwabe
		熊谷仁孝	Yoshitaka Kumagai
技術専門職員	Technical Professionals	宇内克成	Katsunari Unai
馬渡秀夫	Hideo Mawatari	山本友里恵	Yurie Yamamoto
吉川慎	Shin Yoshikawa		
		事務補佐員	Secretaries
技術職員	Technical Staff	今村町子	Matiko Imamura
井上寛之	Hiroyuki Inoue	東端歩	Ayumi Higashibata
		宮崎恵子	Keiko Miyazaki
教務補佐員	Research Assistant	11月30日退職	
芳川雅子	Masako Yoshikawa	宮田美保	Miho Miyazaki
西村光史	Koshi Nishimura	11月10日着任	
佐藤智之	Tomoyuki Sato	土井有紀	Yuki Doi
10月1日着任、3月31日退職			
産業総合研究所へ		臨時用務員	Supply Janitor
		山崎咲代	Sakiyo Yamasaki
研究機関研究員	Research Associates		
浜田盛久	Morihisa Hamada		

## 研究活動 Research Activities

### 機関内共同研究 Institution Collaboration

**Petrological descriptions on the Tsurumi-dake summit lava and implications on its pre-eruptive conditions.**

**H. Ishibashi (Univ. Tokyo), T. Saito (Shinshu Univ.), T. Sugimoto (JMC Geotherm. Eng.)  
K. Takemura**

#### 1. Introduction

Tsurumi volcano is one of the active volcanoes emplaced within the Beppu-Shimabara Graben, Kyushu, Japan. The volcano has been active since more than 60,000 years ago and the latest lava effusion occurred between 7.3-10.5 cal ka BP from tephrochronology and radiocarbon dating (Fujisawa et al., 2002). Tsurumi volcano is chiefly composed of andesitic-dacitic lavas with SiO<sub>2</sub> contents of ca. 56-65wt% and their SiO<sub>2</sub> content tends to decrease toward the younger stage; the summit lava is most basic (Ohta et al., 1990; Sugimoto et al., 2006; Saito et al., 2007). Several petrological and geochemical studies were done for the lavas to clarify their formation mechanism and source characteristics (e.g., Ohta et al., 1990; Ohta and Aoki, 1991; Sugimoto et al., 2006). However, pre-eruptive conditions of the lavas were unknown. Seismological study of Ohkura et al. (2002) revealed that the presence of an aseismic zone at the depth of ca. 4-10km beneath Tsurumi volcano. The distribution pattern of epicenters around the aseismic zone is similar to that of post-eruptive earthquake hypocenters beneath Mt. Pinatubo, Philippines (Hammer and Rutherford, 2003). This similarity makes us to speculate that the aseismic zone corresponds to a magma chamber of Tsurumi volcano. We think it is possible to examine the hypothesis by determining pre-eruptive conditions of volcanic products. In this study, we performed petrological descriptions and tried to determine the pre-eruptive conditions from thermodynamic analyses of constituent mineral chemistry for the summit lava, the latest product of Tsurumi volcano, and the older lava which may belong to early-middle stage deposits (Fujii et al., 2007; Saito et al., 2007).

#### 2. Petrography

We collected rock samples from the summit lava and the older lava adjacent to the summit lava and processed to thin sections for optical observation and EPMA analysis. Both the lavas show common phenocryst assemblage of plagioclase, ortho- and clinopyroxenes, Fe-Ti oxides, hornblend, biotite, quartz, and rarely olivine embedded in holocrystalline-hyalopilitic groundmass. Pyroxene is abundant in the summit lava whereas it is poor in the older lava.

Plagioclase in the summit lava often has dusty zone in contrast to those in the older lava most of which is clear. Hornblende and biotite have opacified rim. Magnetite and Ilmenite often contact with each other. Quartz shows rounded shape, and olivine is surrounded by orthopyroxene. As discussed by Ohta and Aoki (1991), the lavas showed features of magma mixing, such as disequilibrium assemblage of quartz and olivine. It is difficult for such mixed lava to determine its pre-eruptive conditions from phase equilibrium between phenocrysts due to difficulty in identifying coexistent mineral pairs. Thus we focused on crystal clots and mineral inclusions bearing phenocrysts in which hornblende directly contact with other mineral phases (Figure 1). Hornblende phenocrysts have mineral inclusions of plagioclase, ortho- and clinopyroxenes, Fe-Ti oxides and alkali feldspar. Quartz and biotite were not observed in hornblende, indicating that they did not crystallized during hornblende growth.

Major element compositions were analyzed for hornblende-plagioclase pairs in contact with each other. Pairs of magnetite and ilmenite were also analyzed. Compositional differences for the minerals were observed between the summit lava and the older lava. Analyzed plagioclase in the summit lava showed higher An# [=Ca/(Ca+Na+K)] of ca. 0.8 than those in the older lava (An#=0.6-0.7). Hornblendes are pargasitic-magnesiokatophoritic and those in the summit lava are Si-poor compared with those in the older lava. Ti/(Ti+0.5Fe<sup>3+</sup>) ratios of ilmenite and magnetite in the summit lava vary in the range of 0.8-0.9 and 0.2-0.35, respectively. On the other hand the ratios in the older lava are homogeneous with ca. 0.85 for ilmenite and 0.1 for magnetite.

### 3. Pre-eruptive condition estimation

Fe-Ti oxide thermometer (Anderson and Lindsley, 1988) was applied to paired magnetite-ilmenite datasets. Fe-Ti oxide pairs in the summit lava show homogeneous temperature of ca. 800 degree C however estimated oxygen fugacity (fO<sub>2</sub>) vary from 0.8 to 2.4 log unit above quartz-fayalite-magnetite (QFM) buffer. Those in the older lava show homogeneous temperature-fO<sub>2</sub> condition of ca. 700 degree C and QMF+3. These indicate that the summit lava and the older lava erupted at temperature higher than ca. 800 and 700 degree C, respectively.

Hornblende-plagioclase geothermometer (Holland and Blundy, 1994) was applied to coexisting hornblende-plagioclase dataset to estimate pre-eruptive equilibrium temperatures. This thermometer is based on the exchange reaction between plagioclase and hornblende;



This thermometer is very insensitive to pressure and represents equilibrium temperature within 35K (1 sigma). Estimated temperatures vary 850-975 and 840-920 degree C for the summit lava and the older lava, respectively. Hornblende-plagioclase pairs in one crystal clot showed uniform temperature and the variation is caused by temperature difference between each phenocrysts. Maximum estimated temperature is almost similar to experimentally determined hornblende liquidus of H<sub>2</sub>O-rich andesitic magma (e.g., Hertz et al., 2005) and minimum

estimated temperature is higher than temperatures obtained by the Fe-Ti oxides thermometer. We think the estimated temperature for each phenocryst reflects its crystallization temperature and reequilibration was ineffective. This is consistent with very low diffusion coefficient of Al-Si in plagioclase ( $D \sim 10^{-21}$ - $10^{-26}$  m<sup>2</sup>/s at 1000 degree C; Grove et al., 1984).

Hornblende-plagioclase-quartz geobarometer (Bhadra and Bhattacharya, 2007) is based on the following net transfer reaction among the three phases;



Bhadra and Bhattacharya (2007) mentioned that the barometer represents experimental pressure within 2kbar with 83% reliability. This barometer was applied to hornblende-plagioclase dataset with temperatures obtained by hornblende-plagioclase geothermometer to estimate equilibrium pressure. The estimated pressure was ca. 6.7-17 kbar and 16-27 kbar for the summit lava and the older lava, respectively. These unrealistically high pressures are due to undersaturation of quartz component. This barometer tends to overestimate pressure as activity of SiO<sub>2</sub> component decreases. Actually no quartz was observed in hornblende. The minimum pressure estimation yields upper limit of possible pressure; i.e., hornblende crystallization pressure is lower than 16 and 6.7 kbar for the summit lava and the older lava, respectively. Lithostatic pressure of 6.7 kbar corresponds to ca. 17 km depth, which is deeper than the observed aseismic zone.

Coexistence of hornblende and plagioclase requires that liquidus temperatures of both the phases are higher than estimated equilibrium temperatures. The estimated temperatures were compared with hydrous equilibrium experiment of Hertz et al. (2005) in which composition of starting material is similar to the summit lava and the older lava (Figure 2). They showed that the Clapeyron slopes are respectively positive and negative for liquidus curves of hornblende and plagioclase and they intersect at ca. 2.1 kbar; liquidus temperature at the pressure, which is the maximum temperature for coexistence of the phases, is ca. 950 degree C, which coincides with the maximum of estimated temperatures for both the summit lava and the older lava within 1 sigma error. This implies that crystallization pressure of hornblende is near 2.1 kbar under H<sub>2</sub>O-saturated condition. The pressure of 2.1kbar corresponds to the depth of ca. 5.3 km, which is consistent with the roof depth of the aseismic zone. Although further examination about the effect of H<sub>2</sub>O-undersaturation on the pressure estimation is required, we think from the consistency that the aseismic zone beneath Tsurumi volcano may be magma chamber where hornblende phenocrysts grew.

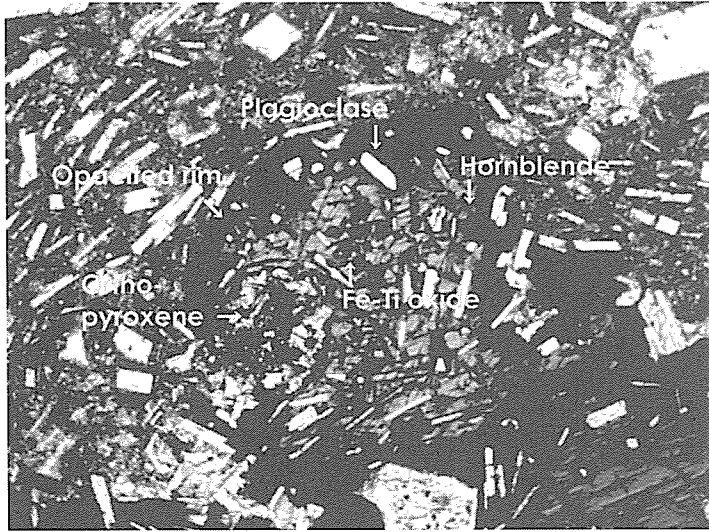


Figure 1. Hornblende phenocryst with mineral inclusions of plagioclase, orthopyroxene, and magnetite (picture width is 1 mm ). Rim of hornblende is broken to opacite.

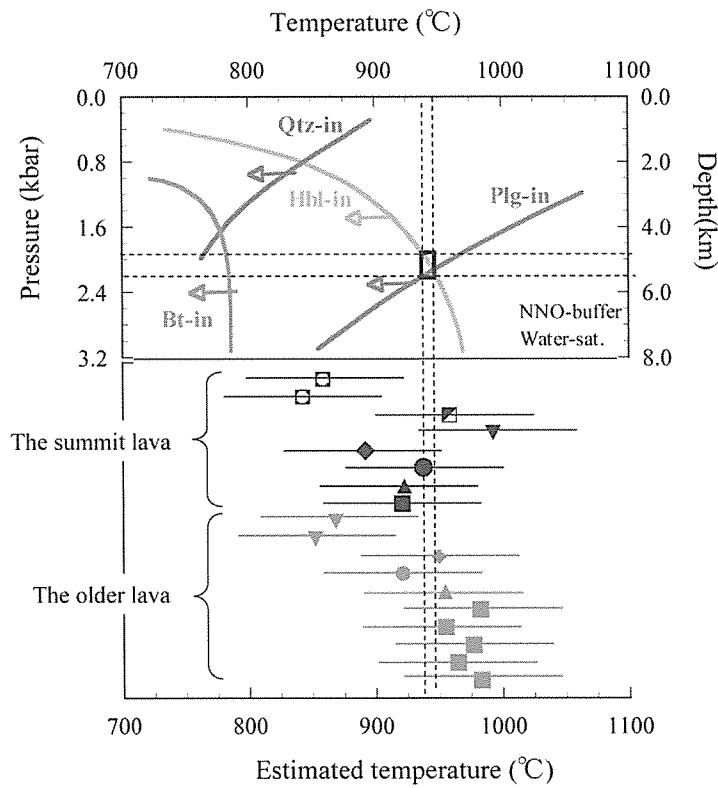


Figure 2. Equilibrium temperatures estimated by the hornblende-plagioclase thermometer and comparison with equilibrium experiment of hydrous andesitic magma (Hortz et al., 2005) which composition is similar to the lavas analyzed in this study. Error bars indicate standard deviation of estimation (2 sigma). The square in the phase diagram indicates pressure range of hornblende-plagioclase stability at maximum estimated temperature. The pressure corresponds to the depth of ca. 5km, which is consistent with the roof depth of the aseismic zone beneath Tsurumi volcano.

## References

- Anderson and Lindsley (1988) Internally consistent solution models for Fe-Mg-Mn-Ti oxides: Fe-Ti oxides. *Am. Min.*, 73, 714-726.
- Bhadra and Bhattacharya, 2007. The barometer tremolite + tschermakite + 2 albite = 2 pargasite + 8 quartz: Constrains from experimental data at unit silica activity, with application to garnet-free natural assemblages. *Am. Min.*, 92, 491-502.
- Fujii et al., 2007. Tentative estimation of the age of Tsurumidake summit lava, Beppu City, by paleomagnetic directions and paleointensities. *Ann. Rep. Inst. Geotherm. Sci., Kyoto Univ.*, FY2007, 6-8.
- Fujisawa et al., 2002. Eruptive activities of Tsurumi volcano in Japan during the past 30,000years. *Jour. Geol. Soc. Japan*, 108, 48-58 (in Japanese with English abstract).
- Hammer and Rutherford, 2003. Petrological indicators of preeruption magma dynamics. *Geology*, 31, 79-82.
- Hortz et al. (2005) Experimental petrology of the 1991-1995 Unzen dacite, Japan. Part I: phase relations, phase composition and pre-eruptive conditions. *J. Petrol.*, 319-337.
- Grove et al., 1984. Coupled CaAl-NaSi diffusion in plagioclase feldspar: Experiments and applications to cooling rate speedmetry. *Geochim. Cosmochim. Acta*, 48, 2113-2121.
- Holland and Blundy, 1994. Non-ideal interactions in calcic amphiboles and their bearing on amphibole-plagioclase thermometry. *Contrib. Mineral. Petrol.*, 116, 433-447.
- Hortz et al., 2005. Experimental petrology of the 1991-1995 Unzen dacite, Japan. Part I: phase relations, phase compositions and pre-eruptive conditions. *J. Petrol.*, 46, 319-337.
- Ohkura et al., 2002. Seismic activity in the Beppu graben, Kyushu, Japan. *Ann. Rep. Inst. Geotherm. Sci., Kyoto Univ.*, FY2002, 2-4.
- Ohta and Aoki, 1991. origin of andesitic magma in Yufu-Tsurumi volcano group –A binary mixing model-. *J. Mineral. Petrol. Economic geology*, 86, 1-15 (in Japanese with English abstract).
- Ohta et al., 1990. Geology and petrography of Yufu-Tsurumi volcano group, Oita prefecture. *J. Mineral. Petrol. Economic geology*, 85, 113-129 (in Japanese with English abstract).
- Saito et al., 2007. The latest lava flows at Tsurumi Volcano, East Kyushu, Japan (2). *Ann. Rep. Inst. Geotherm. Sci., Kyoto Univ.*, FY2007, 9-10.
- Sugimoto et al., 2006. Sr-Nd-Pb isotopic and major and trace element compositions of the Yufu-Tsurumi volcanic rocks: implications for the magma genesis of the Yufu-Tsurumi volcanoes, northeast Kyushu, Japan. *J. Mineral. Petrol. Sci.*, 101, 270-275.

## Trace element in plagioclase in mafic magmatic enclave (MME) analyzed by laser ablation inductively coupled plasma mass spectrometry (LA-ICP-MS)

*K. Nishimura, T. Shibata, S. Yoshikura (Kochi Univ.), M. Yoshikawa*

Late Cretaceous granitoids occur closely associated with gabbroids in the Tanoura Igneous Complex (TIC), Shodoshima Island, SW Japan. The TIC consists of granite, tonalite, gabbro-diorite layered sequence and syn-plutonic mafic to felsic dikes (Yoshikura and Atsuta, 2000; Ishihara et al., 2003). The granite and tonalite include scores of Mafic Magmatic Enclaves (MME; Barbarin, 1988) with various shapes and sizes. We have started analyses of the MMEs to understand mixing and/or mingling processes between coexisting granitic and basaltic magmas. The MME often includes plagioclase crystals with xenoporphyritic texture (Figure 1). Field observations suggested that the plagioclase crystals in MME were derived from the host granite (Yoshikura and Atsuta, 2000). We analyzed trace element concentrations of the plagioclase crystals in MME and in the host granite to confirm this interpretation.

The analysis was performed by a quadrupole inductively coupled plasma mass spectrometry (ICP-MS; XSERIES 2, Thermo Fisher Scientific) equipped with a Nd-YAG laser-ablation microprobe (CETAC LSX 500, Cetac Technologies) at the Institute for Geothermal Sciences, Kyoto University. Relative element sensitivities were calibrated against the NIST 610 glass. Replicate analyses of the NIST 612 glass indicate an analytical precision of less than 10 % (Shibata et al., in prep.). Figure 2 shows the trace element patterns of the plagioclase crystals in the MME and in the host granite, and matrix in the MME. Each concentrations were normalized by an normal mid ocean ridge basalt (N-MORB value; Sun and McDonough, 1989). The patterns of plagioclase crystals in the MME (symbols connected by thin line) agree fairly well with those in the host granite (symbols connected by thick line). This result suggests that the plagioclase crystals in MME were derived from the host granite. Microsampling and Sr isotopic analyses of the plagioclase crystals are currently carried out to further confirm this interpretation.



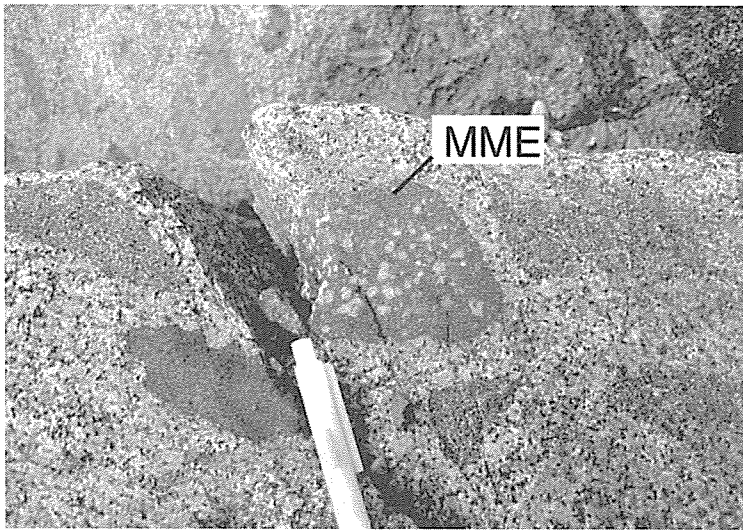


Figure 1. Mafic Magmatic Enclave (MME) showing xenoporphyrific texture observed in the Cretaceous granite, Shodoshima Island, SW Japan.

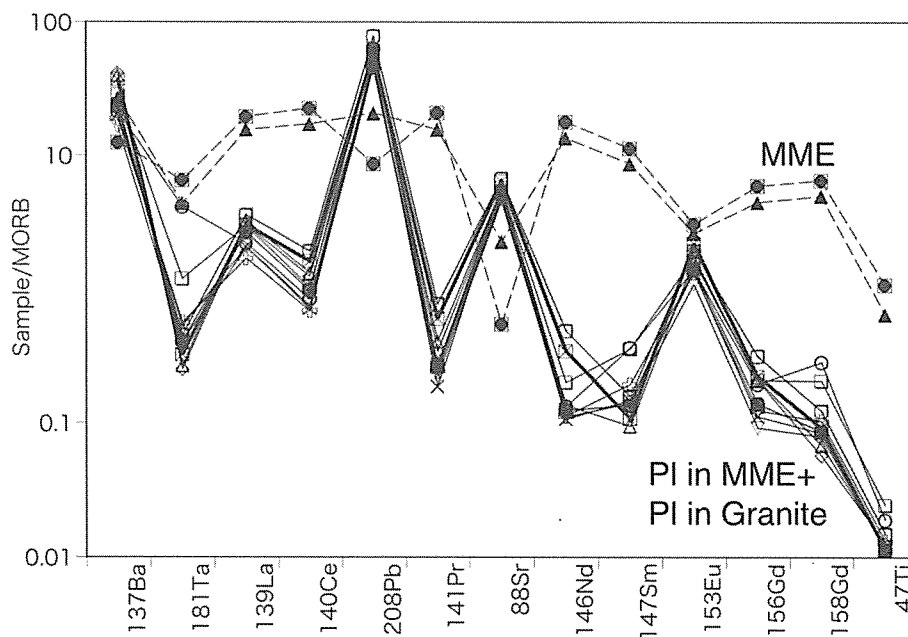


Figure 2. Trace element patterns for plagioclase (PI) crystals in MME (thin line) and in granite (thick line). The patterns for matrix in MME are also shown for comparison (broken line).

#### References

- [1] Barbarin, B. (1988) Canadian Journal of Earth Sciences 25, 49– 59.
- [2] Yoshikura, S., Atsuta, S.(2000) Earth Monthly (in Japanese), 30, 140–145.
- [3] Ishihara, S., Yoshikura, S., Sato, H., Satake, Y., Atsuta, S. (2003), Hutton symposium V, Field Guide book, Geological Survey of Japan, Interim-Report, 28, 41–60.
- [4] Sun, S.S., McDonough, W.F. (1989), in: Magmatism in the Ocean Basins (Saunders, A.D. and Norry, M.J. Eds.), Geological Society of London, Special Publication, 42, 313–345.

## Recent seismic activity in and around the Beppu graben, Kyushu, Japan

*T. Ohkura, H. Mawafari, K. Takemura*

In the Beppu graben, seismic activity was monitored by real-time telemetry system from March 1993 to May 2000 (Annual Report FY2000 and FY2002). However, after May 2000, the real-time observation was suspended and a new network using dial-up system was established.

In July 2007, we established new real-time telemetry system using IP-VPN network and, from April 2008, seismic data of Hi-net, JMA, and Kyushu Univ. around the study area are combined to locate earthquakes in and around the Beppu graben. Fig.1 shows epicentral distribution with seismic stations used in this study. In this figure, all the epicenters are plotted, which were automatically located within the RMS residual travel time of 0.15 second.

We relocated events in the rectangular area of Fig.1 using manually picked P- and S-arrival times. In Fig.2, epicentral distribution in the area is shown with the E-W and N-S cross sections. As indicated in the previous works (Annual Report FY2000 and FY2002), the lower limit

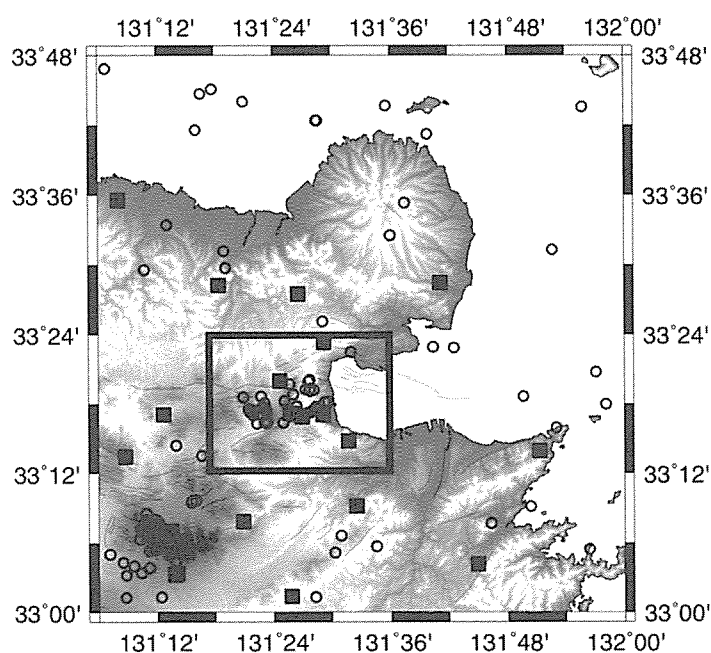


Fig.1 Epicenter distributions (open circles) in the period from April 2008 to March 2008, as determined automatically using IGS, Hi-net, Kyushu Univ. and JMA data. Solid squares show seismic station. Solid lines are active faults. A rectangle denotes the area which are shown in Fig.2.

of seismicity shown in the E-W cross section becomes shallower toward the eastern flank of the active volcanoes; Mt. Garan and Mt. Tsurumi and there is an aseismic zone at a depth of 5 km, where a high electric conductive body is located by electromagnetic surveys (NEDO, 1989).

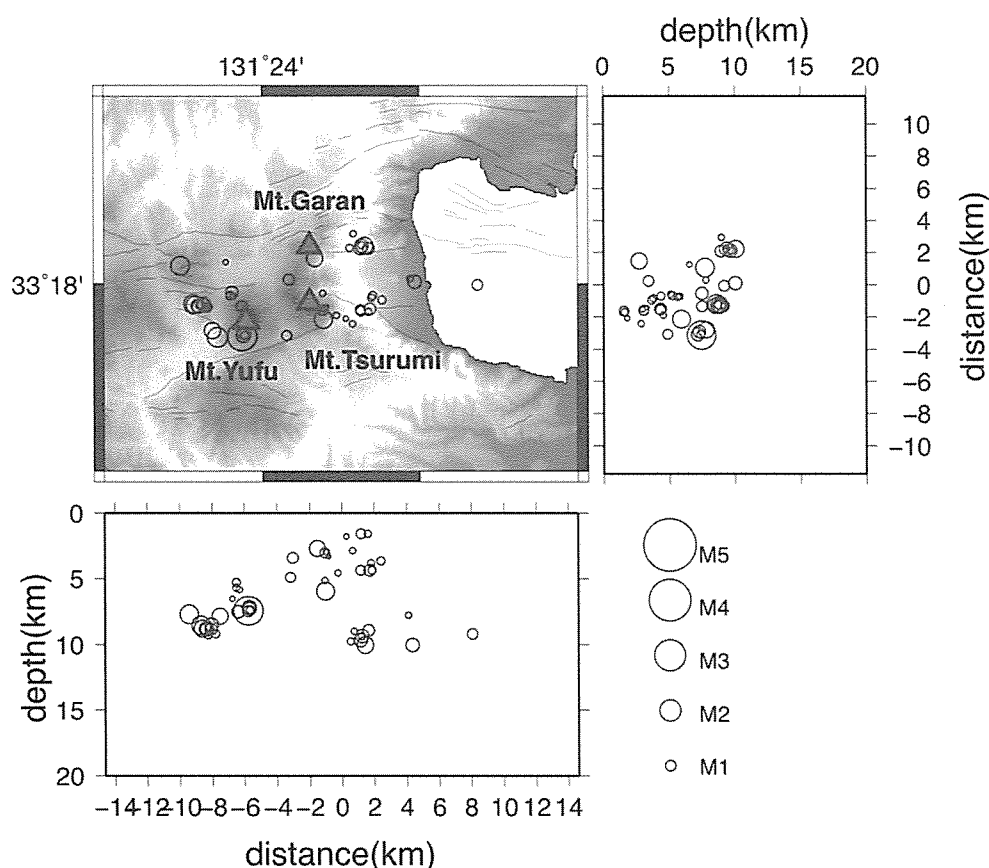


Fig.2 Relocated epicenter distributions in the area shown in Fig.1. period from April 2008 to March 2008 with E-W and N-S cross-sections. Triangles and solid lines show active volcanoes and active faults, respectively.

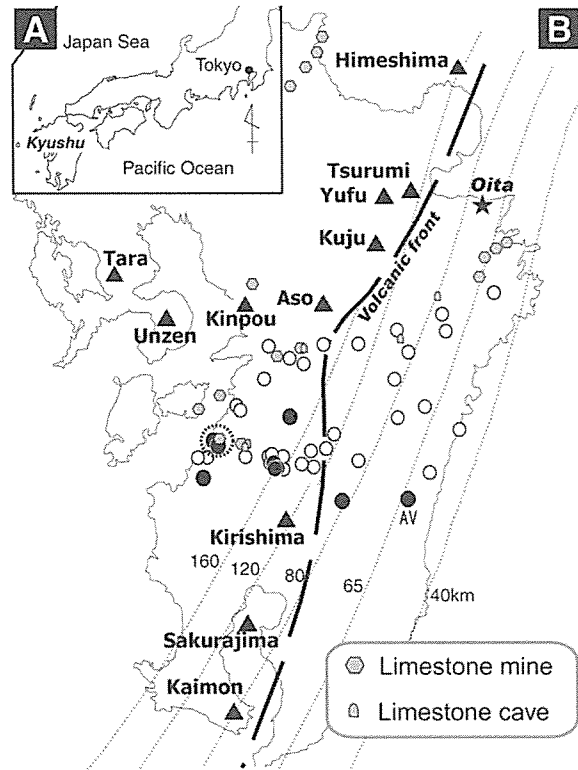
## Waters bearing deep-originated CO<sub>2</sub> discharged from hot spring wells distributed in non-volcanic region between Aso and Kirishima Volcanoes, Kyushu Island, Japan

*S. Ohsawa, M. Yamada, S. Yoshikawa, T. Mishima (Okayama Univ. Sci.), T. Kagiya*

### 1. Introduction

For detection of emerging area of isotopically heavy CO<sub>2</sub> originated from deep earth, we collected 46 water samples from hot spring wells distributed in non-volcanic region between Aso and Kirishima Volcanoes (open and solid circles in Fig.1) and carried out stable-isotopic measurements ( $\delta^{13}\text{C}$  of dissolved inorganic carbon: DIC,  $\delta\text{D}$  and  $\delta^{18}\text{O}$  of H<sub>2</sub>O) and chemical analysis (quantitative analysis of DIC) of the sampled waters.

Fig.1 Location map of the researched hot spring wells (open and solid circles; for differentiation between open and solid, see the result section) with distributions of limestone mass (gray symbols) and the Quaternary volcanoes (solid triangles). The deepest hot spring well researched in this study is 1800m and mean depth of the wells is 840m. The short and long dashed lines show the volcanic front and isopleths of depth of the subducting Philippine-sea plate, respectively. At the place pointed by the solid asterisk, hyper-saline water derived from dehydrated fluid of the subducting oceanic plate has been recognized to be discharged from a hot spring well in Oita area (Amita et al. 2005).



## 2. Results and discussion

Water isotope compositions ( $\delta D$  vs  $\delta^{18}O$ ) of the sampled waters except for sample AV indicate that water ( $H_2O$ ) is in meteoric origin (Fig.2A). AV, which is low temperature saline water, would be a mixed water of pore water of marine sediments (paleo-seawater) to meteoric water.

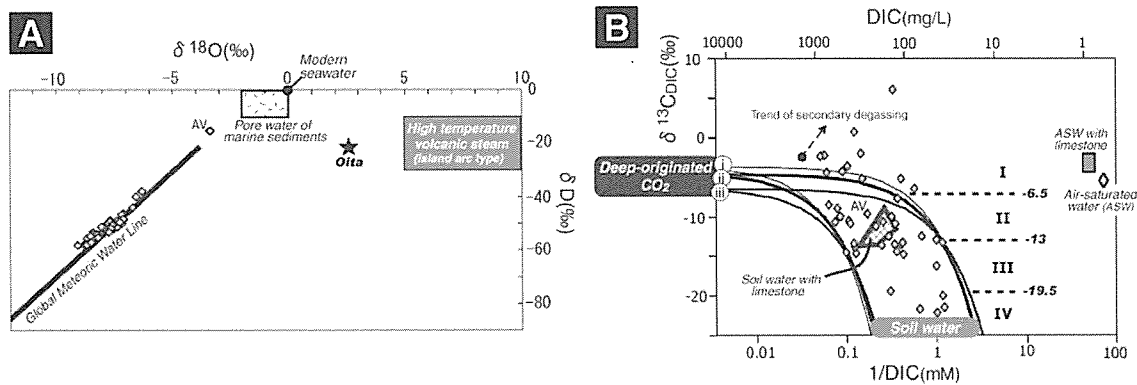


Fig.2 Relation between  $\delta D$  and  $\delta^{18}O$  (A) and relation between  $\delta^{13}C$  and the reciprocal of concentration of dissolved inorganic carbon (B) of sample waters. Deep-originated  $CO_2$ ; i :  $CO_2$  with dehydrated fluid of the subducting oceanic plate at Oita (Amita et al., 2005), ii : magmatic  $CO_2$  at Kirishima Volcano (Sato et al., 1999), iii : mantle  $CO_2$  (e.g., Sano and Marty, 1995).  $\delta^{13}C_i = -2.9\text{‰}$ ,  $\delta^{13}C_{ii} = -4.7\text{‰}$ ,  $\delta^{13}C_{iii} = -6.5\text{‰}$ .

On the other hand, stable carbon isotope ratio ( $\delta^{13}\text{C}$ ) and concentration (Conc) of DIC of the sampled waters have a systematic variation on the  $\delta^{13}\text{C} - 1/\text{Conc}$  diagram (Fig. 2B). The linearly relationship between the  $\delta^{13}\text{C}$  values and the reciprocal of the concentration of the sampled waters suggests that almost every DIC are mixtures of soil  $\text{CO}_2$  with deep-originated  $\text{CO}_2$  and the higher the  $\delta^{13}\text{C}$  value, the more deep-originated  $\text{CO}_2$  is mixed. However, a careful consideration must be given to the data points in and around the crosshatch of soil water with limestone in Fig. 2B, because DIC of such intermediate  $\delta^{13}\text{C}$  value can be formed by the chemical reaction between limestone and soil water ( $\text{CaCO}_3 + \text{H}_2\text{CO}_3 \rightarrow \text{Ca}^{2+} + 2\text{HCO}_3^-$ ; Ohsawa et al., 2002). Fortunately, hot springs having the doubtful data shown by the solid circles in Fig. 1 hardly distribute limestone mass areas except for only two hot springs (see the dashed circle in Fig. 1), therefore mixing ratios of the deep- $\text{CO}_2$  to soil  $\text{CO}_2$  can be roughly led from the  $\delta^{13}\text{C}$  values of DIC. Dividing hot springs into 4 ranks from the  $\delta^{13}\text{C}$  values of DIC; over  $-6.5\text{‰}$ , from  $-6.5\text{‰}$  to  $-13\text{‰}$ , from  $-13\text{‰}$  to  $-19.5\text{‰}$  and below  $-19.5\text{‰}$  the respective positions are expressed on the map by the different symbols (Fig. 3). Here, the contribution ratios of the deep- $\text{CO}_2$  are calculated to be 91%, 59% and 27% when the DIC  $\delta^{13}\text{C}$  is  $-6.5\text{‰}$ ,  $-13\text{‰}$  and  $-19.5\text{‰}$ , respectively, if the  $\delta^{13}\text{C}$  of the deep- $\text{CO}_2$  is  $-4.7\text{‰}$ , which is the mean value of  $\text{CO}_2$  with dehydrated fluid of the subducting oceanic plate ( $-2.9\text{‰}$ ), magmatic  $\text{CO}_2$  ( $-4.7\text{‰}$ ) and mantle  $\text{CO}_2$  ( $-6.5\text{‰}$ ).

It is hard to specify the origin of the high  $\delta^{13}\text{C}$   $\text{CO}_2$  only from  $\delta^{13}\text{C}$  because the  $\delta^{13}\text{C}$  values of  $\text{CO}_2$  with dehydrated fluid of the subducting oceanic plate, magmatic  $\text{CO}_2$  and mantle  $\text{CO}_2$  are close to each other as described above. For the specification of the deep- $\text{CO}_2$ , it is necessary to examine with helium isotope ( $\delta^{13}\text{C}$  vs  $\text{CO}_2/{}^3\text{He}$ ) such as Sano and Marty (1995). We will address such work in the near future, but we will examine the possibility of participation of ancient magmatic  $\text{CO}_2$  in contradistinction to distributions of old igneous rocks, here. Figure 4 is the map expressing the emerging points of high  $\delta^{13}\text{C}$   $\text{CO}_2$  ( $\geq -6.5\text{‰}$ ) shown in Fig. 3 on a distribution map of the Miocene igneous rocks. Only 4 out of 10 hot springs are overlapped at the Miocene volcanics areas (open asterisks in Fig. 4), so DIC of the 6 remainders is possible to be derived from  $\text{CO}_2$  with dehydrated fluid of the subducting oceanic plate or mantle  $\text{CO}_2$ .

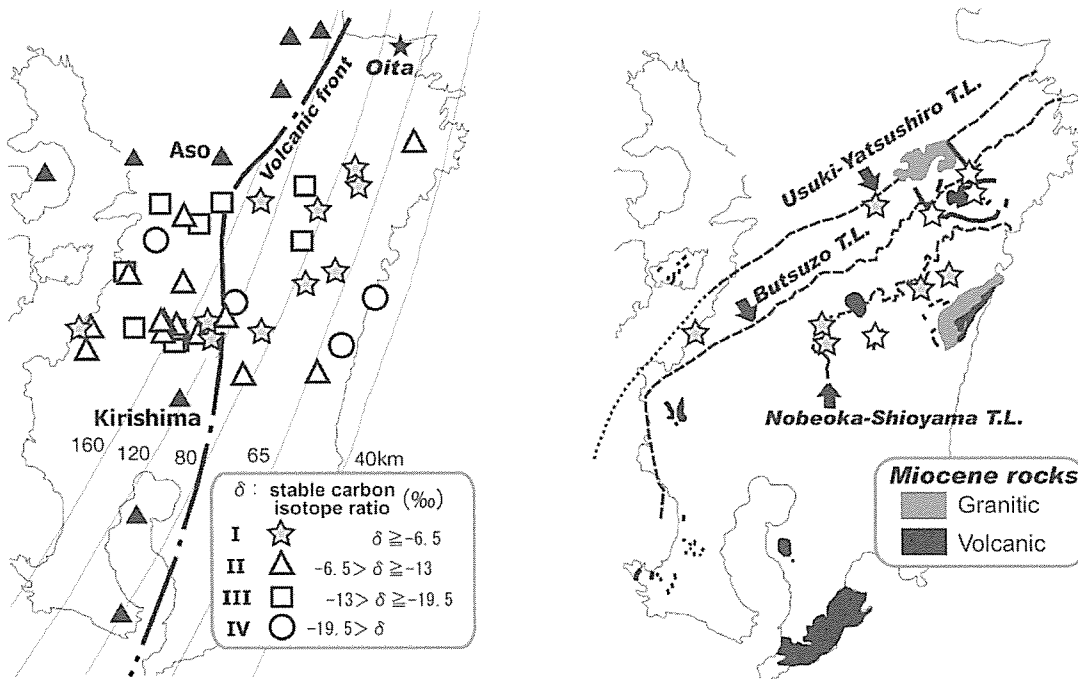


Fig. 3 (left) Hot springs (in Fig. 1B) ranked by the  $\delta^{13}\text{C}$  values of dissolved inorganic carbon (DIC)

Fig. 4 (right) Locally comparison between Miocene igneous rocks and hot springs having high  $\delta^{13}\text{C}$  DIC ( $\geq -6.5\text{‰}$ ) illustrated in Fig. 3. Hot springs shown by open asterisks are overlapped in the distributions of the Miocene volcanics.

## References

- Amita, K., Ohsawa, S., J. Du, Yamada, M. (2005) Origin of Arima-type Deep Thermal Water from Hot Spring Wells in Oita Plain, Eastern Kyushu, Japan. *J. Balneol. Soc. Jpn*, 55, 64-77 (Japanese with English abstract)
- Ohsawa, S., Kazahaya, K., Yasuhara, M., Kono, T., Kitaoka, K., Yusa, Y., Yamaguchi, Y. (2002) Escape of volcanic gas into shallow groundwater systems at Unzen volcano (Japan): evidence from chemical and stable carbon isotope compositions of dissolved inorganic carbon. *Limnology*, 3, 169-173
- Sano, Y. And Marty, B. (1995) Origin of carbon in fumarolic gas from island arcs. *Chem. Geol.*, 119, 265-274
- Sato, M., Mori, T., Notsu, K., Wakita, H. (1999) Carbon and Helium Isotopic Composition of Fumarolic and Hot Spring Gases from Kirishima Volcanic area. *Bull. Volcanol. Soc. Jpn*, 44, 279-283 (Japanese with English abstract)

## Hydrogeological study of limestone cave and speleothems: study of generation process of drip water

*M. Yamada, S. Ohsawa, T. Mishima, H. Mawatari, K. Takemura*

Drip water samples for water isotope ( $\delta D$ ,  $\delta^{18}O$  and Tritium) and major chemical composition analyses were collected from Inazumi limestone cave, Oita Prefecture, in order to understand the behavior of drip water from infiltration to dripping. Quantity of rain and drip water (precipitation and drip rate) also observed near or in there.

The results of precipitation and drip rate measurement (Fig. 1) led to the first conclusions as follows: drip waters have the independent catchment area, respectively. The results of chemical composition analyses (Fig. 2) confirmed the first conclusions and led to the second conclusions as follows: drip waters have the independent contact time with limestone, respectively. In other words, travel time of drip water differ from point to point. The third conclusion was led by the results of water stable isotope analyses (Fig. 3) as follows. The variation of characteristic of drip water was derived from difference of the degree of mixture in soil layer. The difference arises from the degree of progression of crack in limestone. Additionally, tritium analyses data also showed that drip waters have individual travel times, respectively. On these conclusions we have come to final conclusion that characteristic of drip water was governed by the degree of progression of crack.

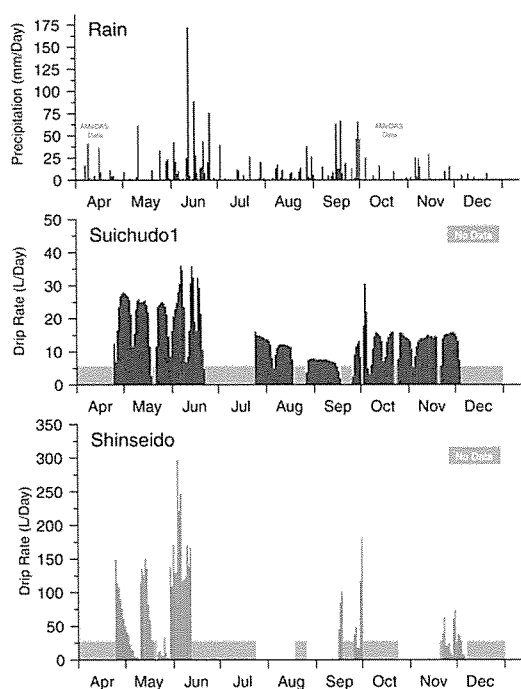


Fig. 1 Result of precipitation and drip rate measurement

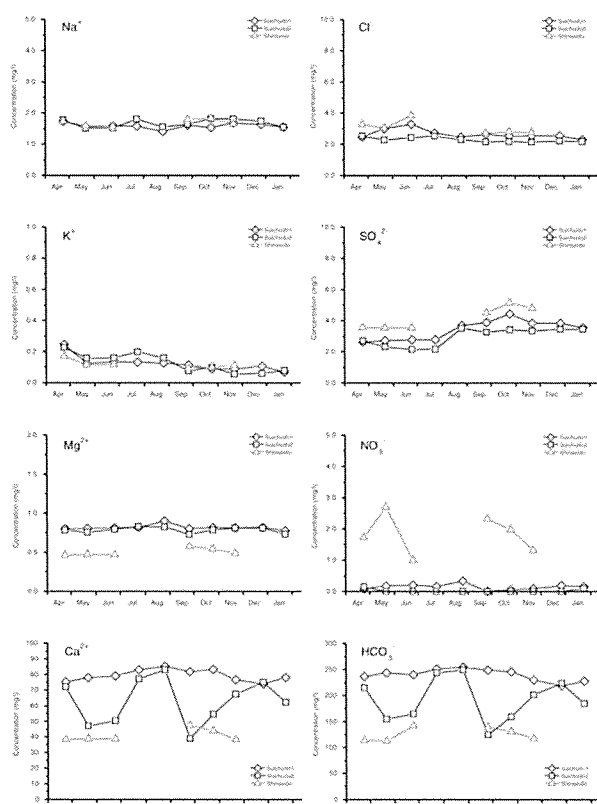


Fig. 2 Time series variation of major chemical composition

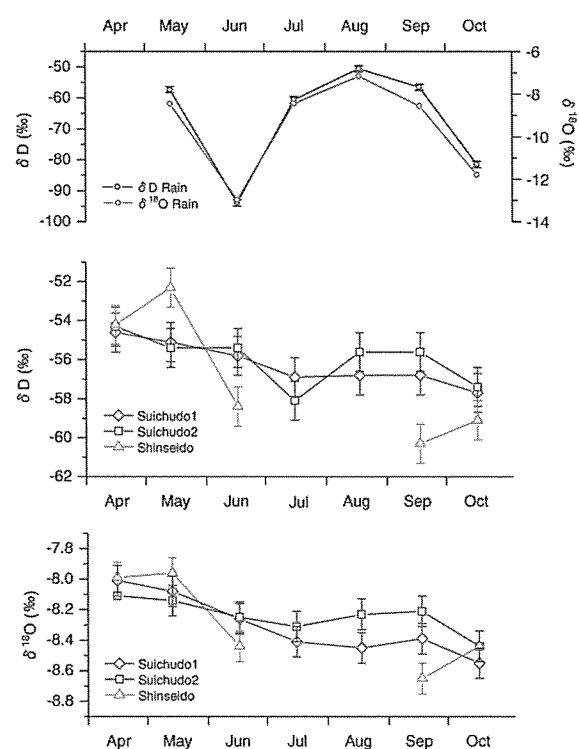


Fig. 3 Time series variation of rain and drip water stable isotopes



**Geochemical and Sr–Nd isotopic characteristics and P–T estimates of mantle xenoliths from the French Massif Central: evidence for melting and multiple metasomatism by silicate-rich carbonatite and asthenospheric melts**

*M. Yoshikawa, T. Kawamoto, T. Shibata, J. Yamamoto*

Ultramafic xenoliths from Mont Briançon, Ray Pic and Puy Beaunit in the French Massif Central show variable mineral compositions that indicate a residual origin after various degrees of partial melting of a fertile peridotite. Furthermore, trace element and Sr–Nd isotopic variations of clinopyroxenes indicate mixing processes between depleted mantle and enriched components such as asthenospheric melt and silicate carbonatite melt. Pyroxene geothermometer and CO<sub>2</sub> geobarometer estimates are 860–1060 °C at 0.92–1.10 GPa for Mont Briançon, 930–980 °C at 0.89–1.04 GPa for Ray Pic, and 840–940 °C at 0.59–0.71 GPa for Puy Beaunit. From south to north, the xenoliths show the following trends: (1) deeper to shallower origin, (2) more depleted mineral compositions, suggesting higher degrees of partial melting, and (3) more enriched isotopes and trace elements, indicating mixing process with a silicate-rich carbonatite melt characterised by high H<sub>2</sub>O and K<sub>2</sub>O, possibly during Variscan subduction.

(Geol. Soc. London, Spec. Issue, in press)

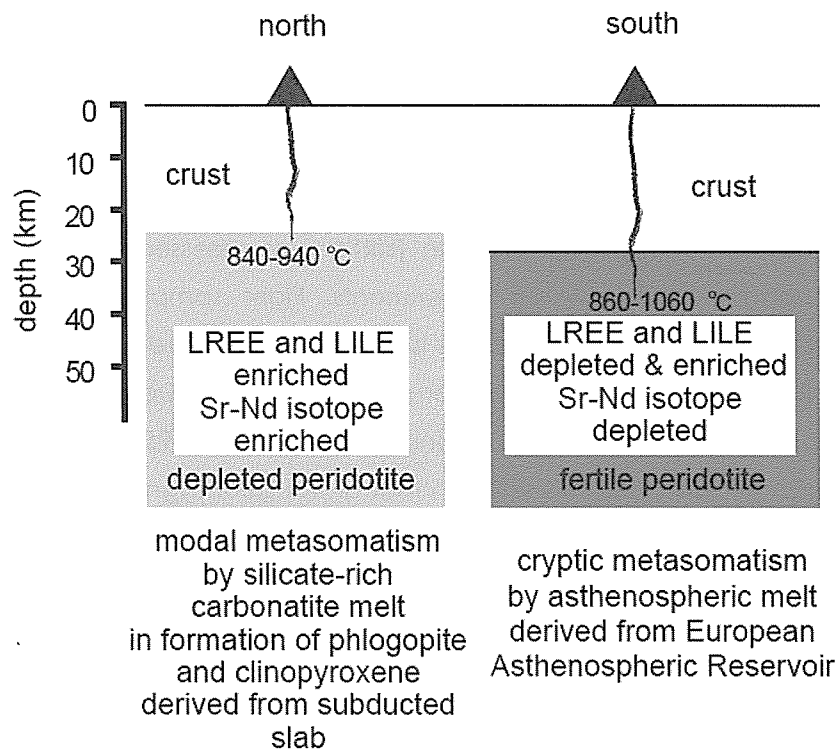


Fig. 1. Schematic diagram of depth and temperature of origin and geochemical characteristics of northern and southern domain xenoliths, Massif Central, France

## 研究報告 Scientific Reports

### Paleomagnetic and rock magnetic studies of subsurface deposits with volcanic materials in Yufu City, Kyushu

S.Fujii, N.Ishikawa (Graduate School of Human and Environmental Studies, Kyoto University),  
K.Takemura

We are conducting paleomagnetic and rock magnetic analyses on subsurface deposits consisting of volcanoclastic materials and their secondary eolian deposits in order to reveal geomagnetic field variation, environmental fluctuation and climate change for the last several ten-thousand-years, and to investigate variations in rock magnetic parameters associated with sedimentation processes of the eolian deposits and soil formation. Samples were obtained from an outcrop of black soil at Tsukahara area and a sediment core drilled at Higashiishimatu area in Yufu City.

[Tsukahara area]

In the outcrop of black soil (1m height) at Tsukahara area, three ash layers (Ash I, II and III in the descending order) are observed. Ash II (16cm thick) at 27 cm below the surface (bs) is Yufudake tephra (2.2ky.B.P.) and Ash III (9cm thick) at 67 cmbs is Kikai-Akahoya tephra (K-Ah: 6.3ky.B.P.). Regarded the ash layers as boundaries, the black soil profile are divided into four units, Soil I to IV in the descending order. Magnetic-orientated 60 samples were collected continuously by pushing 7cc plastic cubes.

The stability of natural remanent magnetization (NRM) was assessed through progressive alternating-field demagnetization (PAFD) experiments. Eight samples of the Tsukahara samples provided stable magnetic components isolated at PAFD levels above 14 mT. Mean directions of the stable component for the lower part of Ash II was Dec=-3.9° and Inc=48.2° ( $\alpha_{95}=8.3^\circ$ ), and for Soil IV was Dec=-6.0° and Inc=50.6° ( $\alpha_{95}=9.8^\circ$ ). The inclination value of the lower part of Ash II is consistent with that of the geomagnetic inclination record at 2.2ky.B.P. from sediment cores in Beppu Bay (Ohno *et al.*, 1991).

Variations of rock-magnetic parameters are shown in Figs. 1-1 and 1-2.

Values of initial magnetic susceptibility ( $X$ ), susceptibility of anhysteresis remanence ( $X_{arm}$ ) and saturation remanence ( $M_r$ ), which reflect mainly the amount of included magnetic materials, show downward increases in Soil I and II, and a downward decrease in Soil III. Soil IV has a different trend;  $X$  values are constant,  $M_r$  values decrease downward, and  $X_{arm}$  values gradually increase downward and then decrease, which implies change in the amount of fine-grained magnetite, especially magnetite of single-domain (SD) size, which can possess anhysteresis remanence (ARM) effectively.  $X$ ,  $X_{arm}$  and  $M_r$  values are higher in

the upper part of Ash II, and lower in Ash III than the other units.

$X_{arm}/X$ ,  $ARM/Mr$  and  $Mr/X$  values, which are influenced by variation in grain size of magnetic minerals, are constant in Soil I and II. In Soil III and IV,  $X_{arm}/X$  and  $ARM/Mr$  values increase downward and then decrease, while  $Mr/X$  values increase downward. Variations in the size of SD magnetite carrying ARM seem to control magnetic properties of Soil III and IV principally. The frequency dependence of  $X$  ( $X_{fd}$ ) is slightly higher in Soil III and IV, implying a higher contribution of ultrafine-sized magnetite. In the upper and lower parts of Ash II,  $ARM/Mr$  values are similar, while  $X_{arm}/X$  and  $Mr/X$  values are higher in the lower part. It is inferred that the grain size of magnetic minerals is finer in the lower part consisting of fine-grained materials. In Ash III with homogenous lithofacies, the three ratios decrease downward, suggesting a downward grain-size decrease of magnetic minerals.

$S$ -ratios are slightly lower in the lower parts of Ash II and Soil IV, which also show higher values of *hard-IRM* (*HIRM*). A contribution of high-coercivity magnetic minerals might have been suggested for the lower parts of Ash II and Soil IV,

#### [Higashiishimatsu area]

The sediment core at Higashiishimatsu area is 6m in length and composed of black soil and brown soil with volcanic ash layers and gravels. Included ash layers are K-Ah layer at 87-100 cmbs and AT layer (26-29 ka) at 230-240 cmbs. The core sample is considered to cover about 50,000 years (Takemura et al, 2006). 160 samples of plastic cube were collected continuously from soil and ash layers, except for volcanic gravels. We also collected powder samples from same horizons where cube samples were obtained, and packed them in plastic bags. We will report results of the core samples from top to 150 cmbs, which are divided into the following three units in the descending order: black soil, K-Ah and black-brown soil units.

All samples of the Higashiishimatsu core showed unstable magnetic behaviors on PAFD experiments below 10mT. No stable magnetic component was obtained.

Variations of rock-magnetic parameters are shown in Figs. 2-1 and 2-2.

In the black soil unit,  $X$ ,  $X_{arm}$  and  $Mr$  values show downward decrease below about 70cmbs, accompanied with downward increases of  $X_{arm}/X$  and  $ARM/Mr$  values. These magnetic features indicate downward decrease in the amount and grain-size of magnetic minerals below about 70 cmbs. Higher values of  $ARM/Mr$ ,  $Mr$  and high-field susceptibility ( $HFS$ ) are observed remarkably at about 50 and 70 cmbs, implying the existence of layers with different magnetic properties. In the black-blown soil unit, a fluctuation of  $X_{arm}$  is distinctive, while  $X$  and  $Mr$  values are constant or slightly decrease downward. Fluctuations in  $X_{arm}/Mr$  and  $ARM/Mr$  correlate to that of  $X_{arm}$ . Variations in the amount and size of magnetic minerals carrying ARM (SD-magnetite) seem to control magnetic properties of the black-blown soil unit. In the black-brown soil unit, higher values of  $X_{fd}$  (~6%) are observed, while  $X_{fd}$  values are 2 % and 3% in the black soil and K-Ah units, respectively. A higher contribution of ultrafine-sized magnetite may be suggested for the black-brown soil unit.

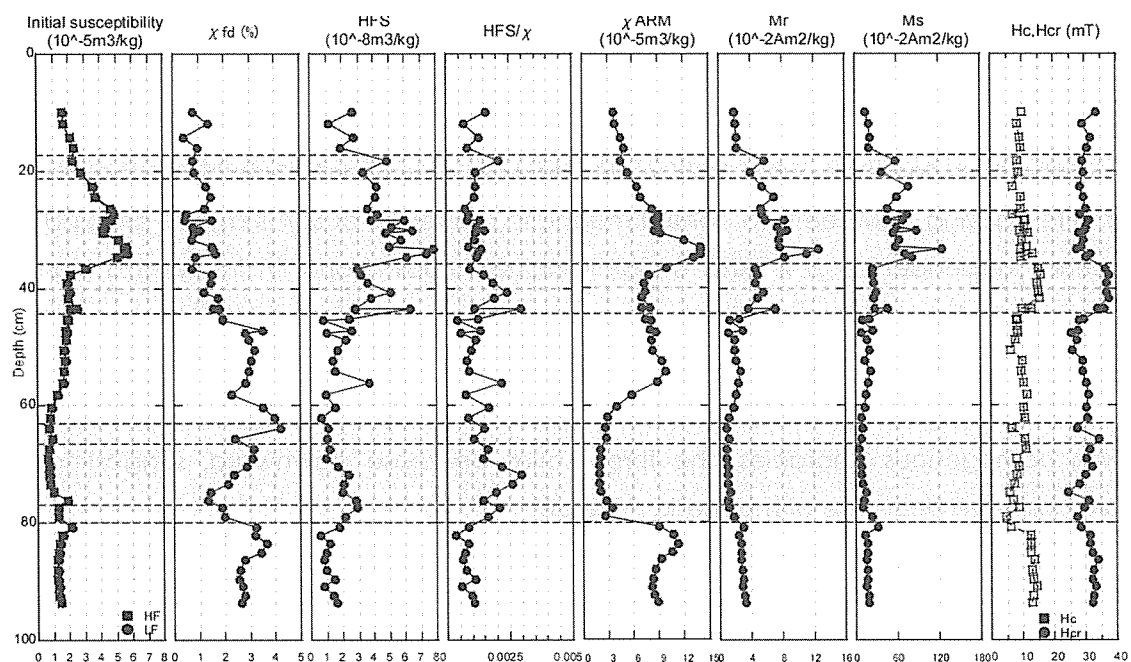


Fig. 1-1. Variations of rock magnetic parameters in the Tsukahara soil profile.

Zones of grey color indicate ash layers. X: initial susceptibility, LF: X of low-frequency measurement, HF: X of high-frequency measurement,  $\chi_{fd}$ : frequency dependency of X, HFS: high-field susceptibility,  $\chi_{ARM}$ : susceptibility of anhysteresis remanence (ARM), Mr: saturation remanence, Ms: saturation magnetization, Hc: coercive force, Hcr: coercivity of remanence.

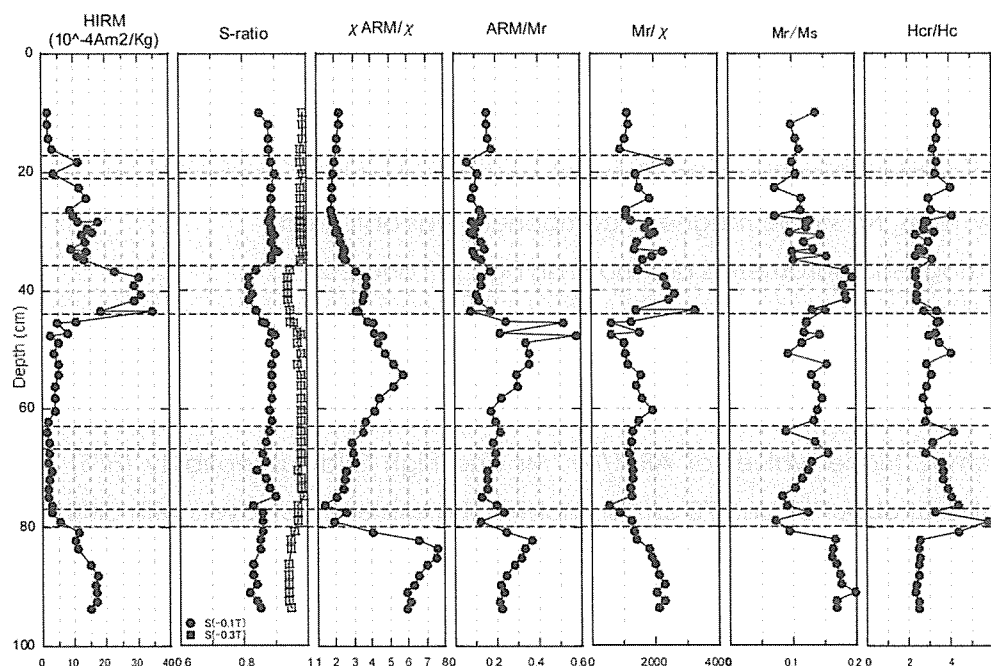


Fig. 1-2. Variations of rock magnetic parameters in the Tsukahara soil profile.

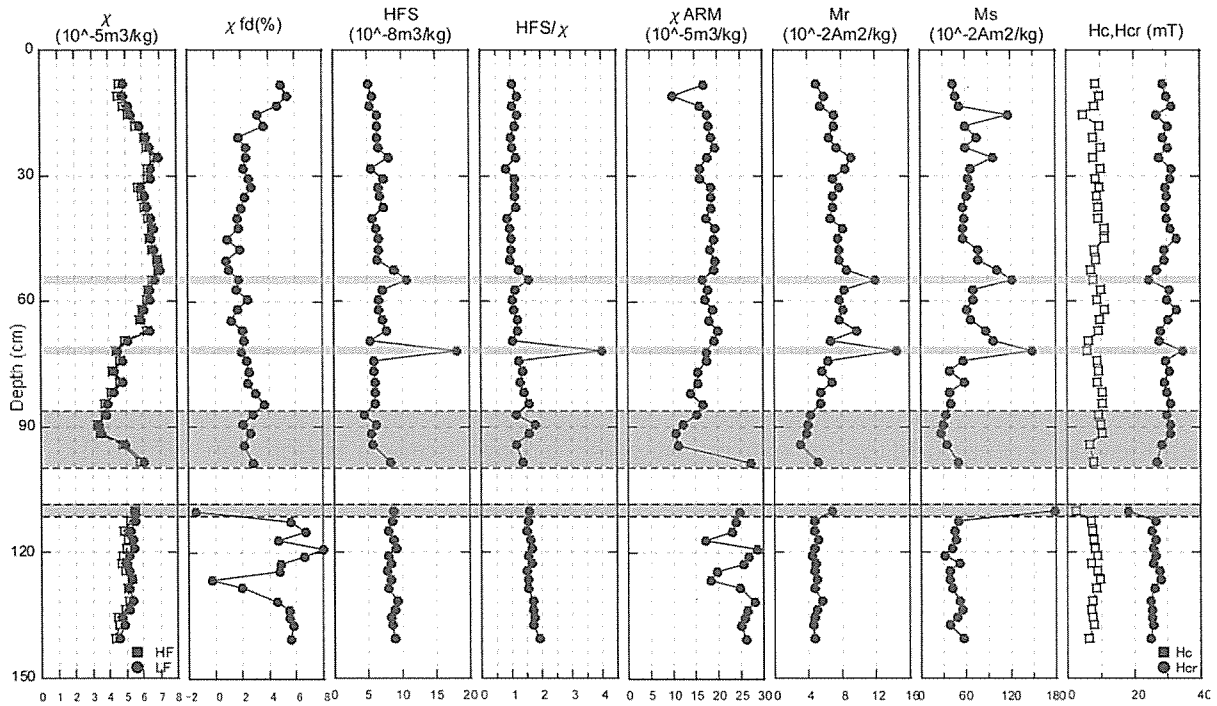


Fig. 2-1. Variations of rock magnetic parameters in the Hlgashiishiamtsu sediment core. Zones of grey and light grey color indicate K-Ah layer and layers with distinctive magnetic properties, respectively. X: initial susceptibility, LF: X of low-frequency measurement, HF: X of high-frequency measurement,  $X_{fd}$ : frequency dependency of X, HFS: high-field susceptibility,  $X_{arm}$ : susceptibility of anhysteresis remanence (ARM),  $M_r$ : saturation remanence,  $M_s$ : saturation magnetization,  $H_c$ : coercive force,  $H_{cr}$ : coercivity of remanence.

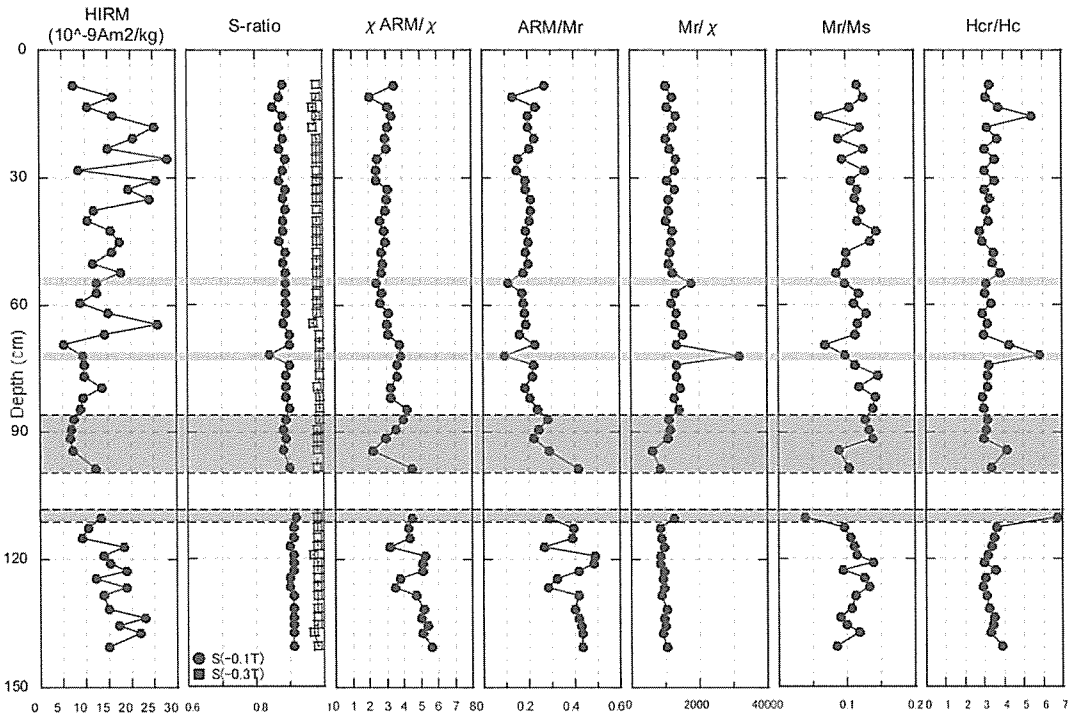


Fig. 2-2. Variations of rock magnetic parameters in the Hlgashiishiamtsu sediment core.

## Isotope Fractionation of Strontium in Solid-Liquid Reactions, I: Isotope Fractionation in $\text{SrCO}_3\text{-Sr}^{2+}$ system

T. Fujii, S. Fukutani (Kyoto Univ.), M. Yoshikawa, T. Shibata

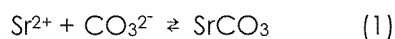
**INTRODUCTION:** Strontium has four naturally occurring isotopes:  $^{84}\text{Sr}$  (isotopic abundance = 0.56%),  $^{86}\text{Sr}$  (9.86%),  $^{87}\text{Sr}$  (7.02%), and  $^{88}\text{Sr}$  (82.56%). These isotopic abundances have natural variations. Isotope fractionations of strontium in chemical exchange reactions have been investigated by various research groups. For example, solvent extraction system using a macrocyclic compound as an extractant gives a large isotope separation factor [1]. The reported distinguishable isotope separation factors suggest that fractionation of Sr isotopes may be detectable even in simple chemical reactions. In this context, we focused on a simple solid-liquid system. Strontium carbonate was selected as the solid phase and a solution containing hydrated  $\text{Sr}^{2+}$  ion was selected as the liquid phase. The isotope fractionation in the precipitation reaction between these two phases was studied.

**EXPERIMENTAL:** 1g of strontium carbonate and 10 mL of 0.05 M sodium carbonate were put in a PP tube. The tube was sealed, and then it was gently shaken at 298K. After a possible aging,  $\text{SrCO}_3$  was precipitated. The precipitant was separated by centrifugation, and the supernatant was filtered by a PTFE membrane (0.20  $\mu\text{m}$  pore size). Sr concentration in the solution was analyzed by ICP-AES. The solid-liquid equilibrium was attained within 3 days. The sample aged 25 days was used for isotopic analysis.

The sample diluted with  $\text{H}_2\text{O}$  was once loaded on a cation-exchange column (DOWEX 50WX8), then it was rinsed by 0.1 M  $\text{HNO}_3$ . Sr was collected in 8 M  $\text{HNO}_3$ . Again, the collected solution was loaded on a column filled with Sr resin (Eichrom), then it was rinsed by 8 M  $\text{HNO}_3$ . Sr was collected in 0.05M  $\text{HNO}_3$ .

Sr in this elution fraction was enriched to be ~70ppm Sr in 1M  $\text{HNO}_3$ . 1  $\mu\text{L}$  aliquot was put onto a rhenium single filament with a tantalum activator. The total amount of Sr loaded on the filament was 70 ng. Similar procedure was performed for our starting material and a Sr standard (SRM-987). Isotopic ratios were determined by multi-collector thermal ionization mass spectrometry (Finnigan, MAT262).

**RESULTS:** The precipitation reaction of  $\text{SrCO}_3$  is written as,



The solubility of  $\text{SrCO}_3$  in  $\text{Na}_2\text{CO}_3$  was shown in Fig. 1. The reported solubility [2] was shown together. It can be seen that our result agree with the reported solubility.

In the present study, we checked the isotopic difference in the equilibrium constant of reaction 1. The isotope fractionation factor  $\alpha_{86,m}$  ( $m=84, 87, \text{ or } 88$ ) is defined as,

$$\alpha_{86,m} = ([^m\text{Sr}]/[^{86}\text{Sr}])_{\text{liquid}} / ([^m\text{Sr}]/[^{86}\text{Sr}])_{\text{solid}} \quad (2)$$

The isotope enrichment factor  $\epsilon_{86,m}$  is defined as,

$$\epsilon_{86,m} = \alpha_{86,m} - 1 \quad (3)$$

$([^m\text{Sr}]/[^{86}\text{Sr}])_{\text{solid}}$  can be substitute as  $[^m\text{Sr}]/[^{86}\text{Sr}]$  of the starting material. The obtained  $\epsilon_{86,m}$ 's are shown in Fig. 2 with  $2\sigma$  analytical errors. Heavier isotopes were preferentially fractionated into the liquid phase. The marine environment is a carbonate system, in which some samples showed Sr isotope fractionations ( $\sim 0.4\text{‰}$  for  $\epsilon_{86,88}$ ). [3] Our results may be correlated with these isotope fractionations.

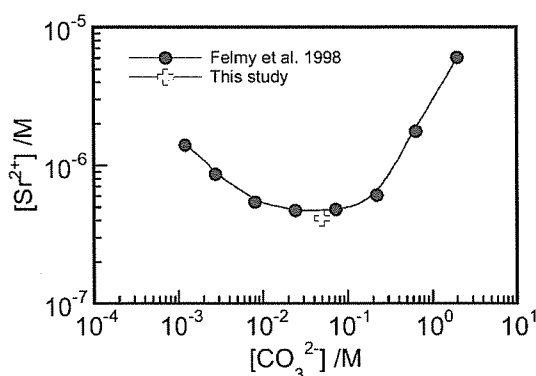


Fig. 1. Solubility of  $\text{SrCO}_3$  in  $\text{Na}_2\text{CO}_3$ .

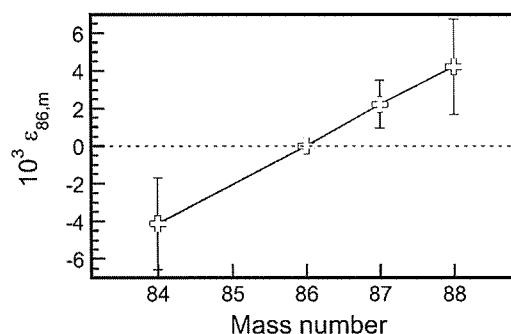


Fig. 2. Isotope enrichment factor.

#### REFERENCES:

- [1] K. Nishizawa *et al.*, J. Nucl. Sci. Technol., **32** (1995) 1230-1235.
- [2] A. R. Felmy *et al.*, J. Chem. Thermodynamics, **30** (1998) 1103-1120.
- [3] J. Fietzke and A. Eisenhauer, Geochem. Geophys. Geosyst., **7** (2006) GC001243.

## Isotope Fractionation of Strontium in Solid-Liquid Reactions, II: *Ab Initio* Calculations of Hydrated $\text{Sr}(\text{II})$ Complexes

T. Fujii, S. Fukutani (Kyoto Univ.), M. Yoshikawa, T. Shibata

**INTRODUCTION:** Strontium 90 ( $^{90}\text{Sr}$ ) is known as one of fission products, and it has a large fission yield. In order to know the chemical behavior of Sr complexes, we study the highly precise isotopic analysis of Sr [1]. The analytical technique will be helpful to understand the fractionation mechanism of Sr isotopes in environmental samples and so on. In parallel with the analytical studies, quantum chemical calculations are performed to check the validity of analytical results. The equilibrium constant of the isotope exchange reaction can be theoretically obtained as the reduced partition function ratio (RPFR) of isotopologs. The RPFR value is usually calculated through harmonic vibration analysis. In this study, we report some *ab initio* calculations of hydrated  $\text{Sr}^{2+}$  complexes.

**COMPUTATIONAL DETAILS:** The orbital geometries and vibrational frequencies of hydrated Sr(II) complexes were calculated by using the conventional Hartree-Fock (HF) approximation and the density functional theory (DFT) as implemented by the Gaussian03 code [2]. The DFT method employed here is a hybrid density functional consisting of Becke's three-parameter non-local hybrid exchange potential (B3) with Lee-Yang-and Parr (LYP) non-local functionals (B3LYP). The 6-31++G\*\* basis set was chosen for H and O, and LanL2DZ was chosen for Sr. The former is an all-electron basis, while the latter is an effective core potential (ECP) basis.

**RESULTS:** The hydrated  $\text{Sr}^{2+}$  species is generally thought to be present as eight-coordinated  $\text{Sr}(\text{H}_2\text{O})_8^{2+}$ . The optimized geometry is shown in Fig. 1, the structure was converged to be the square antiprism with 2.69 Å Sr-O bond length. A structural study on hydrated strontium has been performed by a combination of the extended X-ray absorption fine structure (EXAFS) spectrometry and molecular dynamics (MD).[3] Our result was similar to the reported value, 2.63Å.

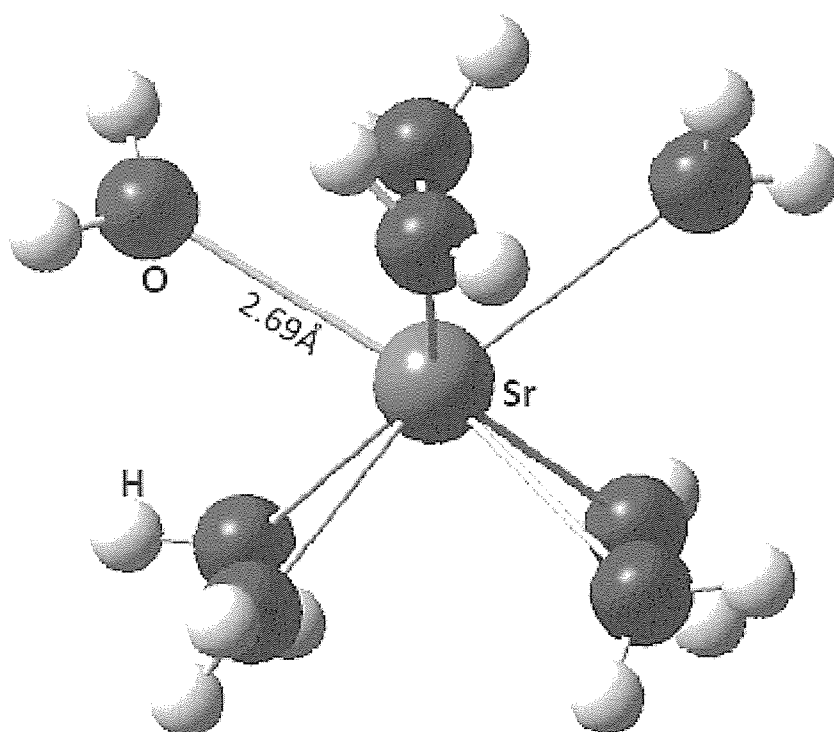


Fig. 1. Equilibrium geometry of  $[\text{Sr}(\text{H}_2\text{O})_8]^{2+}$ .

Then, we examined the hydration enthalpy of  $\text{Sr}(\text{H}_2\text{O})_8^{2+}$ .

$$-\Delta H_{\text{hyd}}^{\circ} = -\Delta E_{\text{b}} + \Delta E_{\text{sol}} + n\Delta H_{\text{vap}} + \Delta nRT - \Delta E(\text{Cp}) \\ -\Delta E_{\text{zp}} + \Delta E_{\text{rel}} + \Delta E_{\text{geom}} \quad (1)$$

In order to relate the calculated quantities to the experimental hydration enthalpy ( $\Delta H_{\text{hyd}}^{\circ}$ ) at 298 K, correction terms were considered in the same way of a report [4]. The  $\Delta H_{\text{hyd}}^{\circ}$  value obtained is shown in Fig.2. The hydration enthalpy of metal cations has been determined by



thermochemical methods and these literature values are shown together for comparison. The  $\Delta H_{\text{hyd}}^{\circ}$  value obtained agreed well with the literature value.

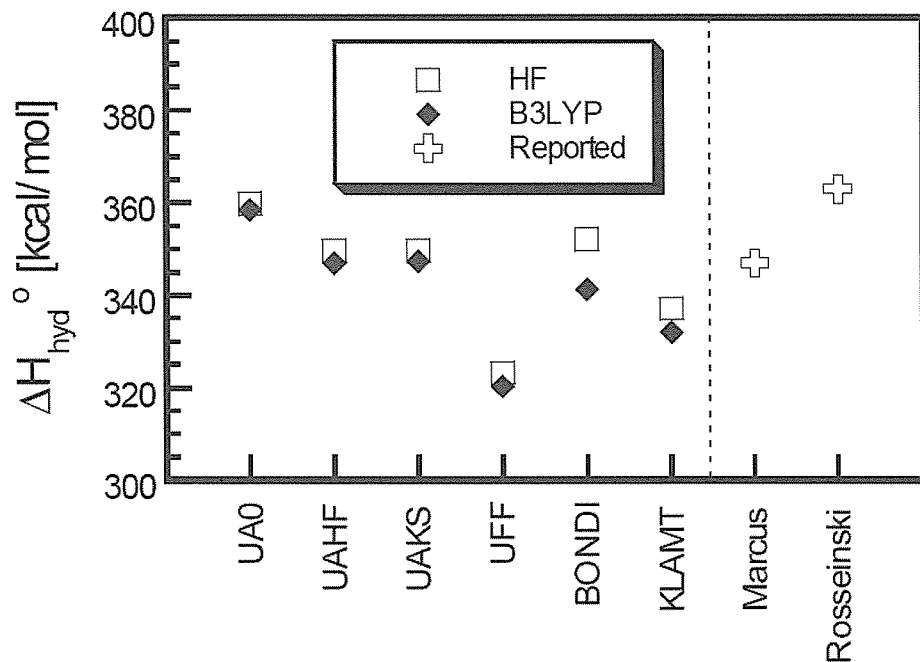


Fig.2 Hydration enthalpy of  $\text{Sr}(\text{H}_2\text{O})_8^{2+}$ .

X-axis showed some molecular cavity calculation codes [2].

The isotope enrichment factor due to this effect can be evaluated from the logarithm of reduced partition function ratio,  $\ln(s/s')f$ . [5] The  $\ln(s/s')f$  values of hydrated  $\text{Sr}(\text{II})$  species were estimated by quantum chemical calculations (Table 1). These values are useful to estimate the degree of isotope fractionation.

Table 1  $\ln(s/s')f$  (‰) of hydrated  $\text{Sr}^{2+}$  species for an isotope pair,  $^{86}\text{Sr}$ - $^{88}\text{Sr}$ .

	HF	B3LYP
$[\text{Sr}(\text{H}_2\text{O})_8]^{2+}$	1.424	1.416
$[\text{Sr}(\text{OH})(\text{H}_2\text{O})_7]^+$	1.540	1.420
$[\text{Sr}(\text{OH})_2(\text{H}_2\text{O})_6]$	1.593	1.508

#### REFERENCES:

- [1] T. Fujii *et al.*, KURRI Prog. Rep. 2007 (2008) 93-93.
- [2] M. J. Frisch *et al.*, Gaussian 03 Revision B.05, Gaussian Inc., Pittsburgh PA, 2003.
- [3] L. X. Dang *et al.*, J. Phys. Chem., 107 (2003) 14119-14123.
- [4] J. Li *et al.*, Inorg. Chem., 35 (1996), 4694-4702
- [5] J. Bigeleisen and M. G. Mayer, J. Chem. Phys., 15 (1947) 261-267.

## Polybaric degassing of H<sub>2</sub>O-saturated island arc basaltic magma recorded in hydrogen content of anorthite-rich plagioclase

*M. Hamada, T. Kawamoto, T. Fujii (Univ Tokyo)*

Anorthite-rich plagioclase (~An<sub>90</sub>) is commonly found in island arc basalt on the volcanic front. Its origin has been discussed as crystallization from H<sub>2</sub>O-rich (H<sub>2</sub>O ≥ 3 wt.%) basaltic magma based on hydrous melting experiments (Sisson and Grove, 1993; Takagi et al., 2005; Hamada and Fujii, 2007). However, melt inclusions hosted by anorthite-rich plagioclase dissolve lower H<sub>2</sub>O (≤ 2 wt.%; Hamada and Fujii, 2007). Hamada and Fujii (2007) explained this contradiction that volatiles might leak from melt inclusions through microcracks in the phenocrysts after entrapment of melt in plagioclase, which suggests that melt inclusions do not always preserve pre-eruptive volatile content of magma. A question remains as to whether island arc basaltic magma on the volcanic front is H<sub>2</sub>O-rich or H<sub>2</sub>O-poor.

Several nominally-anhydrous minerals contain trace amounts of hydrogen in their structure. Recently, hydrogen in nominally-anhydrous minerals is attracting attention as a tool to quantify the dissolved H<sub>2</sub>O in coexisting melt and to monitor the volatile history of magmas (Johnson, 2006). In order to confirm H<sub>2</sub>O content at the time of plagioclase crystallization, we analyzed hydrogen in anorthite-rich plagioclase obtained from the 1986 and 1987 eruptions of Izu-Oshima volcano, using polarized infrared spectra by the procedures of Johnson and Rossman (2003, 2004). Izu-Oshima volcano is located on the volcanic front of Izu arc and issues low-K island arc basalt. The 1986 eruption was the major effusive eruption triggered by injection of new magma, while the 1987 eruption was minor eruption triggered by gas explosion in the conduit.

Plagioclase composition was ranging from An<sub>80</sub> to An<sub>94</sub>. Hydrogen content in plagioclase varied from 40 to 300 ppm H<sub>2</sub>O (Fig.1(a)). Three values of hydrogen contents were found in plagioclase from the 1986 eruption: ~40 ppm H<sub>2</sub>O, 100-180 ppm H<sub>2</sub>O, and 220-300 ppm H<sub>2</sub>O. Assuming partition coefficient of H<sub>2</sub>O between plagioclase and melt is 0.004 (Johnson, 2005), H<sub>2</sub>O contents of coexisting melt correspond to ~1 wt.%, ~3 wt.% and ~6 wt.%, respectively. Hydrogen contents from the 1987 eruption were ranging from 40 to 120 ppm H<sub>2</sub>O.

~3 wt.% H<sub>2</sub>O and ~6 wt.% H<sub>2</sub>O correspond to H<sub>2</sub>O solubility at the estimated depth of magma chambers beneath Izu-Oshima volcano detected by seismic studies: ~4-km deep magma chamber (Ida, 1995) and 8~10-km deep magma chamber (Mikada et al., 1998). Much lower H<sub>2</sub>O content may represent H<sub>2</sub>O solubility at the levels shallower than ~4-km deep magma chamber, i.e. ~1 km deep magma head (Watanabe et al., 1998). Our analytical results suggest that H<sub>2</sub>O content of island arc basaltic magma is higher than analyzed H<sub>2</sub>O content of melt inclusions (≤ 2 wt.%) and that magma is saturated with H<sub>2</sub>O at each level.

Fig.1(b) illustrates our interpretation of analytical results. Plagioclase is assumed to crystallize from H<sub>2</sub>O-saturated melt. Plagioclase in regions A, B and C preserve the equilibrium

hydrogen content at the time of its crystallization. For example, plagioclase in region A moves upward and stagnates at shallower magma chambers, which decreases hydrogen content of plagioclase due to re-equilibration with degassed melt (regions A' and A'' in Fig.1 (b)). The magma erupted in 1986 would have derived from both the ~4 km deep magma chamber and the 8-10 km deep magma chamber without further loss of hydrogen from plagioclase (regions A+A'+B in Fig.1 (b)). In contrast, magma would not have derived directly from the 8~10-km magma chamber in the 1987 eruption inferred from the absence of plagioclase in region A. Plagioclase would have been coexisting with H<sub>2</sub>O-saturated melt at at ~4-km deep magma chamber and shallower levels prior to the 1987 eruption.

We propose the hypothesis that Island arc basaltic magma is H<sub>2</sub>O-rich at depth and undergoes polybaric degassing during ascent. This hypothesis may also explain "excess sulfur degassing" from the island arc volcanoes. This is the issue that the mass of emitted volatiles (especially for sulfur) exceeds the mass of volatiles dissolved in the erupted magma by up to 1 order of magnitude for eruptions of island arc basaltic magmas (Shinohara, 2008). Sulfur is preferentially partitioned into volatile phase, and therefore, the expected volatile degassing at deep may explain "excess sulfur degassing" without large volume of non-erupted magma.

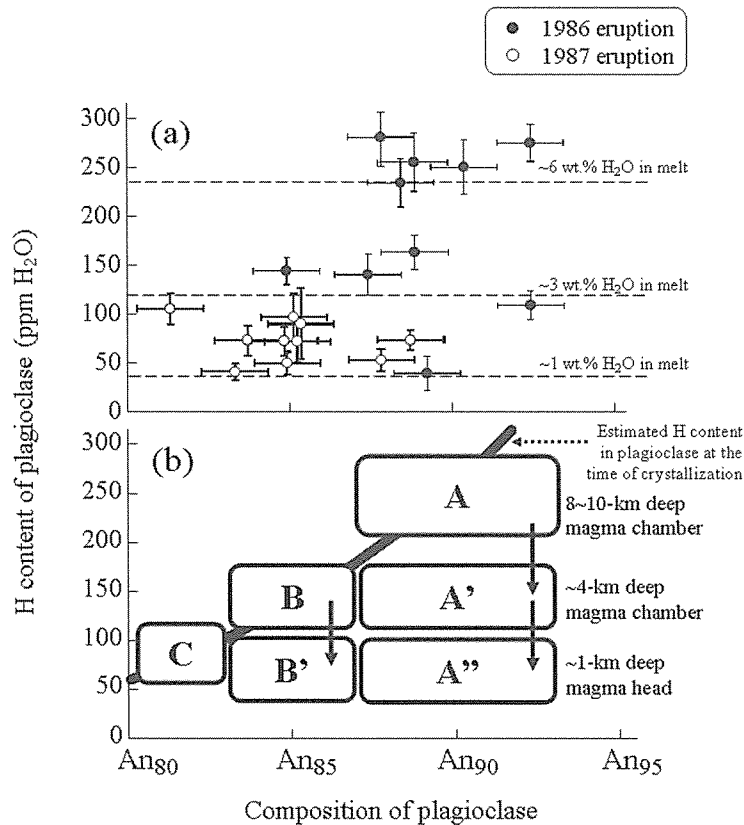


Fig.1 (a) Hydrogen contents of plagioclase phenocrysts from the 1986 and 1987 eruptions. (b) Interpretation of the analytical results shown in (a). The curve is calculated by an empirical formulation of Ca/Na partitioning between plagioclase and melt (Hamada and Fujii, 2007).

## References

- Hamada, M. and Fujii, T. (2007) H<sub>2</sub>O-rich island arc low-K tholeiite magma inferred from Ca-rich plagioclase-melt inclusion equilibria. *Geochem. J.* 41, 437-461.
- Ida, Y. (1995) Magma chamber and eruptive processes at Izu-Oshima volcano, Japan: buoyancy control of magma migration. *J. Volcanol. Geotherm. Res.* 66, 53-67.
- Johnson, E. A. (2005) Magmatic water contents recorded by hydroxyl concentrations in plagioclase phenocrysts from Mount St. Helens, 1980-1981. *Geochim. Cosmochim. Acta* 69, A743.
- Johnson, E. A. and Rossman, G. R. (2003) The concentration and speciation of hydrogen in feldspars using FTIR and <sup>1</sup>H MAS NMR spectroscopy. *Am. Mineral.* 88, 901-911.
- Johnson, E. A. and Rossman, G. R. (2004) A survey of hydrous species and concentrations in igneous feldspars. *Am. Mineral.* 89, 586-600.
- Johnson, E. A. (2006) Water in nominally anhydrous crustal minerals: speciation, concentration, and geologic significance. *Rev. Mineral. Geochem.* 62, 117-154.
- Mikada, H., Watanabe, H., Sakashita, S. (1994) Evidence for subsurface magma bodies beneath Izu-Oshima volcano inferred from a seismic scattering analysis and possible interpretation of the magma plumbing system of the 1986 eruptive activity. *Phys. Earth Planet. Int.* 104, 257-269.
- Saito, G., Uto, K., Kazahaya, K., Shinohara, H., Kawanabe, Y., and Satoh, H. (2005) Petrological characteristics and volatile content of magma from the 2000 eruption of Miyakejima Volcano, Japan. *Bull. Volcano.* 67, 268-280.
- Shinohara, H. (2008) Excess degassing from volcanoes and its role on eruptive and intrusive activity. *Rev. Geophys.* 46, 1-31.
- Sisson, T. W. and Grove, T. L. (1993) Experimental investigations of the role of H<sub>2</sub>O in calc-alkaline differentiation and subduction zone magmatism. *Contrib. Mineral. Petrol.* 113, 143-166.
- Takagi, D., Sato, H. and Nakagawa, M. (2005) Experimental study of a low-alkali tholeiite at 1-5 kbar: optimal condition for the crystallization of high-An plagioclase in hydrous arc tholeiite. *Contrib. Mineral. Petrol.* 149, 527-540.
- Watanabe, H., Okubo, S., Sakashita, S. (1998) Drain-back process of basaltic magma in the summit conduit detected by microgravity observation at Izu-Oshima volcano, Japan. *Geophys. Res. Lett.* 25, 2865-2868.

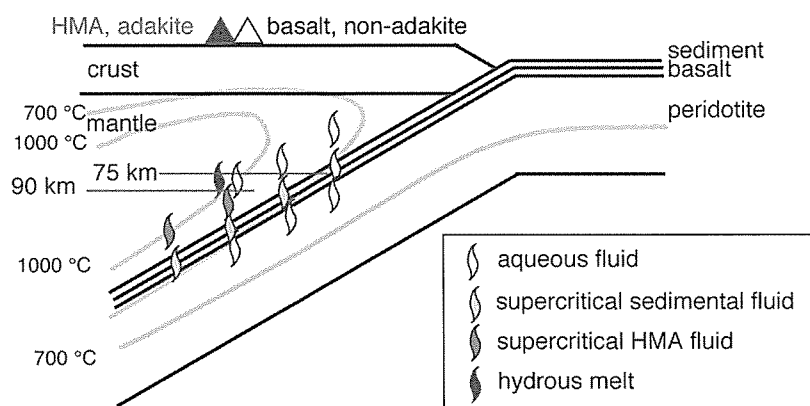


**Supercritical fluids from downgoing slab beneath volcanic arcs: critical endpoints in sediment  
– H<sub>2</sub>O and high Mg andesite – H<sub>2</sub>O systems**

**T. Kawamoto, M. Kanzaki (Misasa), K. Mibe (ERI Univ Tokyo)  
K. N. Matsukage (Ibaraki, now at Ehime Univ), S. Ono (IFREE, JAMSTEC)**

Subduction zone magmatism is triggered by addition of slab-derived component into overlying mantle wedge. Whether this component is aqueous fluids from dehydration or partial melts of subducting oceanic crust remains an open question. Based on our high-pressure and high-temperature radiography experiments at SPring-8 (Mibe et al., 2004, GCA 68, 5189, Mibe et al., 2007, JGR 112, B03201), we suggest surprisingly shallow pressures of critical endpoints between aqueous fluids and high-Mg andesite (2.9 GPa, 87 km depth) or sediment (2.6 GPa, 75 km depth). We also carried out a test using albite with 50 and 64 wt% H<sub>2</sub>O at SPring-8; we see two fluids with 50 % H<sub>2</sub>O at 1.4 GPa while one single fluid with 50 % H<sub>2</sub>O at 1.7 GPa. These indicate the critical endpoint in albite and H<sub>2</sub>O system located between 1.4 and 1.7 GPa, which is consistent with the previous studies (Shen & Keppler 1997 Nature 386, 710, Stalder et al. (2000) Am Miner 85, 68). This simple test guarantees an ability of the present X-ray radiography method to determine the critical endpoints in silicate melts and aqueous fluids within an uncertainty of plus/ minus 10 % relative or 0.15 GPa.

We suggest that slab-derived fluids should be supercritical fluids at the top of subducting slab beneath the volcanic arcs. Under relatively hot conditions, dense liquid-like supercritical fluids are input from dehydrating slab to the overlying mantle wedge (Figure). Such dense supercritical fluids should react with mantle peridotite changing its composition to high Mg andesite. Such a high Mg andesitic supercritical fluids will separate to HMA liquid and fluids when it intersect 90 km deep during its ascent. This separation can produce double magmatism in hot subduction zones: basalt and sanukite or basalt and adakite [Tatsumi & Ishizaka (1982) Lithos 15, 161, Yogodzinski & Kelemen 1998 EPSL. 158, 53]. The sanukite and adakite can be produced by reaction of the melt and mantle, while basalt through fluid-induced partial melting of mantle.



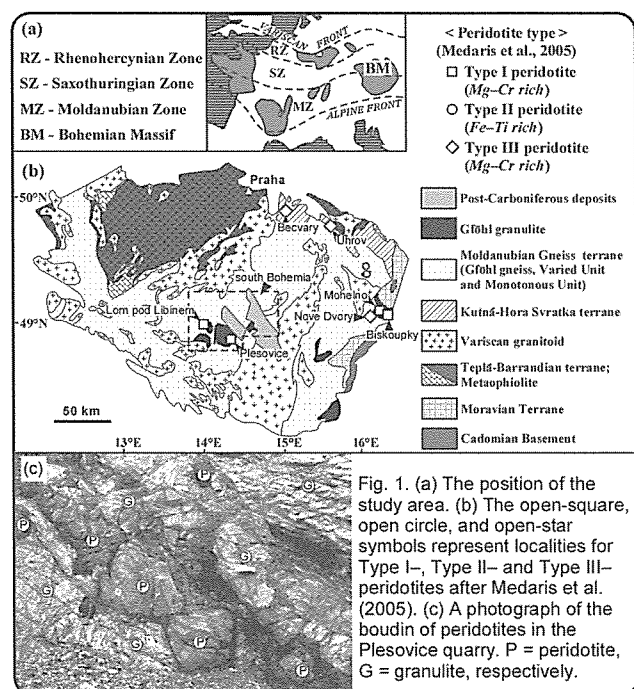
# Major element compositions of Mg–Cr rich garnet-bearing peridotites in the Moldanubian zone of the Bohemian Massif.

K. Naemura (Kyoto Univ.), T. Shibata, T. Hirajima (Kyoto Univ.)

## INTRODUCTION

In the Variscan Orogen, the Gfohl Unit in the Moldanubian zone of the Bohemian Massif appears to be unusual members of high-pressure collisional belts in containing diverse types of orogenic peridotites (Medaris et al., 2005). Study on such orogenic peridotites give insight about the crust–mantle interaction in the root zone of the Variscan orogenic belt. The Gfohl Unit, which occupies the highest structural position of the Moldanubian zone, consists of a lower “Gfohl gneiss unit” of migmatitic, granitic orthogneiss and an overlying “Gfohl granulite unit” of quartzofeldspathic high-pressure granulite, both of which contain bodies of orogenic peridotites (Fig. 1a, b). It has been demonstrated that two contrasting types of Mg–Cr rich peridotite occur in the Gfohl Unit: namely Type I peridotites in the Gfohl granulite (Mohelno, Biskoupky in Fig. 1b) unit and Type III peridotites in the lower Gfohl gneiss unit (Nove Dvory, Uhrov and Becvary) (Medaris et al., 2005). Type I peridotite consists of spinel and garnet peridotites, is devoid of garnet pyroxenite or eclogite layers, has depleted major element and REE compositions, was equilibrated in a very high-pressure condition (up to 1300 °C). On the other hand, Type III peridotite consists of garnet peridotites without chromian spinels, contains garnet pyroxenite and eclogite layers, shows a range of LREE depletion to enrichment, was equilibrated in a very high-pressure condition (up to 5 GPa ~ 160–170 km) (Medaris et al., 2005).

In this study, we analyze the major element composition of Type I peridotites to demonstrate the compositional differences between the Type I peridotites and Type III peridotites. Analyzed samples were collected from the south Bohemian region of the Moldanubian zone (Fig. 1b). Garnet-bearing peridotites have been collected from a locality (Plesovice, Figs. 1b, c) from the Blansky les massif, and a locality near the town of Prahatic (Lom pod Libinem quarry, Fig. 1b) from the Prahatic massif. Occurrences and petrographic characteristics of the investigated Czech peridotites are summarized in the following sections:



## 1. Plešovice peridotite

Peridotite boudins and lenses, measuring about  $1 \times 1$  m to  $5 \times 20$  m, is well exposed in the Plešovice quarry (Fig. 1c) which locates at the eastern end of the Blanský les granulite (Naemura et al., 2008). All of the rocks directly collected from the outcrop contain both spinel and garnet, thus classified as spinel–garnet peridotites. On the other hand, the abundant loose blocks, ranging ca.  $2 \times 2 \times 2$  m, collected from this quarry in 2005 are garnet peridotites which lacks chromian spinels. Both spinel–garnet peridotite and garnet peridotite consist of large (5–20 mm) spheroidal to lobate garnet grains in a fine- to medium-grained, inequigranular polygonal groundmass of olivine, orthopyroxene, clinopyroxene, and minor amount of phlogopite and apatite, with or without spinel (Naemura et al, submitted).

## 2. Lom pod Libidem peridotite

Peridotite boudins and lenses, measuring  $3 \times 10$  m to  $10 \times 30$  m, are enclosed by granulite in a quarry (Medaris et al., 2005). All of the samples collected from this outcrops are characterized by the relatively abundant phlogopite and they contain both garnet and spinel, therefore classified as spinel–garnet peridotite. These peridotites consists of large (ca. 5 mm) spheroidal garnet grains in a relatively fine- to medium-grained, matrix of olivine, orthopyroxene, clinopyroxene, phlogopite and chromian spinel. Frequently spinel grains are found in garnet. Based on this texture, Medaris et al. (2005) proposed that spinel was the earliest aluminous phase in the peridotite in this locality.

## PERIDOTITE CHEMISTRY

21 samples of garnet peridotites were analyzed for major elements by XRF techniques at the Institute for geothermal Sciences, Beppu, Japan. We prepared the powders of rock samples and made glass-beads following the method of Sugimoto et al. (2007). The major elements were determined by use of the WDS type apparatus of X-ray fluorescence (XRF) System3270 (Rigaku, Japan) in the Beppu Geothermal Research Laboratory. Detailed analytical conditions and the preparations for standard are shown in Sugimoto et al. (2007).

Variations for elements in garnet-bearing peridotites are illustrated in Fig. 2, where  $\text{SiO}_2$ ,  $\text{TiO}_2$ ,  $\text{Al}_2\text{O}_3$ ,  $\text{Fe}_2\text{O}_3$ ,  $\text{CaO}$ ,  $\text{Na}_2\text{O}$ ,  $\text{K}_2\text{O}$  and  $\text{P}_2\text{O}_5$ , are plotted against  $\text{MgO}$ . The compositions of Type I peridotites and Type III peridotites from the literature (Medaris et al., 2005) and the variation trend for the well documented Ronda massif (Frey et al., 1985), are included for comparison.

Czech Type I peridotites (represented as boxes in Fig. 2), including our data, show decreases in  $\text{SiO}_2$ ,  $\text{TiO}_2$ ,  $\text{Al}_2\text{O}_3$ ,  $\text{CaO}$ ,  $\text{Na}_2\text{O}$  with an increase in  $\text{MgO}$  (Fig. 2a–h). Such negative correlations are comparable to those for the Ronda massif. Among the Czech type I peridotites analyzed so far, spinel–garnet peridotites in the Plešovice show the highest  $\text{MgO}$  contents.

There are significant scatter in the data of Type III peridotites (cf.  $\text{TiO}_2$  in Fig. 2b). Although variation trends for Type III peridotites are similar to those for Type I peridotites, there are systematic differences: higher  $\text{SiO}_2$ ,  $\text{TiO}_2$ ,  $\text{Fe}_2\text{O}_3$  contents (Figs. 2a, b, d) and lower  $\text{CaO}$ ,  $\text{Na}_2\text{O}$  contents (Figs. 2e, f) than those of Type I peridotites for a given  $\text{MgO}$  value. The variation trends for Type III peridotites are also slightly deviate from those for the Ronda massif. Both  $\text{K}_2\text{O}$  and  $\text{P}_2\text{O}_5$  do not show a clear trend (Figs. 2g, h). Among Czech peridotites, Type I peridotites analyzed in this study show higher  $\text{K}_2\text{O}$  contents (Fig. 2g). This is consistent with the existences of phlogopites in these peridotites. In Fig. 2h, it is shown that Czech peridotites generally contain significant amount of  $\text{P}_2\text{O}_5$ . This was supported by the existences of apatites

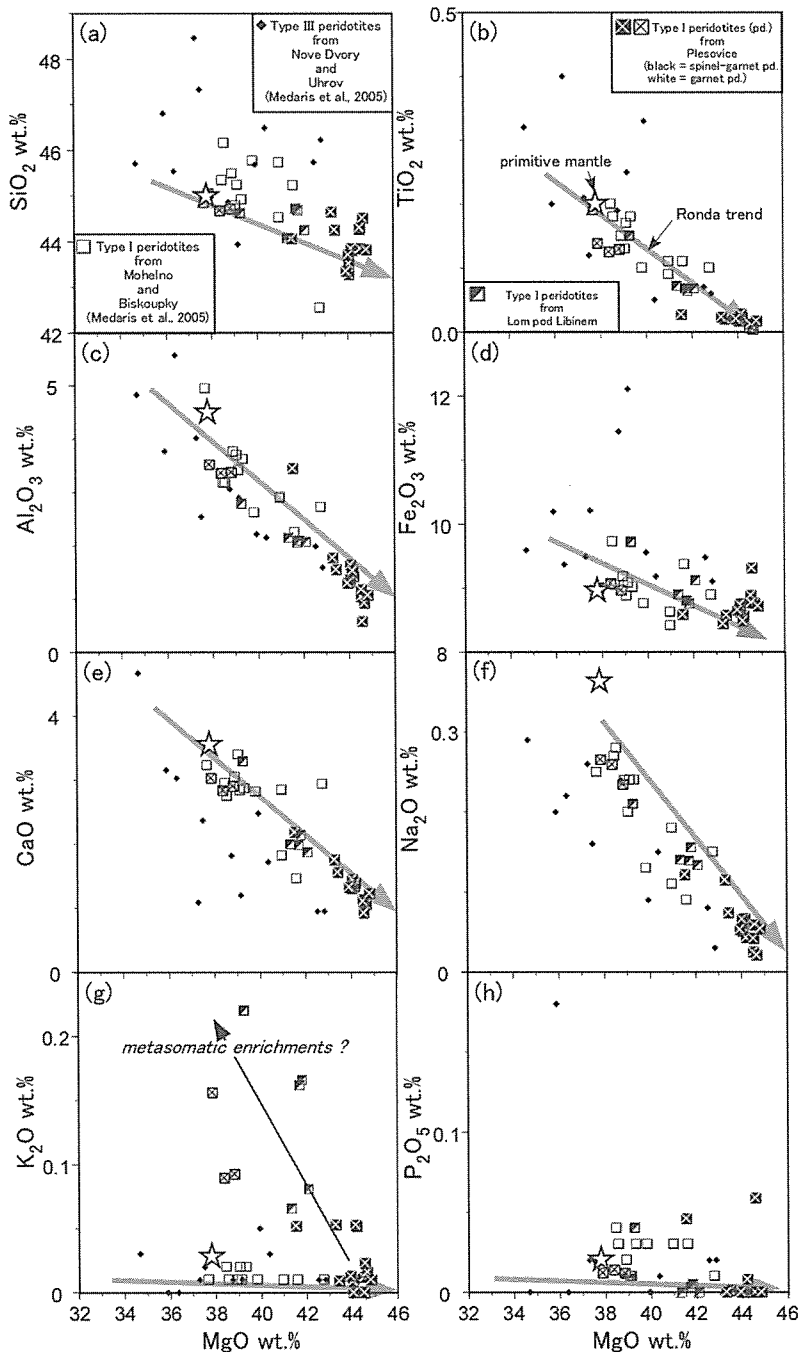


Fig. 2. Oxide variation diagrams for Czech peridotites in the Gfohl Unit. The composition of primitive mantle source (☆) (McDonough & Sun, 1995) and the Ronda variation trend (→) (Frey et al., 1985) are shown for comparison.

in Type I peridotites from the Plesovice peridotites (e.g., Naemura et al., 2008).

We also analyze the trace amount of Cr and Ni in both peridotites and granulites by use of XRF techniques. The variations of these elements are shown in Fig. 3. Cr in the Czech peridotites shows a significant scatter. Particularly, the spinel-garnet peridotites from the Plesovice show the wide range of Cr (ca. 1800–4500 ppm). Ni and  $\text{MgO}$  in the Czech peridotites show a positive correlation that is consistent with the Ronda trend.

#### THE ORIGIN OF THE COMPOSITIONAL TREND — PARTIAL MELTING or METASOMATISM?

Medaris et al. (2005) have shown that there are systematic differences



between the major element compositions of Type I and Type III peridotites. Based on the existences of abundant veins and layers of pyroxenites and eclogites in Type III peridotites, Medaris et al. (2005) suggested that such differences probably reflect the modifications of Type III peridotites by the percolation of mafic melts. On the other hand, major element compositions of Type I peridotites are typically plot on the "Ronda variation trend", which is considered to be formed by the partial melting of the pyrolite-like mantle source (Frey et al., 1985). However, the higher K<sub>2</sub>O and P<sub>2</sub>O<sub>5</sub> contents in the Type I peridotites (Figs. 2g, h) can not be explained by this partial melting model. These elements were probably added to the peridotites from the external sources. Patricularly, K<sub>2</sub>O and MgO for the Plesovice and Lom pod Libinem peridotites show a negative correlation (black arrow in Fig. 2g). This may suggest that the observed trend for these peridotites may partly caused by the metasomatic enrichments. To understand the nature of such metasomatisms, trace-elements- and REE-analyses of these peridotites will be useful.

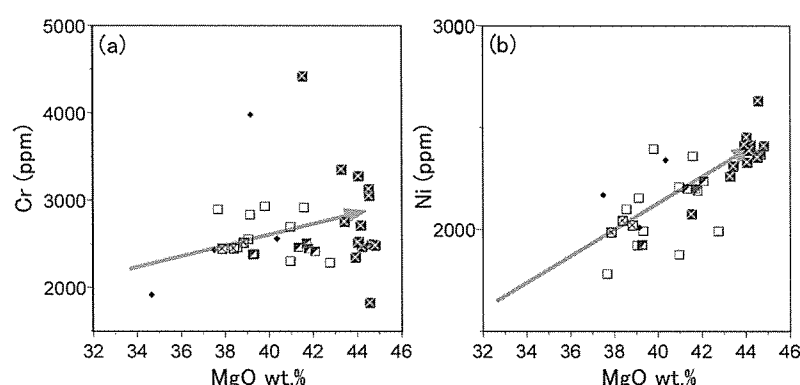


Fig. 3. Variation diagrams for Cr and Ni in Czech peridotites from the Gfohl Unit.

## REFERENCES

- Medaris Jr., L.G., Wang, H.H., Jelinek, E., Mihaljevic, M. & Jakes, P. (2005) Characteristics and origins of diverse Variscan peridotites in the Gföhl Nappe, Bohemian massif, Czech Republic. *Lithos* **82**, 1-23.
- Naemura, K., Yokoyama, K. & Hirajima, T. (2008) Age determination of thorianite in phlogopite-bearing spinel-garnet peridotite in the Gfohl Unit, Moldanubian zone of the Bohemian Massif. *Journal of Mineralogical and Petrological Sciences* **103**, 285–290.
- Sugimoto, T., Shibata, T. & Yoshikawa, M., XRF analyses of major elements of silicate rocks including ultrabasic rocks and carbonate rocks by a single calibration line method (submitted).
- Frey, F.A., Suen, C.J. & Stockman, H.W. (1985) The Ronda high temperature peridotite: Geochemistry and petrogenesis. *Geochimica et Cosmochimica Acta* **49**, 2469-2491.
- McDonough, W.F. & Sun, S.-s. (1995). The composition of the Earth. *Chemical geology* **120**, 223-253.

**Interactions between hydrothermal circulation and magmatic activity beneath a spreading centre, example of the Oman ophiolite.**

**M. Python, T. Shibata S. Arai (Kanazawa University)**

Dykes are omnipresent features in the mantle section of the Oman ophiolite. They usually are considered as the residue of melt circulation within the mantle. Nevertheless all the dykes present in the Oman mantle are not of magmatic origin and about 2% of them show petrological characteristics (textures, mineralogy, chemistry, etc.) that may be explained in the frame of a high-*T* hydrothermal circulation within the mantle. These hydrothermal dykes are composed mainly of pure diopside ( $Mg\# > 0.95$ ) highly depleted in Fe, Al, Cr, Ti and all other incompatible elements, we called them "diopsidite" dykes. We interpreted them as the result of very high-*T* hydrothermal activity in the upper mantle (see Python et al., 2007a, b).

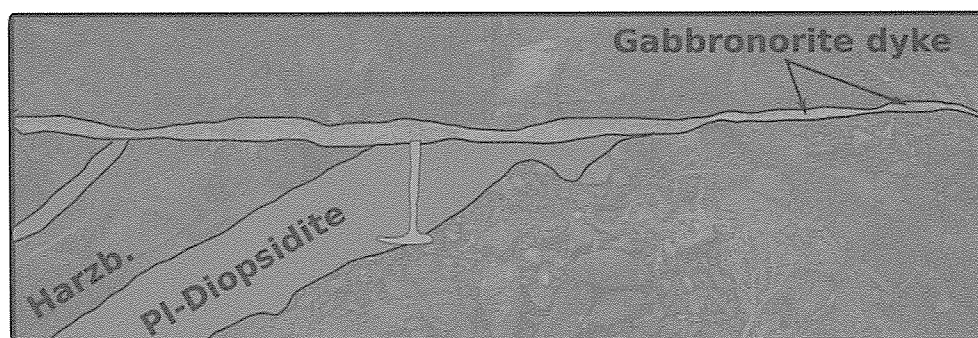


Fig. 1: Field view of a magmatic dyke (gabbronorite) crosscutting a diopsidite dyke

In the field, some diopsidite dykes are crosscut by magmatic dykes, showing that these two features formed more or less contemporaneously and may have interact to some extent (see Fig. 1). At the contact with a diopsidite dyke, a few millimetres to few tens of centimetre wide reaction zone exists, where the chemistry of the primary minerals in harzburgites or magmatic dykes is modified. Chromian spinels, olivines and plagioclases showing respectively exceptionally high Cr# (up to 0.85), forsterite (to 0.98) and anorthite (to 0.99) contents. The process leading to the genesis of the diopsidites affect a region larger than the dyke itself, and the reaction zone between the diopsidite and the magmatic dyke is the result of the close interaction between hydrothermal circulation and magmatic activity within the mantle. We analysed one diopsidite dyke crosscut by a gabbronorite dyke and the lithologies within the resulting reaction zone between these two features. the reaction zone is composed of fine grained diopsides and anorthites which chemical composition is intermediate between the composition of the magmatic dyke and that of the diopsidite. Hydrous phases are very scarce and represented by amphiboles in equilibrium with highly calcic plagioclase ( $An\% > 98\%$ ).

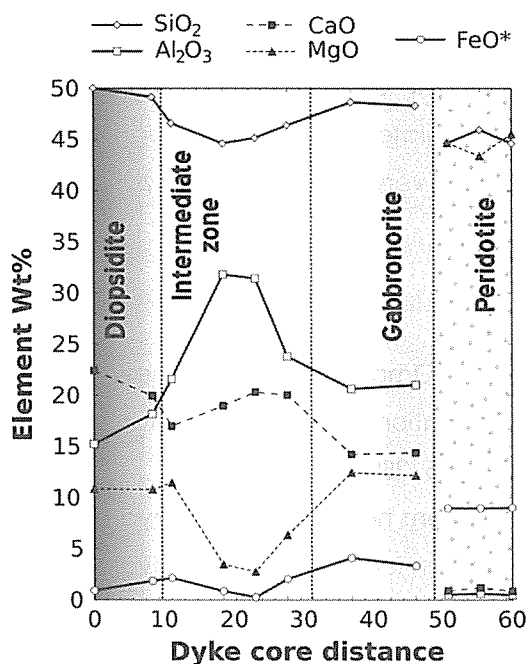


Fig. 3: Profile showing the evolution of the major element chemistry from the diopsidite to the gabbronorite through the reaction zone

The diopsidite dykes themselves present large chemical heterogeneities, which probably result from their metamorphic origin. On the other hand, when not included in the reaction zone, their host rocks are relatively homogeneous. The diopsidite is globally richer in Ca and Si than the gabbronorite and poorer in Al (see Figs. 2 and 3). The intermediate zone between the two type of dykes is comparatively poor in Si and rich in Al, but a chemical evolution between a Si-poor and Al-rich endmember and the "diopsidite" endmember is visible (Figs. 2 and 3). The intermediate zone show impoverishment in Si and enrichment in Al that could be the consequence of the variations (accumulation for Si and evacuation for Al) of these elements in the diopsidite compared to the gabbronorite.

The intermediate zone is strongly depleted in Mg and Fe and enriched in Ca (Fig. 3), suggesting that the hydrothermal fluid responsible of the genesis of the diopsidite was Ca saturated and poor in Fe and Mg. Fe and Mg follow identical spacial variations, which are opposite to that of Ca (Fig. 3). The effect of the the fluid, thus the water/rock ratio was probably the higher close to the centre of the intermediate zone (Fig. 3).

Out of the active magmatic zones (absence of any mafic dyke), an intermediate zone between the mantle and diopsidite dyke exists. In this case, the mineralogical and chemical composition of this reaction zone is quite different: rich in hydrous minerals (antigorite, tremolite), it is devoid of Al and very rich in Mg. the mantle probably reacted with a Ca-rich hydrous fluid leading to the formation of antigorite and tremolite. The lack of Al as well as the richness in Mg of the environnement may explain the chemical differences between the reactions zones close or far from a magmatic dyke.

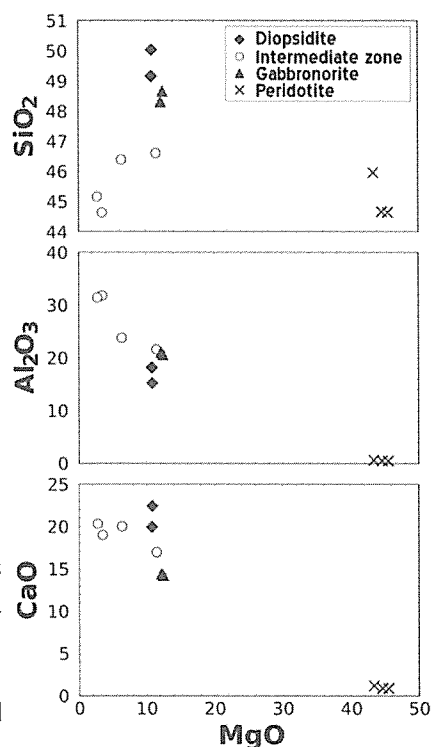
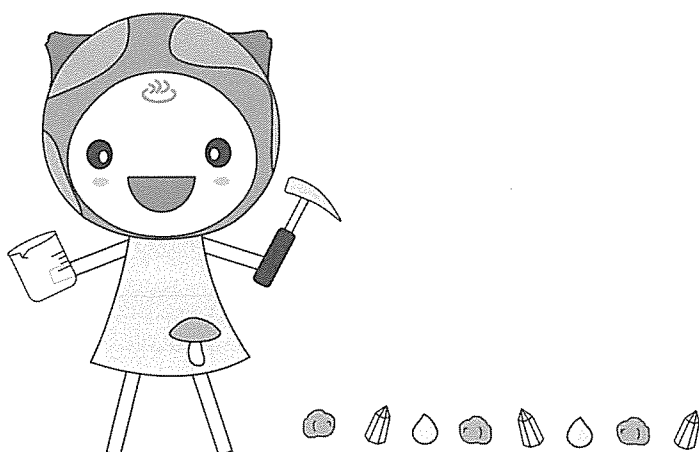


Fig. 2: Whole rock major elements composition of the various lithologies implicated in the diopsidite genesis and its reaction with the surrounding rocks

In an active magmatic zone (in the presence of a gabbro-norite dyke), the hydrothermal fluid reacted with the magma at very high-T, leading to the formation of the observed assemblage of diopside and anorthite with low amount of amphibole. The chemical composition of the minerals in the reaction zone is intermediate between the magmatic and the hydrothermal compositions, showing that there is a very narrow mixing zone where hydrothermal and magmatic processes interacted.

#### References:

- Python, M., Ceuleneer, G., Ishida, Y., Barrat, J.-A. & Arai, S. Oman diopsidites: a new lithology diagnostic of very high temperature hydrothermal circulation in mantle peridotite below oceanic spreading centres Earth Planet. Sci. Lett., 2007a, 255, 289-305
- Python, M., Ishida, Y., Ceuleneer, G. & Arai, S. Trace element heterogeneity in hydrothermal diopside: evidence for Ti depletion and Sr-Eu-LREE enrichment during hydrothermal metamorphism of mantle harzburgite J. Mineral. Petrol. Sci., 2007b, 102, 143-149



*Chīnetsu☆chan*

# **Sr-Nd isotopic ratios of Wakurayama dacite as adakite from the Matsue city, inner zone of Southwest Japan Arc**

**D. Sato (Shimane Univ.), T. Shibata, A. Kamei, I. Matsumoto (Shimane Univ.)**

## **INTRODUCTION**

Sr-Nd isotopic ratios of Wakurayama dacite as adakite, Matsue city, Southwest Japan have been examined. The activity of Wakurayama dacite is about 5 Ma ago [1, 2]. We made clear that this dacite is adakite [3]. In this study, petrological details of Wakurayama dacite became clear. We classified this dacite by the color of the surface of the rock and texture under the microscope. And Sr-Nd ratios and bulk chemical compositions of rocks were determined.

## **RESULTS AND DISCUSSIONS**

Wakurayama dacite is basically divided into three groups which are Gray, Olive and Red groups by their color. Those groups can be also distinguished compared with the amount of the minerals, with bulk rock chemical compositions and with Sr-Nd isotopic ratios. These groups having flowed in order of Gray group, Olive group and Red group became clear by their stratigraphy. In addition, the important geochemical feature is that tholeiitic rock series and calc-alkaline rock series are coexistent in one volcano. That is Gray group (FeO\*/MgO ratio: 2.55 in average), Olive group (FeO\*/MgO ratio: 6.42 in average) and Red group (FeO\*/MgO ratio: 2.51 in average) are tholeiite, calc-alkaline and tholeiitic rock series respectively. And almost all rocks of Wakurayama dacite as adakite show high in Al (18.96 wt% in average), low in Mg (1.36 wt% in average), high in Sr (636 ppm in average) and low in Y (10 ppm in average). Above chemical features of wakurayama dacite is very similar with adakites [4]. That is Wakurayama dacite magma may derived from the subducted materials like oceanic sediment.

## **References**

- [1] Miyajima et al. (1972): Mem. Fac. Lit. & Sci., Shimane Univ., Nat. Sci., 5, 131-140.
- [2] Kano et al. (1993): Geology of Matsue district. Geol. Soc. Jpn, p126.
- [3] Sato and Matsumoto (2008): GCA, Abstract Vol. 199 A824.
- [4] Defant and Drummond (1990): Nature, 662-665

(submitted to 2009 Goldschmidt Conference)

## The lateral variations of Sr, Nd and Pb isotopic and trace element compositions for Quaternary volcanics from Kyushu, Japan

*T. Shibata, T. Kobayashi (Kagoshima Univ.), T. Sugimoto, O. Ujike (Toyama Univ.)  
J. Itoh (AIST), K. Takemura*

The Quaternary volcanoes are widely distributed in Kyushu Island, Japan. Philippine Sea plate is subducting beneath Kyushu. Clear distribution of deep seismic foci is observed below the Quaternary volcanoes in southern area, but not in northern area. Thus, no contribution of subducting slab to the magma source, or volcanic activity similar to the within-plate type volcanism have been emphasized for the magma genesis of this area [e.g. 1,2]. However, volcanic rocks with island arc type chemistry are reported from some Quaternary volcanoes from north Kyushu [e.g. 3,4] so that the magma genesis is still controversial. Therefore, we studied lateral variations of Sr, Nd and Pb isotopic and trace element compositions for Quaternary volcanics from Kyushu to investigate the magma genesis. From the results, a clear variation of Sr/Y ratio, decreasing from north to south, is observed along the volcanic front. Some of the Sr/Y ratio of the most northern part of Kyushu shows the value  $>100$ . The all analyzed Pb isotope compositions show a single linear trend in  $^{208}\text{Pb}/^{204}\text{Pb}$  v.s.  $^{206}\text{Pb}/^{204}\text{Pb}$  diagram. The linear trend of Pb isotope ratios is situated between the ranges of mid ocean ridge basalt, shikoku basin basalt and tereginious sediment which might be a constituent of the subducting slab. The similar relationships are found in Sr and Nd isotopic systematics. The isotopic characteristics of the Quaternary magma in Kyushu can be explained by the magma generation process of island arc, in spite of the lack of deep seismic foci. It is considered that high and low Sr/Y ratios suggest the contributions of partial melt and aqueous fluid derived from subducting slab, respectively [e.g. 5]. If this is the case, high Sr/Y ratio observed from northern part of Kyushu indicates that the subducting slab is partially molten in the area.

### References

- [1] Notus et al, JVGR, 181 (1990)
- [2] Kita et al, JVGR, 99 (2001)
- [3] Otha et al, GANKO, 1 (1990)
- [4] Itoh, GANKO, 541 (1990).
- [5] Defant and Drummond, Nature, 662 (1990).

## Temporal variations of geochemical characteristics of volcanic rocks from north of Kofu Basin, central Japan, and the role of Philippine Sea Plate

*T. Shibata, M. Yoshikawa, S. Koshimizu (YIES)*

Slab derived materials are believed to be added to the mantle wedge from subducting oceanic crust in subduction zone. It is considered that the mechanism is dehydration or partial melting of subducting slab. However, the detail of mechanism is still controversial (Nakamura et. al., 2006, *Nature Geoscience*, Seghedi et al., 2006, *Lithos*). To make these clear, it is generally recognized that spatial and/or temporal variations of geochemistry of the subduction zone magmas are useful.

The Pacific plate (PAP) and Philippine Sea plate (PSP) is subducting beneath Chubu District in Japan. The subduction of PSP started from 15 Ma. After an inactive duration, subduction of PSP restarted from 6 Ma, and the direction of the subduction has been changed for NNW to WEW at 1.5 Ma (Kamata, 1999). In this area, volcanic activity has been occurred from Neogene to Quaternary. Therefore, it is expected that temporal geochemical variations of magmas related to the changes of PSP subduction are observed from lavas of this area. We collected the samples from the lavas and dykes of the Traga-thoge, Mizugamori, Kengamine, Kurofujii volcanoes, and analyzed major element, trace element and Sr – Nd – Pb isotopic compositions.

In the silica-alkali diagram, data are plotted on the boundary of tholeiite and high alumina basalt rock series. The patterns of trace elements show typical characteristics of island arc magma such as enrichment of LILE and depletion of HFSE. It can be considered that the mantle wedge beneath this area is MORB type mantel, because  $\text{TiO}_2$  is  $< 0.9$  wt% and the Zr/Nb ratio is nearly constant ( $\text{Zr/Nb} = 25 - 35$ ), and similar to the ratio of MORB. It is observed that the Sr/Y ratios of Neogene volcanics are lower compared with those of Quaternary volcanics. This suggest that the mechanism of slab material addition to the mantel wedge has changed from slab dehydration (Neogene) to slab melting (Quaternary). From the model calculation using Sr-Nd-Pb isotopic compositions, it can be suggested that 1) the mantel wedge was already metasomatised by PSP derived materials at Neogene, 2) the fluid derived from PAP has induced the Neogene magma generation, and 3) Quaternary magams can be produced by partial melt of PSP. From these, we can conclude that the leading edge of PSP away from, but close to below the volcanic center at Neogene, and PSP has reached below the volcanic center at Quaternary.

## **Development of observation techniques for inaccessible and extremely acidic crater lakes: Installation of temperature telemetry buoys, dredging of lake sediments, and sampling of lake waters**

**A. Terada, S. Yoshikawa**

We describe direct observation techniques for inaccessible and extremely acidic crater lakes surrounded by steep crater walls. Observation equipment and an attached weight suspended beneath a pulley are lowered to the lake surface or lake bottom under gravity along a rope stretched between opposite sides of the crater rim. The weight is tied to the observation equipment using paper string that dissolves in the lake water. This enables the rapid descent of the system from the top of the crater rim to the lake, the automatic deployment of the weight from the observation equipment once the system reaches the lake, and the simple manual retrieval of the system from the lake to the crater rim following the completion of observations.

Using the above technique, we deployed two temperature telemetry buoys, including wireless thermometers, upon the crater lake of Aso volcano, Japan, to monitor water temperature. We manually ran a 400 m polypropylene rope (8 mm diameter) between opposite sides of the crater rim. The strength of the rope was sufficient to lower 3–5 kg of equipment to the lake surface. The protective buoy housing the wireless thermometer is made of expanded polystyrene (EPS), enabling it to float on the lake surface. The buoy has a 1-mm-thick coating of polyurethane resin to prevent UV damage. The buoys were fixed at the lake bottom using anchors and 18 m fluororesin ropes initially tied to the system using paper string, enabling the system to readily descend to the lake surface along the stretching rope. The paper strings dissolved several minutes after the equipment had landed on the lake surface, at which point the anchor descended to the lake bottom.

To obtain samples of lake sediments, we developed a mud sampler that consists of a stainless steel frame covered by a polyester mesh net. A doughnut-shaped fluororesin block, designed to prevent chemical contamination of the dredged sample, was used as a weight inside the net. The mud sampler and an attached weight suspended beneath two pulleys were lowered to the lake bottom under gravity along the polypropylene rope. The attached weight was tied to the sampler using paper string. We also obtained a sample of lake water using a polypropylene bottle with a weight tied beneath the bottle using paper string.

These techniques are expected to contribute to the monitoring of active crater lakes and the underlying hydrothermal system.

(Bull. Geotherm. Soc. Japan, in press)



# Geothermal activity within the western slope geothermal zone of Aso volcano, Japan: Development of a new geothermal field in 2006

A. Terada, Y. Sudo (Aso Volcano Museum)

Unusual geothermal activities occurred at Yoshioka hot spring, Aso volcano, from November 2005. Prior to this date, the area was a minor geothermal field, emitting only 0.2 MW of hot water. Steam flux increased significantly to 15–30 MW in October 2006, accompanied by small explosions. After November 2006, the new fumarole maintained a largely constant heat-discharge rate of approximately 4.6 MW, almost 10 times higher than that of existing natural fumaroles within the WSGZ (0.5 MW). The total heat-discharge rate at Yoshioka is 5.2 MW, equivalent to half of the total amount of the WSGZ. Hence, we consider that the geothermal events at Yoshioka differ from typical hydrothermal eruptions. We infer that the geothermal events at Yoshioka in 2006 resulted from an increase in volcanic fluid flux from a deep aquifer to the steam-dominated reservoir beneath Yoshioka, resulting in the formation of a new geothermal field.

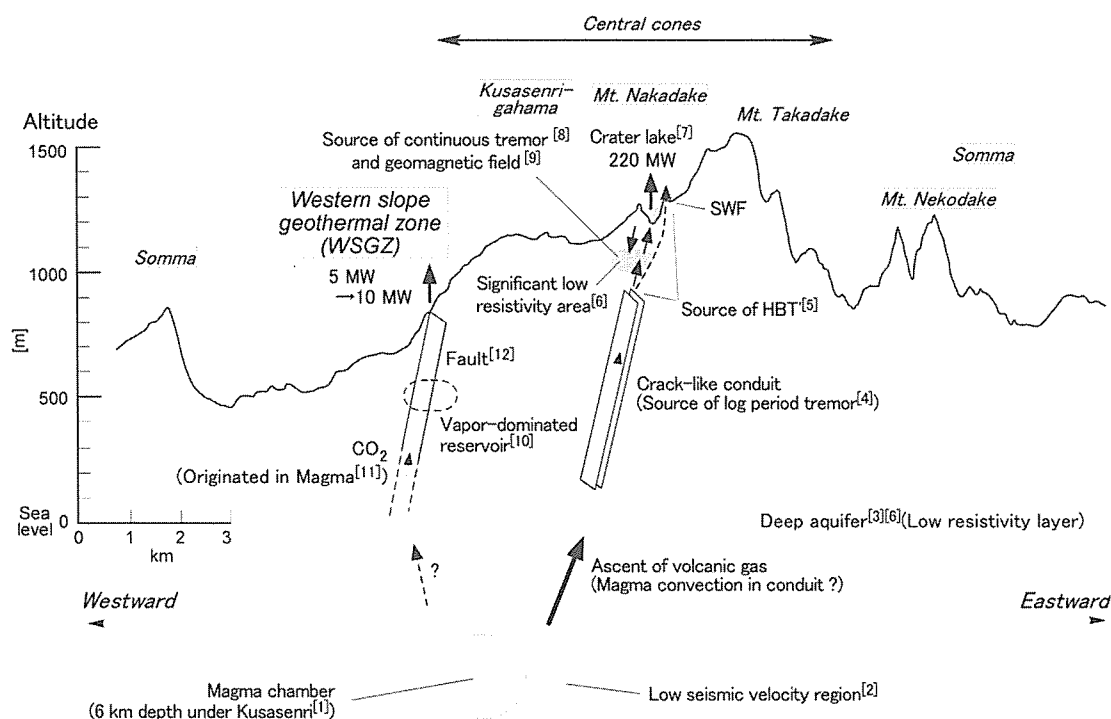


Fig. Heat-flow model of Aso volcano based on the results of geophysical and geochemical studies. SWF: fumaroles within the south wall of the Nakadake 1st Crater. HBT: isolated hybrid volcanic tremor (Mori *et al.*, 2008). Superscript numbers refer to the following references: [1] Sudo *et al.* (2006); [2] Sudo and Kong (2001); [3] Hase *et al.* (2005); [4] Yamamoto *et al.* (1999); [5] Mori *et al.* (2008); [6] Kanda *et al.* (2008); [7] Terada *et al.* (2008); [8] Takagi *et al.* (2006); [9] Tanaka (1993); [10] Parmentier and Hayashi (1981); [11] Yamada (2005); and [12] Yamasaki *et al.* (1978).

(Geothermics, submitted)

## Quantitative Evaluation of Geothermal Activities at the Central Cones of Aso Volcano, Japan

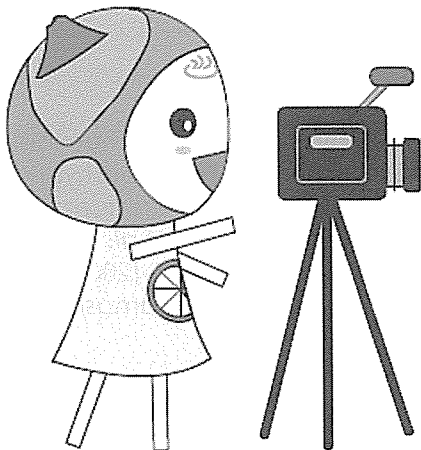
A. Terada, T. Kagiya, S. Yoshikawa

For quantitative evaluations of geothermal activities of Aso volcano, Japan, an aerial infrared survey is carried out on early morning by use of a helicopter. At Nakadake, one of the central cones of Aso volcano, aerial infrared photographs reveal that no temperature anomalies exist out of the 1st Crater of Nakadake. The total heat-discharge rate from Aso volcano is estimated to be 120 – 200 MW in the calm period. The most of heat is discharged from hot crater lake of the Nakadake 1st Crater. Heat-discharge rate from the West-flank Geothermal Field (WFGF) is estimated to be 9.9 MW. The Yoshioka Hot Spring (one of the WFGF) that notable geothermal events occurred in 2006 discharges over 5 MW of heats corresponding to the half of the heat-discharges from the WFGF.

**Table. Results of heat-discharge rates (MW) through fumaroles, steaming grounds, ponds or lakes and hot springs of Aso volcano.**

	Fumaroles	Steaming grounds	Ponds or lakes	Hot springs	
1st Crater					
Yudamari	-	-	110 - 220 <sup>(b)</sup>	-	
"S"	<100 <sup>(a)</sup>	2.0<	-	-	
"SE"	-	0.64	-	-	
"SW-1"	-	0.27	-	-	
"SW-2"	-	0.005	-	-	
Total	<100	2.92<	110	-	Total
Yunotani	1	0.09	0.17	0.78 <sup>(c)</sup>	2.04
Yoshioka	5	0.41	-	0.20 <sup>(d)</sup>	5.61
Jigoku	-	0.42	-	1.86 <sup>(c)</sup>	2.28
-Tarutama					
Total	6	0.92	0.17	2.84	9.93

(Disaster Prevention Research Institute annuals, 51, 275-290)



## Nd and Sr isotopic study of felsic plutonic rocks in northern Oman ophiolite, Oman

N. Tsuchiya (Iwate Univ.), Y. Adachi (Niigata Univ.), S. Miyashita (Niigata Univ.), T. Shibata  
M. Yoshikawa

### INTRODUCTION

The presence of felsic rocks in ophiolite suites has been reported by numerous authors, and is called plagiogranite (Coleman and Peterman, 1975; Coleman and Donato, 1979). Four major models are under debate to explain the formation of these rocks: (1) late-stage differentiation of a parental MORB melt, (2) partial melting of gabbroic rocks, (3) immiscibility in an evolved tholeiitic liquid, and (4) assimilation and partial melting of previously altered dikes (e.g., Koepke et al., 2007). Recently, Koepke et al. (2004; 2007) described that hydrous partial melting of cumulate gabbro is most likely process explaining the petrogenesis of oceanic plagiogranite magma. However, since the experimental results after Koepke et al. (2004; 2007) could not reproduce the entire chemical variation of felsic rocks in ophiolite, petrogenesis of felsic magmas should be further studied in detail.

The Oman ophiolite contains a particularly well-preserved sequence; exposure is almost continuous along strike and almost completes vertical sections. Plagiogranites occur both as high-level intrusives in axis stage and as late intrusive complexes intruding into various stratigraphic units (Lippard et al., 1986). Among them, the late intrusive complex attract special interest because of the coexistence of various rock types such as layered and massive gabbros, diorites, and plagiogranites. Sr and Nd isotopic study is a useful tool identifying primary magmatic signature and possible tectonic site of formation, however, very little has been stated about isotopic signature of plagiogranites. The purpose of this study is to investigate Sr and Nd isotopic characteristics of plagiogranites and related rocks in the Oman ophiolite, and to elucidate the petrogenesis of these rocks.

### OUTLINE OF GEOLOGY AND PETROLOGY

Fig. 1 shows distribution of the felsic plutonic complex and related rocks in the northern Oman ophiolite around Sohar to Wadi Jizi. In general, they are composed mainly of gabbroic to dioritic rocks with subordinate amounts of plagiogranites. Among them, Lasail complex, Suhaylah complex, and granitic dikes intruding mantle sequence in Wadi Fizh are chosen for Sr and Nd isotopic analysis (Fig. 1).

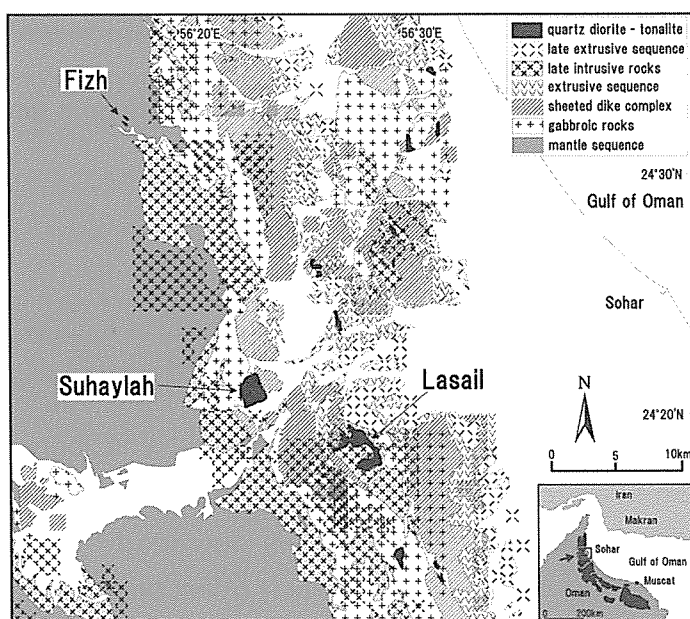


Fig. 1: Distribution of the felsic plutonic complex and related rocks in the northern Oman ophiolite.

Lasail complex feeds the Lasail Unit volcanic rocks, felsitic sheets, and andesitic cone-sheets around Lasail Mine (Alabaster et al., 1982; Lippard et al., 1986). Lasail complex, dimension of  $4.7 \times 3.8$  km, consists of gabbroic to tonalitic rocks and is intruded into the base of the lava of Geotimes Unit. The gabbroic rocks are composed of layered gabbro (gabbro-norite and anorthositic leucogabbro-norite associated with minor amounts of dunite, wehrlite, websterite, and olivine gabbro) and massive gabbro (hornblende gabbro-norite, hornblende gabbro, and hornblende diorite). The layered gabbro is intruded by the massive gabbro, and often occurs as large blocks in the massive gabbro. These gabbroic rocks are intruded by small intrusions of hornblende diorite to hornblende tonalite. The tonalitic rocks are characterized by MME (mafic magmatic enclaves) swarms of fine-grained gabbro to diorite in central to eastern part of the complex. The assemblage of these rocks belongs to the opx-series classified by Umino et al. (1990). Stakes and Taylor (2003) described bulk rock chemistry and oxygen isotopic study of the rocks from the Lasail complex.

Suhaylah complex, dimension of  $1.5 \times 1.5$  km, is intruded into cumulate gabbros at a lower contact and into dike complex and basalt at an upper contact. It is composed of hornblende quartz diorite including basaltic 'pillows' and dismembered dikes, and is intruded by hornblende tonalite at central to eastern part. At the northern part of the complex, hornblende quartz diorite intrudes into the upper gabbro, and included many blocks of the gabbroic rocks. Stakes and Taylor (2003) described bulk rock chemistry and oxygen isotopic study of the rocks from the Suhaylah complex.

Small intrusive bodies of biotite granites and tourmaline granites are intruded into harzburgite in the upper part of the mantle sequence at the upper stream of the Wadi Fizh. These granites occur as small dikes less than 10 m thick, and show WNW-ESE strikes and steep northward contact with host harzburgite. These rocks are characterized by leucocratic and

fine-grained texture with or without remarkable foliation. Similar granitic intrusive rocks, fine-grained and foliated biotite granite to aplite, occur in the lower part of the Samail Nappe (Oman ophiolite), and are described as igneous rocks associated with emplacement (Browning and Smewing, 1981). These granites are intruded into the upper part of the mantle sequence and near the base of the layered series, and distributed mainly in the Khor Fakkan (UAE) Block and in the southeastern part of the Haylayn block near Rustaq. Lippard et al. (1986) reported biotite K-Ar age of  $85 \pm 3$  Ma from the biotite aplite intruding the amphibolite sheet and the overlying harzburgite at Sharm in the UAE.

Bulk chemistry of the Lasail and Suhaylah complex show wide range of composition, but each complex show distinct trend from gabbroic to tonalitic rocks. Tonalitic to quartz dioritic rocks from the Lasail and Suhaylah complex are characterized by extreme depletion in incompatible elements;  $K_2O$ ,  $P_2O_5$ , and  $TiO_2$ , while biotite granites from the upper stream of the Wadi Fizh shows particularly higher  $K_2O$  contents.

Koepke et al. (2004; 2007) described that hydrous partial melting of cumulate gabbro is most likely process explaining the petrogenesis of oceanic plagiogranite magma.  $TiO_2$  contents of felsic rocks from the Lasail and Suhaylah complex, however, shows clearly higher concentrations than that obtained by experimental results after Koepke et al. (2004).

## ANALITICAL METHOD

The analytical methods for Sr and Nd isotope analyses are essentially the same as those of Yoshikawa et al. (2001), Shibata et al. (2003), and Shibata and Yoshikawa (2004). Extraction procedures for Rb, Sr, Sm, and Nd were described by Shibata et al. (2003). Isotopic analyses were performed on a TIMS (ThermoFishers MAT262) with static multi-collector mode following Yoshikawa et al. (2001). The  $^{87}Sr/^{86}Sr$  and  $^{143}Nd/^{144}Nd$  ratios were normalized to  $^{86}Sr/^{88}Sr = 0.1194$  and  $^{146}Nd/^{144}Nd = 0.7219$ , respectively. The decay constants of  $^{87}Rb$  is  $1.42 \times 10^{-11}/y$  (Steiger and J'ager, 1977) and of  $^{147}Sm$  is  $6.54 \times 10^{-12}/y$  (Lugmair and Marti, 1978).

## RESULTS AND DISCUSSIONS

A mean error of each isotopic analyses was  $\pm 0.000009$  to  $16$  for  $^{87}Sr/^{86}Sr$  and  $\pm 0.000009$  to  $34$  for  $^{143}Nd/^{144}Nd$ . Initial  $^{87}Sr/^{86}Sr$  ( $Sr_i$ ) and initial  $^{143}Nd/^{144}Nd$  ( $Nd_i$ ) ratios and  $\epsilon Sr$  and  $\epsilon Nd$  values are calculated from assumed age of 95 Ma (Hacker, 1994) for Lasail and Suhaylah complex and of 85 Ma (Lippard et al., 1986) for biotite granites from the Wadi Fizh. The  $\epsilon Sr$  and  $\epsilon Nd$  values were calculated using the following chondritic uniform reservoir (CHUR) parameters;  $^{87}Sr/^{86}Sr = 0.7045$  and  $^{87}Rb/^{86}Sr = 0.0827$ ,  $^{143}Nd/^{144}Nd = 0.512638$  and  $^{147}Sm/^{144}Nd = 0.1966$ .

Fig. 2 shows  $\epsilon Nd$ - $\epsilon Sr$  diagram for the felsic plutonic complex and related rocks in the Oman ophiolite. Data from various igneous rocks in the Oman ophiolite (McCullogh et al. 1980; 1981; Benoit et al., 1996) are also plotted for comparison. Igneous rocks in the Oman

ophiolite are plotted in a horizontal trajectory from an origin at the mantle array, indicating the possibility of contamination with seawater (McCulloch et al. 1980; 1981). In Fig. 2, rocks from the Lasail and Suhaylah complex are plotted within the data from various igneous rocks in the Oman ophiolite, though the plots are characterized by higher  $\epsilon_{\text{Sr}}$  values than the mantle array. On the other hand, the biotite granites intruding into mantle sequence at Wadi Fizh are characterized by particularly lower  $\epsilon_{\text{Nd}}$ . This indicates the possibility that the biotite granites have been derived from isotopically different source materials probably related to continental crust.

Fig. 2 shows  $\epsilon_{\text{Nd}}$ - $\epsilon_{\text{Sr}}$  diagrams for each rock type from the Lasail complex. The gabbro-norite shows the lowest value of  $\epsilon_{\text{Sr}}$ , and is characterized by fresh lithology without hydrous minerals nor alteration products. This indicates the possibility that the gabbro-norite retains magmatic  $\epsilon_{\text{Sr}}$  value with negligible seawater contamination, and that the source materials of the gabbro-norite has slightly higher  $\epsilon_{\text{Sr}}$  value compared with those of MORBs. In other words, the source materials of the gabbro-norite may have some relationships to the rocks contaminated with seawater.

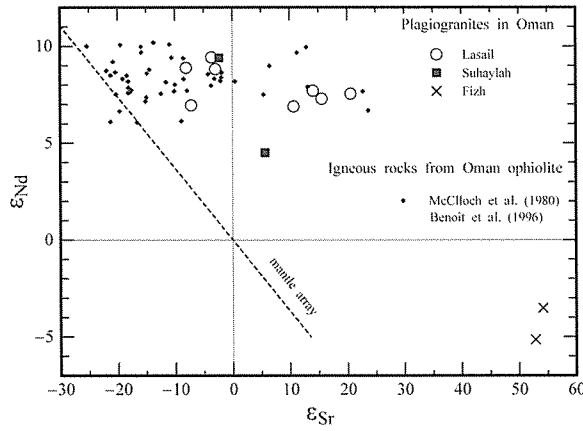


Fig. 2:  $\epsilon_{\text{Nd}}$  -  $\epsilon_{\text{Sr}}$  diagrams for the felsic plutonic complex and related rocks in the Oman ophiolite.

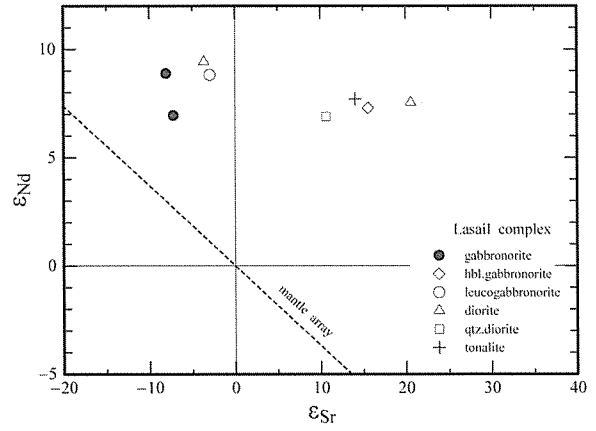


Fig. 3:  $\epsilon_{\text{Nd}}$  -  $\epsilon_{\text{Sr}}$  diagrams for each rock type from the Lasail complex.

Fig. 4 shows  $^{87}\text{Sr}/^{86}\text{Sr}_{\text{initial}}$  ( $\text{Sri}$ ) vs. wt %  $\text{SiO}_2$  diagram, and Fig. 5 shows  $^{143}\text{Nd}/^{144}\text{Nd}_{\text{initial}}$  ( $\text{Ndi}$ ) vs. wt%  $\text{SiO}_2$  diagram for the Lasail and Suhaylah complex. From these figures,  $\text{Sri}$  is increasing with differentiation, but  $\text{Ndi}$  shows no remarkable variation with differentiation. This indicates that the isotopic variation is resulted from seawater alteration with differentiation.

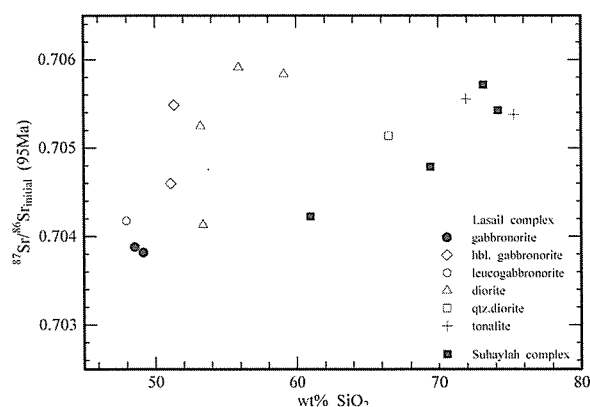


Fig. 4:  $^{87}\text{Sr}/^{86}\text{Sr}_{\text{initial}}$  (SrI) vs. wt%  $\text{SiO}_2$  diagram for the Lasail and Suhaylah complex.

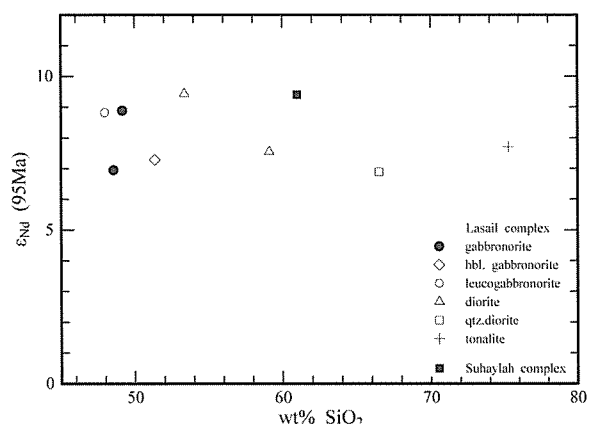


Fig. 5:  $^{143}\text{Nd}/^{144}\text{Nd}_{\text{initial}}$  (NdI) vs. wt%  $\text{SiO}_2$  diagram for the Lasail and Suhaylah complex.

## CONCLUDING REMARKS

From the examination of Sr and Nd isotopic signature, igneous rocks in the Oman ophiolite are variously contaminated with seawater as described by McCulloch et al. (1980; 1981). In the case of rocks from the Lasail and Suhaylah complex, they are characterized by rather higher  $\epsilon_{\text{Sr}}$  values than the mantle array. The gabbro from the Lasail complex shows the lowest value of  $\epsilon_{\text{Sr}}$ , and probably retains magmatic  $\epsilon_{\text{Sr}}$  values with negligible seawater contamination. This suggests that the gabbro magma has produced by the melting of the rocks with higher  $\epsilon_{\text{Sr}}$  values than those of MORBs, e.g., the axis stage rocks interacted with seawater. On the other hand, the biotite granites intruding into mantle sequence at Wadi Fihz are considered to be produced by partial melting of continental materials during the emplacement stage on the Arabian continental margin.

## Reference

- Alabaster, T., Pearce, J.A., and Malpas, J. (1982) The Volcanic Stratigraphy and Petrogenesis of the Oman Ophiolite Complex. *Contributions to Mineralogy and Petrology*, 81, 168--183.
- Benoit, M., Polve, M. and Ceuleneer, G. (1996) Trace element and isotopic characterization of mafic cumulates in a fossil mantle diapir (Oman ophiolite), *Chemical Geology*, 134, 199--214.
- Browning, P. and Smewing, J.D. (1981) Processes in magma chambers beneath spreading axes: evidence for magmatic associations in the Oman ophiolite. *Journal of Geological Society, London*, 138, 279--280.
- Coleman R.G. and Peterman Z.E. (1975) Oceanic plagiogranite. *Journal of Geophysical Research*, 80, 1099--1108.
- Coleman R.G. and Donato, M.M. (1979) Oceanic plagiogranite revisited. In: Barker, F. (ed), *Trondhjemites, dacites, and related rocks*. Elsevier, Amsterdam, pp. 149--167.
- Hacker, B.R. (1994) Rapid emplacement of young oceanic lithosphere, argon geochronology

- of the Oman ophiolite. *Science*, 265, 1563--1569.
- Koepke, J., Feig, S.T., Snow, J., Freise, M. (2004) Petrogenesis of oceanic plagiogranites by partial melting of gabbros: an experimental study. *Contributions to Mineralogy and Petrology*, 146, 414--432.
- Koepke, J., Berndt, J., and Feig, S.T. (2007) The formation of SiO<sub>2</sub>-rich melts within the deep oceanic crust by hydrous partial melting of gabbros. *Contributions to Mineralogy and Petrology*, 153, 67--84.
- Lippard, S.J., Shelton, A.W., and Gass, I.G. (1986) *The Ophiolite of Northern Oman*. Memoir of Geological Society, London, vol. 11, 178 pp., Blackwell Scientific Publications, Oxford.
- Lugmair, G.W., Marti, K. (1978) Lunar initial <sup>143</sup>Nd/<sup>144</sup>Nd: Differential evolution of the Lunar crust and mantle. *Earth and Planetary Science Letters*, 39, 349--357.
- McCulloch, M.T., Gregory, R.T., Wasserburg, J. and Taylor, H.P. (1980) A neodymium, strontium, and oxygen isotopic study of the cretaceous Samail ophiolite and implications for the petrogenesis and seawater-hydrothermal alteration of oceanic crust. *Earth and Planetary Science Letters*, 46, 201--211.
- McCulloch, M.T., Gregory, R.T., Wasserburg, J. and Taylor, H.P. (1981) Sm-Nd, Rb-Sr, and <sup>18</sup>O/<sup>16</sup>O isotopic systematics in an oceanic crustal section: evidence from the Samail ophiolite. *Journal of Geophysical Research*, 86, 2721--2736.
- Steiger, R.H., Jäger, E. (1977) Subcommittee on Geochronology: convention on the use of decay constants in geo- and cosmochemistry. *Earth and Planetary Science Letters*, 36, 359--362.
- Shibata, T., Yoshikawa, M. and Tatsumi, Y. (2003) An analytical method for determining precise Sr and Nd isotopic compositions and results for thirteen rock standard materials: Frontier Research on Earth Evolution 1, IFREE Report for 2001--2002, pp. 363--367, Institute for Frontier Research on Earth Evolution, Japan Marine Science and Technology Center, Yokosuka, Japan.
- Stakes D.S. and Taylor, H.P. (2003) Oxygen isotope and chemical studies on the origin of large oceanic plagiogranite bodies in northern Oman, and their relationship to the overlying massive sulfide deposits. In: Dilek, Y. and Robinson, P.T. (eds), *Ophiolites in earth history*. Geological Society, London, Special Publications, 218, 315--351.
- Umino, S., Yanai, S., Jaman, A.R., Nakamura, Y., and Iiyama, J.T. (1990) The transition from spreading to subduction: Evidence from the Samail ophiolite, northern Oman mountains, in *Ophiolites: Oceanic Crustal Analogues*, edited by Malpas, J. et al., pp. 375--384, Geol. Surv. Dep., Minist. of Agric. and Nat. Resour., Nicosia, Cyprus, 1990.



## Wide-band MT survey in Aso caldera

*M. Utsugi, T. Kagiya, K. Komori, H. Inoue*

Aso Volcano is one of the most active volcanoes in Japan. Activity of this volcano started about 300 ka. Four huge plinian eruptions, forming Aso-1 to Aso-4 pyroclastic flows, formed a large caldera. This caldera surrounded by the outer ring is the largest of the world and stretching 18 km east-west and 24 km north-south. More than 10 central cones of basalt to

rhyolite line up in the east-west on the caldera floor. Only Nakadake cone among them repeated historical eruptions of basaltic magma, and it has a great crater (Nakadake-crater), which is still active.

In 2008, to investigate the resistivity structure beneath Aso volcano and caldera, we made the wide-band MT (MagnetoTelluric) survey along a survey line which traverses the caldera to northeast-southwest passing Nakadake crater. The number of total survey points is 16. Using our observed data, we made tow-dimensional inversion analysis and we estimated the resistivity structure in the

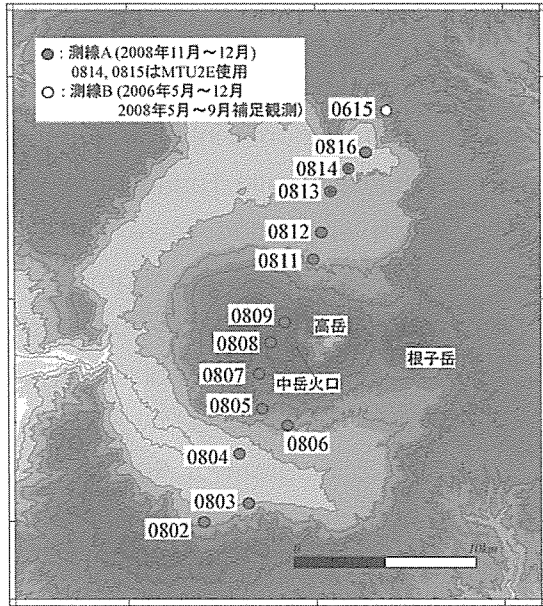


Fig. 1 Observation points of 2008 MT

cross section which traverses the Aso caldera. As a result of this analysis, some characteristic features were discovered for the subsurface structure of Aso volcano. One of them is the existence of the extremely low resistivity layer at a few hundreds meter depth beneath the Aso central cones. The resistivity of this layer is 1 – tens of  $\Omega m$  and this low resistivity suggests the underground water that contains a lot of volcanic gases distributes in this layer.

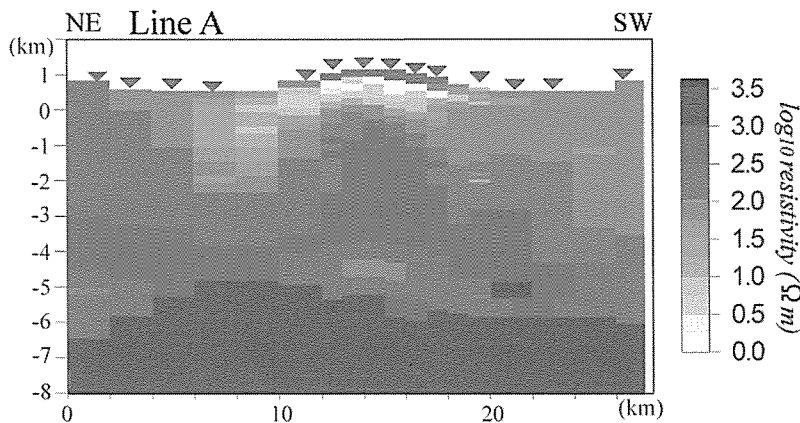


Fig. 2. Resistivity structure of Aso caldera.

## Diffusive fractionation in mantle with magma channels: an index to mantle depletion

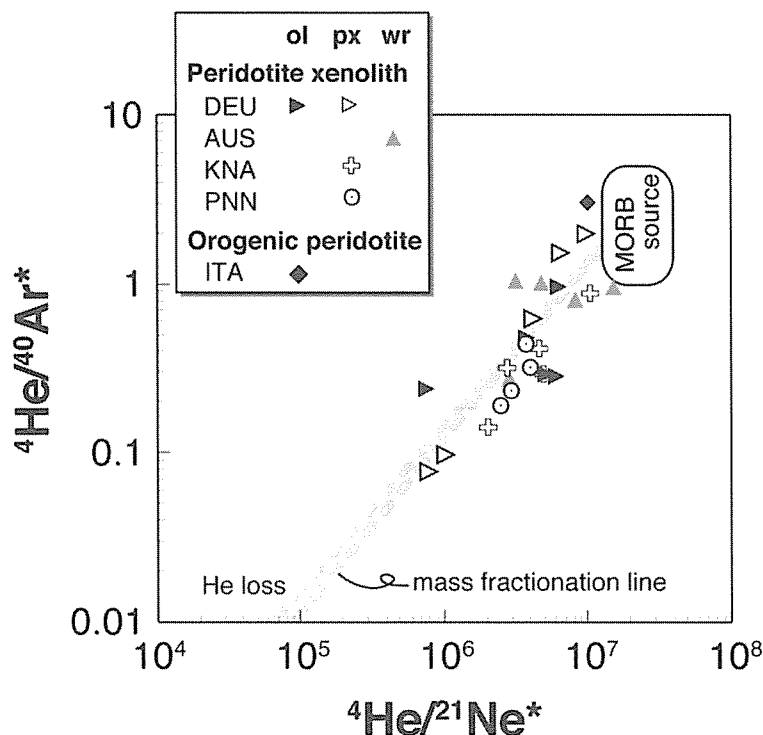
*J. Yamamoto, K. Nishimura, T. Sugimoto, K. Takemura, N. Takahata (Tokyo Univ.)  
Y. Sano (Tokyo Univ.)*

The relative composition of secondary nuclides generated by nuclear reactions converges with the production ratio over time. The production value thereby serves as an initial value to elucidate evolutive processes of the mantle. In fact,  $^4\text{He}/^{40}\text{Ar}^*$  is particularly useful as an indicator for examining consequences of degassing of oceanic basalt. The current mantle is inferred to have  $^4\text{He}/^{40}\text{Ar}^*$  of ca. 1–5. The  $^4\text{He}/^{40}\text{Ar}^*$  in the magma would be elevated because He preferentially diffuses away from crystalline phases in the source mantle into the magma if partial melting or infiltration of exotic magma occurs in the source mantle. Furthermore, He is considerably more soluble than Ar in silicate melts, which engenders more extensive degassing of Ar relative to He: the degassing increases the  $^4\text{He}/^{40}\text{Ar}^*$  of residual magma. In this view, it is noted that low  $^4\text{He}/^{40}\text{Ar}^*$  (ca. 0.1) has been reported occasionally for basaltic magma (Honda et al., 1993; Harrison et al., 2004; Marty et al., 1994; Nuccio et al., 2008) and frequently for mantle-derived xenoliths (e.g., Yamamoto et al., 2004). Possible low (U+Th)/K in the source mantle results in low  $^4\text{He}/^{40}\text{Ar}^*$ . Figure 1 presents a diagram of  $^4\text{He}/^{40}\text{Ar}^*$  and  $^4\text{He}/^{21}\text{Ne}^*$  for peridotites. Actually,  $^4\text{He}/^{21}\text{Ne}^*$  of the peridotites is correlated with  $^4\text{He}/^{40}\text{Ar}^*$ . It is indicative of a significant and systematic elemental fractionation of  $^4\text{He}$  from nonatmospheric  $^{21}\text{Ne}$  and  $^{40}\text{Ar}$  (Honda and Patterson, 1999; Patterson et al., 1994) rather than low (U+Th)/K in the source mantle.

Matsuda and Marty (1995) and Burnard (2004) proposed a similar model by which He can be enriched in melt during partial melting following diffusion from crystalline phases into magma. Complementary residual mantle and magma derived from it are expected to have low  $^4\text{He}/^{40}\text{Ar}^*$ . The same diffusive fractionation will occur in phenocrysts in ascending magma (Harrison et al., 2004; Nuccio et al., 2008).

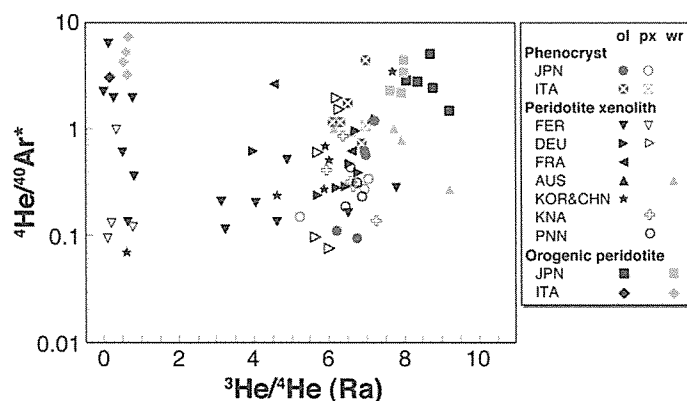
As demonstrated by results of this study, the diffusive loss of a lighter element or isotope from solid phase to melt is a key phenomenon that is useful for tracing pristine chemical and isotopic compositions of mantle-derived materials. Therefore, we test this assumption quantitatively in combination with the influence of subsequent accumulation of radiogenic  $^4\text{He}$  and  $^{40}\text{Ar}$  using published noble gas data for peridotites, phenocrysts, and ocean island basalts along with newly obtained noble gas data on phenocrysts in volcanic rocks from Japan.

By crushing olivine and pyroxene phenocrysts in volcanic rocks from Kyushu Island, Japan, we determined  $^3\text{He}/^4\text{He}$  of 3–7 Ra and  $^{40}\text{Ar}/^{36}\text{Ar}$  of up to 1750 (Fig. 2).



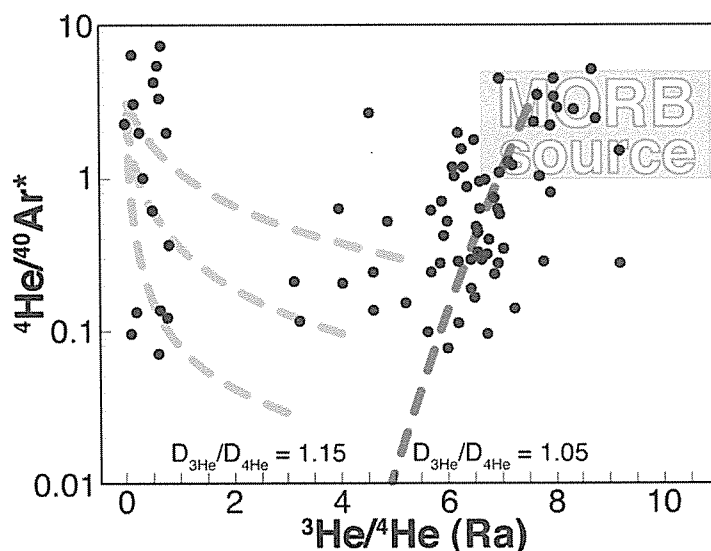
These values are lower than those of MORB.  $^4\text{He}/^{40}\text{Ar}^*$  (down to 0.1) is much lower than the production ratio of  $^4\text{He}/^{40}\text{Ar}^*$  (1–5). The present results show no systematic difference from published data of subarc and subcontinental mantle materials. Overall, the  $^3\text{He}/^4\text{He}$  of the subarc and subcontinental mantle are roughly separable

**Figure 1.**  $^4\text{He}/^{40}\text{Ar}^*$  versus  $^4\text{He}/^{21}\text{Ne}^*$  diagram of data obtained from peridotites with crushing experiments, where \* indicates correction for atmospheric contamination. Data sources are as follows: peridotite xenoliths from Germany (DEU) (Buikin et al., 2005; Gautheron et al., 2005), Australia (AUS) (Matsumoto et al., 2000), Kenya (KNA) (Hopp et al., 2007), and Pannonian (PNN) (Buikin et al., 2005); orogenic peridotites from Italy (ITA) (Matsumoto et al., 2005). Data with  $^{21}\text{Ne}/^{22}\text{Ne}$  and  $^{40}\text{Ar}/^{36}\text{Ar}$  of less than 0.03 and 320, respectively, are not shown. Actually,  $^{21}\text{Ne}$  can be generated nucleogenically from ( $\alpha$ , n) reaction on  $^{18}\text{O}$  and (n,  $\alpha$ ) reaction on  $^{24}\text{Mg}$  (Wetherill, 1954). The  $^4\text{He}/^{21}\text{Ne}^*$  production ratio in the mantle is estimated as  $2.2 \times 10^7$  (Leya and Wieler, 1999; Yatsevich and Honda, 1997). The  $^4\text{He}/^{21}\text{Ne}^*$  of the lithosphere is determined primarily by its chemical composition, which is unlikely to change dramatically between reservoirs. Therefore, the  $^4\text{He}/^{21}\text{Ne}^*$  of the mantle is likely to be constant, as is true for  $^4\text{He}/^{40}\text{Ar}^*$ .



**Figure 2.**  $^3\text{He}/^4\text{He}$  versus  $^4\text{He}/^{40}\text{Ar}^*$  diagram of phenocrysts from quaternary volcanoes in Kyushu island, Japan (JPN) with data obtained by crushing mantle-derived materials. Data sources are as follows: phenocrysts from Italy (ITA) (Marty et al., 1994; Nuccio et al., 2008); phenocrysts from Siberia, Russia (SBR) (Harrison et al., 2004); peridotite xenoliths from Far Eastern Russia (FER) (Yamamoto et al., 2004), Germany (DEU) (Buikin et al., 2005; Gautheron et al., 2005), France (FRA) (Gautheron et al., 2005), Australia (AUS) (Matsumoto et al., 2000), Korea (KOR), China (CHN) (Kim et al., 2005), Kenya (KNA) (Hopp et al., 2007) and Pannonian (PNN) (Buikin et al., 2005); orogenic peridotites from Japan (JPN) (Matsumoto et al., 2001), and Italy (ITA) (Matsumoto et al., 2005).

into two regimes: data with  $^3\text{He}/^4\text{He}$  more than 3 Ra and less than 1 Ra. The  $^3\text{He}/^4\text{He}$  of the former samples have a positive correlation with  $^4\text{He}/^{40}\text{Ar}^*$ . The  $^3\text{He}/^4\text{He}$  and  $^4\text{He}/^{40}\text{Ar}^*$  of phenocrysts overlap with those of subcontinental mantle xenoliths. Although noble gas compositions of phenocrysts are affected considerably by diffusive fractionation in ascending magma (Fig. 3), they have little effect on the noble gases in the mantle xenoliths because it takes 100 years for He/Ar fractionation of ca. 15% for a mantle xenolith with 5 cm diameter. Therefore, the low  $^4\text{He}/^{40}\text{Ar}^*$  of the mantle xenoliths is inferred to result from another kinetic fractionation in the mantle.



**Figure 3.**  $^3\text{He}/^4\text{He}$  versus  $^4\text{He}/^{40}\text{Ar}^*$  diagram of subcontinental mantle peridotites. Data are from Fig. 4. The shaded area shows a trend of the diffusive noble gas fractionation from the source mantle (gray rectangle) using  $D_{^3\text{He}}/D_{^4\text{He}}$  of 1.15 and  $D_{^4\text{He}}/D_{^{40}\text{Ar}}$  of 3.16. A dark gray broken line is the best-fitting exponential curve to sets of data with  $^3\text{He}/^4\text{He}$  of more than 4 Ra, which corresponds to the diffusion curve with  $D_{^3\text{He}}/D_{^4\text{He}}$  of 1.05. Light gray broken lines show the radiogenic change of the depleted mantle, which originally has  $^3\text{He}/^4\text{He}$  of 3.1, 4.1, and 5.2 Ra and  $^4\text{He}/^{40}\text{Ar}^*$  of 0.03, 0.1, and 0.3, respectively. The radiogenic change is based on an original source mantle with K/U of 12 700 and Th/U of 3.1, in which K, Th, and U contents are presumed to be unaffected by the depletion. Numbers labeling the broken lines denote the elapsed time (kiloyear).

Possibly, the correlation for the mantle xenoliths results from diffusive fractionation accompanied by magma migration in the mantle. During generation and migration of magma in the mantle, lighter noble gases diffuse rapidly out into the magma. This diffusive fractionation can explain low  $^4\text{He}/^{40}\text{Ar}^*$  and somewhat low  $^3\text{He}/^4\text{He}$  in the residual mantle. Furthermore, the combination of the diffusive fractionation and subsequent radiogenic ingrowth explain the fact that data from subcontinental mantle xenoliths have extremely low  $^3\text{He}/^4\text{He}$  and various  $^4\text{He}/^{40}\text{Ar}^*$ . Assuming this concept to be true,  $^3\text{He}/^4\text{He}$  and  $^4\text{He}/^{40}\text{Ar}^*$  provide useful indices for tracking mantle evolution.

For more details on the diffusive fractionation of noble gases in the mantle, refer to the paper below.

Yamamoto, J., Nishimura, K., Sugimoto, T., Takemura, K., Takahata, N., Sano, Y. (2009) Diffusive fractionation of noble gases in mantle with magma channels: origin of low He/Ar in mantle-derived rocks. *Earth Planet. Sci. Lett.* 280, 167-174

## **Cathodoluminescence zoning and Ti content in quartz from the Cape Ashizuri Igneous Complex in Kochi Prefecture, Japan**

**M. Yokoyama, S. Yoshikura (Kochi Univ.), T. Shibata, H. Nishido (Okayama Univ. of Sci.)**

### **Introduction**

Recently, several studies have shown that igneous quartz preserves cathodoluminescence (CL) zoning that can be used as a sensitive petrogenetic tool (e.g., Wark et al., 2007). For example, the CL zoning of quartz was used to reveal the magma chamber processes such as magma mingling and mixing between two contrasting felsic and mafic magmas (Müller et al., 2000; Wiebe et al., 2007).

The CL emission is reflected in the trace elements content and/or lattice defect. In the case of quartz, the spectral response is characterized by emission spectra about 400nm (blue-CL) and 700nm (red-CL). It is reported that the cause of the blue CL is concentration of titanium (e.g., Wark and Spear, 2005) and Ti content in quartz increases with increasing crystallization temperature (e.g., Wark and Watson, 2006).

In this paper, we report the results of SEM-CL zoning and Ti content determined by EPMA and LA-ICP-MS in situ microanalysis in quartz, and the comparison of Ti content obtained by two methods was made.

### **Cape Ashizuri Igneous Complex**

The Cape Ashizuri Igneous Complex is a Middle Miocene trench-proximal A-type granitoid pluton emplaced into the Neogene Shimanto accretionary complex in Kochi Prefecture, southwest Japan. The Complex exhibits a concentrically zoned structure made up of three zones (Fig. 1). The outer zone (Zone I) consists of medium- to coarse-grained, subsolvus biotite granite. The middle zone (Zone II) is characterized by abundant mafic magmatic enclaves (MME) and syn-plutonic mafic dikes in the biotite granite or heterogeneous hybrid. The inner zone (Zone III) comprises essentially medium-grained, hypersolvus alkali granite enclosing various types of syenitic and mafic magmatic enclaves. Clearly post-plutonic mafic dikes with chilled fine-grained margins crosscut all the lithologies.

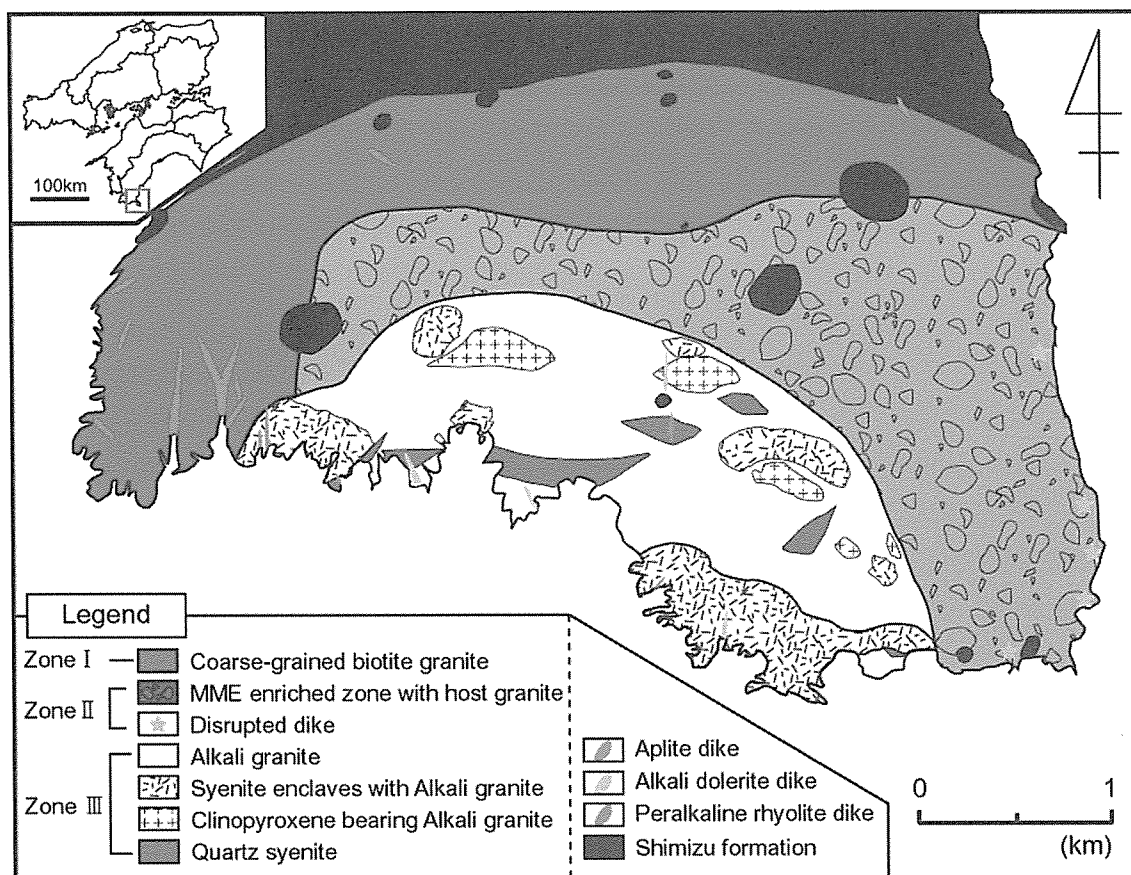


Fig. 1 Geological map of the Cape Ashizuri Igneous Complex.

There are many lines of field and petrographic evidence for coexisting of mafic and felsic magmas and extensive interactions between them in all the zones, particularly in the Zone II : pillow-shaped MME with crenulated and chilled margins enclosed either singly or in swarms within a granitic host; fine-grained igneous textures and magmatic mineralogy of MME; double/composite MME; syn-plutonic mafic dikes being broken into MME (disrupted dike); composite dikes with felsic margins; quartz and polycrystalline granitic ocelli rimmed with fine aggregates of clinopyroxene and/or hornblende; corroded K-feldspar with dendritic plagioclase overgrowths (rapakivi feldspar) in hybrid rocks; plagioclase with K-feldspar or dendritic plagioclase rims (anti-rapakivi feldspar) in hybrid rocks; development of "xenoporphyrritic" texture in MME; quenched textures of apatite (acicular) and Fe-Ti oxides (skeletal) in MME; pipe-like granitic blobs rising in the mafic host. These observations are interpreted in terms of a periodic injection of mafic magmas into the crystallizing felsic magma chamber, and mingling and mixing between these two contrasting magmas. These magmatic processes played an important role in producing many of the compositional and petrographic features of the MME, syn-plutonic dikes and their host granitic rocks in the Cape Ashizuri Igneous Complex.

## **Analytical methods**

### **Cathodoluminescence (SEM-CL)**

SEM-CL images and spectral information of quartz were analyzed on carbon-coated polished sections using the Gatan Mini-CL and Oxford Mono-CL2, which is attached to the JEOL 5410LV at Okayama University of Science. CL analyses were performed using an accelerating voltage of 15 kV and a beam current between 1.5 and 2.0 nA.

### **EPMA**

Ti contents in quartz were determined by wavelength dispersive electron probe microanalyser (JEOL 8900 Superprobe) at Okayama University of Science. EPMA operated at an accelerating voltage of 15 kV, at a beam current of 120 nA, at a counting time of 240 sec, and with a beam diameter of 10  $\mu\text{m}$ . The precision of the analyses (at 3 sigma) was 18 ppm, and limit of detection is 18 ppm for Ti.

### **LA-ICP-MS**

LA-ICP-MS analyzed on non-carbon-coated sections (about 100 $\mu\text{m}$  in thickness) using the Inductively Coupled Plasma Mass Spectrometer on the X SERIES 2 (Thermo Scientific) equipped with a Laser Abrasion micro-sampler on the CETAC LSX 200 (Cetac Technologies) at Institute for Geothermal Science, Kyoto University. For the analysis, the laser system is 266nm Nd-YAG laser that is operated at energy level of 6-20, laser pulse repetition of 5 Hz, spot size of 50  $\mu\text{m}$ . Laser irradiation method is "soft-ablation", which increase energy level from 6 to 10 for 2 seconds and from 10 to 20 for 3 seconds. The "soft-ablation" was used to suppress the breaking of analytical spot on quartz.

## **Results and discussions**

Results of SEM-CL, EPMA and LA-ICP-MS analyses are shown in Figures 2 and 3 and Table 1. As shown in Fig. 2, variations in Ti content determined by EPMA correspond to blue CL intensity variations in individual CL contrasted growth zones. On the other hand, Ti contents analyzed by LA-ICP-MS are constantly higher than those analyzed by EPMA and there is no positive relationship with blue-CL intensity (Table 1 and Fig. 3).

It seems that the difference of these results depends on the difference of analytical volume of each technique. The analytical volume of SEM-CL and EPMA could be equal. In contrast, the analytical volume (sampling volume in case of LA-ICP-MS) by LA-ICP-MS is much larger than that of EPMA and SEM-CL. The large sampling volume of LA-ICP-MS straddles several zones with different CL intensity. In addition, there is a possibility that micro-inclusions with Ti-rich phases exist within the volume ablated by the laser.

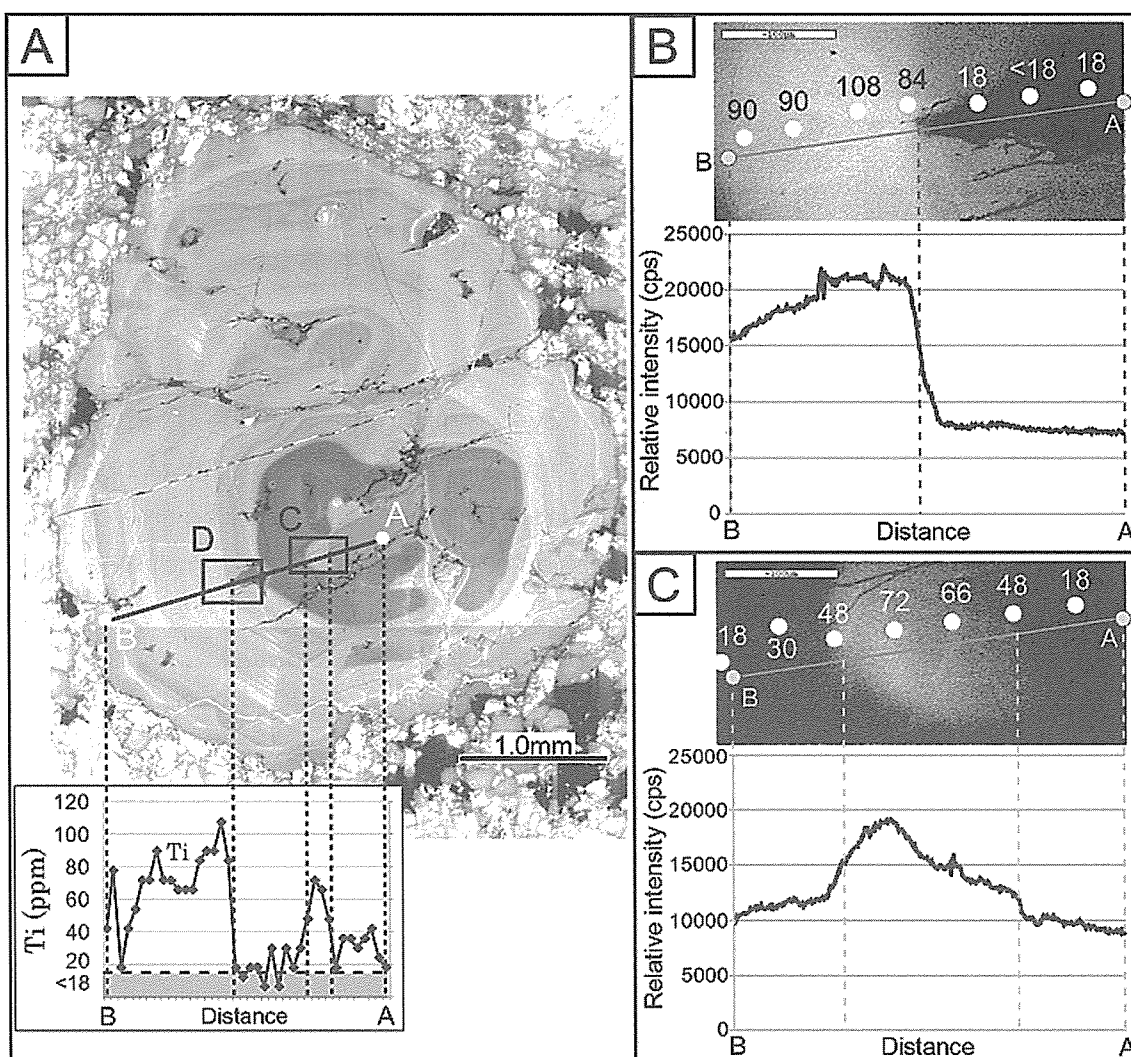


Fig. 2. A.: CL zoning in quartz from granitic MME in Zone II and Ti line profile. B: Detailed CL image and line profile of blue CL intensity in area D in Fig. 2A. C: Detailed CL image and line profile of blue CL intensity in area C in Fig. 2A.

Müller et al. (2003) evaluate the three in situ microanalytical methods of SIMS, EPMA and LA-ICP-MS in determining Ti in natural quartz samples and compared the analytical results from view point of the spatial resolution and limits of detection. They reported the dramatic difference LA-ICP-MS and other two analytical methods and also attribute it to the difference in sampling volume. They reach the conclusion that EPMA is the most reliable in situ microanalysis for obtaining quantitative trace element data in quartz at concentration in excess of a few 10's of ppm and at the  $<10 \mu\text{m}$  scale at the moment.



Table 1. Trace element contents in quartz and nist grass analysed by LA-ICP-MS

elements / point No.	point 1	point 2	point 3	point 4	nist 612	nist 614
<sup>27</sup> Al	13815	13076	12504	12732	8531	8469
<sup>47</sup> Ti	631	654	716	621	38	10
<sup>49</sup> Ti	595	601	599	683	61	14
V	18	23	25	30	49	1
Cr	n.d.	n.d.	n.d.	n.d.	57	6
<sup>56</sup> Fe	1230	1216	1147	1597	60	21
Zr	59	57	68	60	8	1
Nb	8	10	6	7	12	0
Hf	11	11	10	14	22	1
Ta	2	3	3	4	18	0
Pb	10	7	10	13	196	12

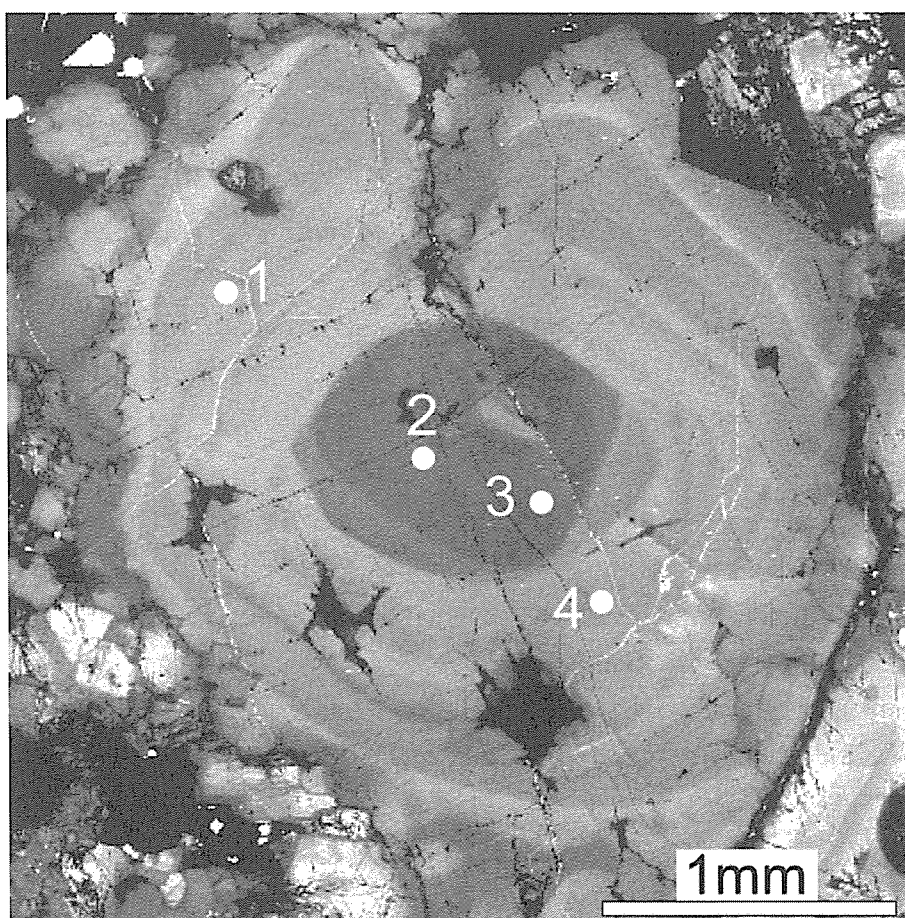


Fig. 3 CL zoning in quartz from granitic MME in Zone II and points ablated by laser for ICP-MS analysis of trace elements shown in Table 1.

## References

- Müller, A., Seltmann, R., Behr, H. -J., 2000, Application of cathodoluminescence to magmatic quartz in a tin granite case study from the Schellerhau Granite Complex, Eastern Erzgebirge, Germany. *Mineralium Deposita*, v. 35, pp. 169-189.
- Müller, A., Wiedenbeck, M., van den Kerkhof, AM., Kronz, A., Simon, K., 2003, Trace elements in quartz – a combined electron microprobe, secondary ion mass spectrometry, laser-ablation ICP-MS, and cathodoluminescence study. *European Journal of Mineralogy*, v. 15, pp. 747-763.
- Wark, D. A., and Spear, F. S., 2005, Ti in quartz: Cathodoluminescence and thermometry. *Geochimica et Cosmochimica Acta*, v. 69, supplement, p. A592.
- Wark, D. A., and Watson, E. B., 2006, TitaniQ: A titanium-in-quartz geothermometer. *Contributions to Mineralogy and Petrology*, v. 152, pp. 743-754.
- Wiebe, R. A., Wark, D. A., Hawkins, D. P., 2007, Insights from quartz cathodoluminescence zoning into crystallization of the Vinalhaven granite, coastal Main. *Contributions to Mineralogy and Petrology*, v. 154, pp. 439-453.

## **Major element compositions of least altered harzburgite from the Hayachine-Miyamori Ophiolitic complex**

***M. Yoshikawa, K. Ozawa (Univ. Tokyo), T. Shibata***

Bulk-rock major element compositions of peridotite provide direct information on partial melting, melt extraction, and melt fertilization processes in the upper mantle. However, the original bulk-rock compositions, particularly those for trace elements, are quite susceptible to low-temperature processes such as serpentinization. There is a way to recover the primary compositions for major elements or compatible trace elements. Niu et al. (1997), for example, attempted to reconstruct primary bulk-rock compositions of serpentinized abyssal peridotites by mass balance calculation based on mineral chemical compositions and estimated primary modes. Recently, Niu (2004) further reported bulk-rock major and trace element analyses on serpentinized abyssal peridotites and argued that magmatic signatures could be preserved in bulk-rock major and trace element compositions, although he admitted that some of MgO is lost by sea-floor weathering. However, the approach was criticized by Walters (1999) and Baker & Beckett (1999). Moreover, such reconstruction for incompatible trace elements encounters enormous difficulties. It is desirable to find fresh peridotites with limited secondary alteration to avoid ambiguity in reconstruction of bulk chemical composition.

The Hayachine-Miyamori ophiolitic complex in the Kitakami Mountains, northeastern Japan is located in the Hayachine Tectonic Belt, which is one of the oldest geological terrane in Japan and consists of ultramafic tectonite and cumulate members corresponding to the lower ultramafic sections of ophiolites (e.g. Ozawa, 1984; Ehiro, 2000). Peridotites in this complex are extensively serpentinized (most of them contains > 60 % serpentine; Ozawa,

1988). The tectonite member is divided into two suites on the basis of spinel Cr-number ( $Cr\# = 100 \times Cr / (Cr + Al)$ ): aluminous spinel ultramafic suite (ASUS;  $Cr\# < 40$ ) and chromite-bearing ultramafic suite (CSUS;  $Cr\# > 40$ ; Ozawa, 1988). We found a least serpentinized boulder of peridotite belonging to CSUS. Peridotites belonging CSUS generally contain phlogopite and  $K_2O$ -rich and  $TiO_2$ -poor hornblend with rare occurrence of apatite (Ozawa and Shimizu, 1995). The presence of primary amphibole in refractory peridotites (harzburgite and dunite) and the major, trace element and Sr-Nd isotopic compositions of clinopyroxene and amphibole are attributed to open-system melting with influx of slab-derived materials around 500Ma (e.g. Ozawa, 1994; Ozawa & Shimizu, 1995; Yoshikawa and Ozawa, 2007; Yoshikawa et al., 2007). Here, we report a bulk-rock major element composition of the spinel harzburgite boulder (73003-1) by using new XRF method established by Sugimoto et al. (submitted), which is applicable to wide range of silicate rocks from ultramafic to felsic rocks. The sample 73003-1 is plotted in the field of the Horoman orogenic lherzolite complex when plotted in MgO variation diagrams, excepting in the MgO-CaO and MgO- $Al_2O_3$  variation diagrams (Fig. 1). The sample 73003-1 is characterized by high CaO and low  $Al_2O_3$  contents than other orogenic peridotites. Similar feature was observed from the Victoria peridotite xenoliths (Yaxley et al., 1991). Yaxley et al. (1991) suggested carbonatite metasomatism for the high CaO and low  $Al_2O_3$  of the xenoliths from the following lines of evidence; (1) replacement of primary orthopyroxene by clinopyroxene and olivine, which may be attributed to the reaction between orthopyroxene and  $CO_2$ -rich melt to produce clinopyroxene and olivine, (2) presence of accessory apatite, which can be produced by reaction from primary olivine + diopside + carbonatite melt to secondary orthopyroxene + haloapatite, (3) high bulk-rock  $CaO/Al_2O_3$  value and extreme large ion lithophile element (LILE) enrichment without concomitant  $TiO_2$  enrichment, which are characteristics of carbonatite melt. CSUS peridotites have petrological and geochemical features consistent with (2) and (3), although the replacement of orthopyroxene by clinopyroxene + olivine has not been observed in CSUS peridotites. They contain spinel with higher  $Cr\#$ , indicating higher degree of melting than ASUS peridotites underwent (e.g. Ozawa, 1988), because the  $Cr\#$  of spinel is a good indicator of degree of melting (e.g. Dick and Bullem, 1984). Modal composition of clinopyroxene generally decreases with increase in degree of melting (e.g. Dick et al., 1984). The modal abundances of clinopyroxene in CSUS peridotites, however, are as high as or even higher than in ASUS peridotites (Fig. 2), suggesting addition of clinopyroxene by influx of a  $CaO$ -rich agent. Increase of modal composition of clinopyroxene by metasomatism with silicate-carbonatite melt derived from subducted slab was suggested from Puy Beaunit peridotite xenoliths, Massif Central, which have high LILE/HFSE (high field strength element) ratios (Fig. 2; Yoshikawa et al., in press). The Nd model age and Re depletion model age of sample 73003-1 are around 500 Ma (Yoshikawa and Ozawa, 2007; Yoshikawa et al., 2007). On the basis of the above observations, we infer that CSUS peridotites underwent influx of a silicate-carbonatite melt most probably from subducted slab around 500Ma.

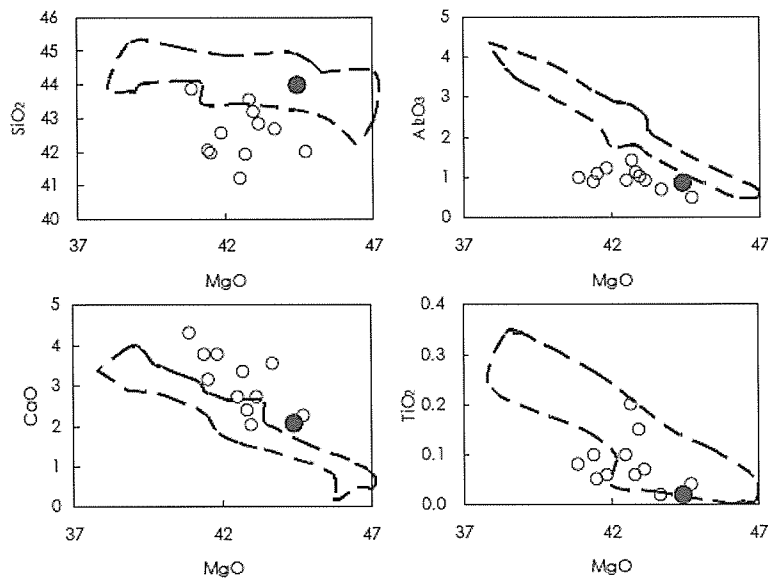


Fig.1. MgO-Oxide (wt %) variation diagrams for bulk-rock. The broken lined area is as the fields of peridotites from the Horoman peridotite complex (Obata and Nagahara, 1987; Takazawa et al., 1992; Yoshikawa and Nakamura, 2000). Symbols are ●, 73001-1 spinel harzburgite and ○, the Victorain peridotite xenoliths (Yaxely et al., 1997).

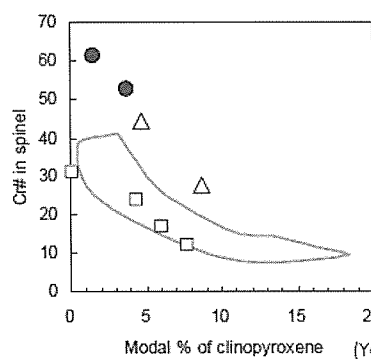


Fig. 2. Relationship between Cr#  $[100 \times \text{Cr}/(\text{Cr}+\text{Al})]$  in spinel and modal composition of clinopyroxene. Symbols are ●, CSUS peridotites; □, ASUS peridotites; △, the silicate-carbonatite metasomatized xenoliths from the Massif Central (Yoshikawa et al. in press). Data of the ASUS and CSUS peridotites are from Ozawa and Shimizu (1995). The range of the Massif Central xenoliths is also shown (Yoshikawa et al., in press and reference is herein).

## References

- Baker, M.B., Beckett, J.R., 1999. The origin of abyssal peridotites: a reinterpretation of constraints based on primary bulk compositions. *Earth Planet. Sci. Lett.* 171, 49-61.
- Dick, H.J.B., Bullen, T., 1984. Chromian spinel as a petrogenetic indicator in abyssal and alpine-type peridotites and spatially associated lavas. *Contrib. Mineral. Petrol.* 86, 54-76.
- Dick, H.J.B., Fisher, R.L., Bryan, W., 1984. Mineralogic variability of the uppermost mantle along mid-ocean ridges. *Earth Planet. Sci. Lett.* 69, 88-106.
- Ehiro, M., 2000. Relationships in tectonic framework among the South Kitakami and Hayachine Tectonite Belts, Kurosegawa Belt, and "Paleo-Ryoke Belt". *Mem. Geol. Soc. Japan* 56, 53-64.
- Niu, Y., 2004. Bulk-rock major and trace element compositions of abyssal peridotites: Implications for mantle melting, melt extraction and post-melting processes beneath mid-ocean ridges. *J. Petrol.* 45, 2423-2458.
- Niu, Y., Langmuir, C.H., Kinzler, R.J., 1997. The origin of abyssal peridotites: A new perspective. *Earth Planet. Sci. Lett.* 152, 251-265.
- Obata, M., Nagahara, N., 1987. Layering of alpine-type peridotite and the segregation of partial melt in the upper mantle. *J. Geophys. Res.* 92, 3467-3473.
- Ozawa, K., 1984. Olivine-spinel geospeedometry: Analysis of diffusion-controlled Mg-Fe<sup>2+</sup> exchange. *Geochim. Cosmochim. Acta* 48, 2597-2611.
- Ozawa, K., 1988. Ultramafic tectonite of the Miyamori ophiolitic complex in the Kitakami

- Mountains, Northeast Japan: hydrous upper mantle in an island arc. *Contrib. Mineral. Petrol.* 99, 159-175.
- Ozawa, K., 1994. Melting and melt segregation in the mantle wedge above a subduction zone: Evidence from the Chromite-bearing peridotites of the Miyamori ophiolite complex, northeastern Japan. *J. Petrol.* 35, 647-678.
- Ozawa, K., Shimizu, N., 1995. Open-system melting in the upper mantle: Constraints from the Hayachine-Miyamori ophiolite, northeastern Japan. *J. Geophys. Res.* 100, 22315-22335.
- Takazawa, E., Frey, F.A., Shimizu, N., Obata, M., Bodinier, J.L., 1992. Geochemical evidence for melt migration and reaction in the upper mantle. *Nature* 359, 55-58.
- Waletr, J.M., 1999. Comments on 'Mantle Melting and Melt Extraction Processes beneath Ocean Ridges: Evidence from Abyssal Peridotites' by Yaoling Niu. *J. Petrol.* 40, 1187-1193.
- Yaxley, G.M., Crawford, A.J., Green, D.H., 1991. Evidence for carbonatite metasomatism in spinel peridotite xenoliths from western Victoria, Australia. *Earth Planet. Sci. Lett.* 107, 305-317.
- Yoshikawa, M., Nakamura, E., 2000. Geochemical evolution of the Horoman peridotite complex: Implications for melt extraction, metasomatism, and compositional layering in the mantle. *J. Geophys. Res.* 105, 2879-2901.
- Yoshikawa, M., Ozawa, K., 2007. Rb-Sr and Sm-Nd isotopic systematics of the Hayachine-Miyamori ophiolitic complex: Melt generation process in the mantle wedge beneath an Ordovician island arc. *Gondwana Res* 11, 234-246.
- Yoshikawa, M., Suzuki, K., Ozawa, K., 2007. Osmium isotopic composition of harzburgite from the Hayachine-Miyamori ophiolitic complex. *Ann. Report FY2007 Institute for Geothermal Sciences*, 39-40.
- Yoshikawa, M., Kawamoto, T., Shibata, T., Yamamoto, J. (in press) Geochemical and Sr-Nd isotopic characteristics and P-T estimates of mantle xenoliths from the French Massif Central: evidence for melting and multiple metasomatism by silicate-rich carbonatite and asthenospheric melts. *Geol. Soc. London. Spec. Issue.*



## 公表論文 Publications

### < 原著論文 >

- Ahmed, H. A., Helmy, H. M., Arai, S., Yoshikawa, M. (2008) Magmatic unmixing in spinel from late Precambrian concentrically-zoned mafic-ultramafic intrusions, Eastern Desert, Egypt, *Lithos*, 104, 85-98.
- Arakawa, M., Yamamoto, J., Kagi, H. (2008) Micro-Raman thermometer for CO<sub>2</sub> fluids: Temperature and density dependence on Raman spectra of CO<sub>2</sub> fluids. *Chemistry Letters* 37, 280-281.
- Bianchini M., Yoshikawa, M., Sapienza, G. T. (in press) Comparative study of ultramafic xenoliths and associated lavas from South-Eastern Sicily: nature of the lithospheric mantle and insights on magma genesis. *Miner. Petrol.*
- Furukawa, Y., Temperature- and fluid-controlled seismicity in the Beppu graben, Kyushu, Japan, *J. Volcanol. Geotherm. Res.*, 181, 61-66, 2009.
- Furukawa, Y., Convergence of aqueous fluid at the corner of the mantle wedge: Implications for a generation mechanism of deep low-frequency earthquakes, *Tectonophys.*, 469, 85-92, 2009.
- Furukawa, Y., Temperature Structure under the Kinki Area, the Southwest Japan Subduction Zone, *J. Balneol. Soc. Japan*, 2009 印刷中
- 古川邦之, 三好雅也, 新村太郎, 柴田知之, 荒川洋二 (印刷中) 阿蘇カルデラ北西壁に分布する先阿蘇火山岩動との地岩石学・岩石学的研究: 先カルデラ火山活動における噴火活動とマグマ供給系, *地質学雑誌*.
- Hamada, M., Fujii, T. (2008) Experimental constraints on the effects of pressure and H<sub>2</sub>O on the fractional crystallization of high-Mg island arc basalt. *Contrib. Mineral. Petrol.*, 155, 767- 790.
- Helmy, H.M., Yoshikawa, M., Shibata, T., Arai, S., Tamura, A. (2008) Corona structure from arc mafic-ultramafic cumulates: the role and chemical characteristics of late magmatic hydrous liquids, *Journal of Mineralogical and Petrological Sciences*, 103, 333-344.
- Ishibashi, H. (2009) Non-Newtonian behavior of plagioclase-bearing basaltic magma: Subliquidus viscosity measurement of the 1707 basalt of Fuji volcano, Japan. *J. Volcanol. Geotherm. Res.*, 181, 78-88.
- Ishibashi, H., Arakawa, M., Ohi, S., Yamamoto, J., Miyake, A., Kagi, H. (2008) Relationship between Raman spectral pattern and crystallographic orientation of a rock-forming mineral: a case study of Fo<sub>89</sub>Fa<sub>11</sub> olivine. *J. Raman Spectroscopy*, 39, 1653-1659.
- Kagiyama, T., Morita, Y., (2008) First steps in understanding caldera forming eruptions(invited), *J. Disaster Res.*, 3, 270-275.
- 鍵山恒臣 (2008) 噴火卓越型火山活動と地熱活動卓越型火山活動ー新しい視点で見る火山活動ー(招待), *地熱学会誌*, 30, 193-204.
- 鍵山恒臣 (2007) 富士山の地下構造, 富士火山, 山梨県環境科学研究所, 137-150.

- Kanda, W., Tanaka, Y., Utsugi, M., Takakura, S., Hashimoto, T., Inoue, H., A preparation zone for volcanic explosions beneath Naka-dake crater, Aso volcano, as inferred from magnetotelluric surveys, *J. Volcanol. Geotherm. Res.*, 178, 32-45, 2008.
- Kanda, W., Utsugi, M., Tanaka, Y., Hashimoto, T., Fujii, I., Hasenaka, T., Shigeno, N., A heating process of Kuchi-erabu-jima volcano, Japan as inferred from geomagnetic field variation and electrical structure, *Earth Planets Space*, 61, 1-14, 2009.
- 小森省吾, 鍵山恒臣, 宇津木充, 寺田暁彦, 井上寛之, スリグトモ ワヒュー, 田中良和, 星住英夫 (2008) 雲仙火山北東部における浅部比抵抗域と熱水の関係, *火山 2 集*, 53, 131-136.
- Kusumoto, S., Takemura, K. (2008) Control Factors on Initial Caldera Geometry; Quantitative Estimation by Numerical Simulation. *Jour. School of Marine Science and Technology, Tokai Univ.*, 6, 15-26.
- Mori, T., Sudo, Y., Tsutsui, T., Yoshikawa, S., Characteristics of isolated hybrid tremor (HBT) during a calm activity period at Aso Volcano, *Bull. Volcanol.*, 2008, 70, 1031-1042 (DOI 10.1007/s00445-007-0185-7).
- Mori, T., Suzuki, T., Hirabayashi, J., Nogami, K., Ohwada, M., Yoshikawa, S., Depth estimation of fumarolic gas source deduced by fume pressure measurement, *Earth, Planets and Space*, 2008, 60 (No. 8), 889-893
- Nakagawa, T., Okuda, M., Yonenobu, H., Miyoshi, N., Fujiki, T., Gotanda, K., Tarasov, P.E., Morita, Y., Takemura, K., Horie, S. (2008) Regulation of the Monsoon Climate by Two Different Orbital Rhythms and Forcing Mechanisms. *Geology*, 36, 491-494.
- Nakamura T., Hashimoto T., Terada, A., Katsube, Y., Maruyama, J., Tsuda, T. (2008) Field observation of water vapor distribution in volcanic plumes with a Raman Lidar, Reviewed and revised papers presented at the 24th International Laser Radar Conference, 23-27 June 2008, Boulder, CO, USA., 1029 – 1032.
- Nishimura, K., (2009) A trace-element geochemical model for imperfect fractional crystallization associated with the development of crystal zoning, *Geochim. Cosmochim. Acta.*, 73, 2142-2149.
- Nishimura, K., Amita, K., Ohsawa, S., Kobayashi, T., Hirajima, T., (2008) Chemical characteristics and trapping P-T conditions of fluid inclusions in quartz veins from the Sanbagawa metamorphic belt, SW Japan, *Journal of Mineralogical and Petrological Sciences*, 103, 94-99.
- 岡本響, 大倉敬宏, 瀬野徹三 (2008) , 九州地方中南部におけるフィリピン海スラブ内地震活動, *地震 2*, 61, 77-99.
- 齋藤武士, 大沢信二, 橋本武志, 寺田暁彦, 吉川慎, 大倉敬宏 (2008) 阿蘇火山湯だまりの水・熱・塩化物イオン収支. *日本地熱学会誌*, 30, 107-120.
- 真田哲也, 高松信樹, 山崎一, 網田和宏, 大沢信二 (2008) 泉質の異なる温泉水の混合における希土類元素の挙動. *温泉科学*, 58, 81-97.
- Sano, Y., Kameda, A., Takahata, N., Yamamoto, J., Nakajima, J. (2009) Tracing extinct spreading center in SW Japan by helium-3 emanation. *Chem. Geol.* in press.
- 柴田知之, 芳川雅子, 奥水達司 (2008) 甲府盆地北縁周辺に分布する火山岩類の地球化学的特徴の時間変化と沈み込み帯の構造との関係, *MAGMA*, 89, 1 – 16.
- Srigutomo, W., Kagiyama, T., Kanda, W., Mune Kane, H., Hashimoto, T., Tanaka, Y., Utada, H., Utsugi, M., (2008) Resistivity structure of Unzen Volcano derived from Time Domain

- Electromagnetic (TDEM) survey, J. Volcanol. Geotherm. Res., 175, 231-240.
- Takano, B., A. Kuno, A., Ohsawa, S., Kawakami, H. (2008) Aqueous sulfur speciation possibly linked to sublimic volcanic gas-water interaction during a quiescent period at Yugama crater lake, Kusatsu-Shirane volcano, Central Japan. J. Volcanol. Geotherm. Res., 178, 145-168.
- 竹村恵二(2008) 横尾遺跡周辺の地質と地形および横尾遺跡立地との関連. 大分市教育委員会
- 竹村恵二(2008) 関西圏の地質・断層—関西の地盤・プロジェクトと関連して. 地盤工学会関西支部 50 周年記念誌, 38-41.
- 竹村恵二, 水谷崇亮, 利藤房男(2008) 関西国際空港の建設と地盤工学的諸問題 3. 地盤調査(その1). 地盤工学会誌, 56-5(604), 32-39. 口絵写真 9-11.
- Terada, A., Sudo, Y. Geothermal activities at the western slope geothermal zone at Aso volcano, Japan: Development of new geothermal field in 2006, Geothermics, submitted.
- 寺田暁彦, 吉川慎 (2009) 接近困難な強酸性火口湖における観測技術—水温モニタリング・湖水および湖底泥の採取—, 日本地熱学会誌, 31, 117-128.
- 寺田暁彦, 大島弘光, 松島喜雄, 鍵山恒臣(2008) 有珠火山 2000 年新山からの総放熱率とその変遷—1977 年噴火後の貫入マグマ冷却過程との比較, 日本地熱学会誌, 30, 259-270.
- Terada, A., Hashimoto, T., Kagiyama, T., Sasaki, H. (2008) Precise remote-monitoring technique of water volume and temperature of a crater lake in Aso volcano, Japan: Implication for a sensitive window of volcanic hydrothermal system, Earth Planets Space, 60, 705-710.
- Terada, A., Kagiyama, T., Oshima, H. (2008) Ice Box Calorimetry: A handy method for estimation of heat discharge rates through a steaming ground, Earth Planets Space, 60, 699-703.
- 筒井智樹, 及川純, 鍵山恒臣, 富士火山人工地震構造探査グループ (2007) 人工地震で見た富士火山の内部構造, 物理探査, 60, 131-144.
- 内田東, 佐藤孝久, 山下隆丞, 寺田暁彦, 噴気地における地表面温度と放熱率の経験的關係—赤外カメラと氷箱熱流計測による同時観測実験—, 火山, 印刷中.
- Utada, H., Takahashi, Y., Morita, Y., Koyama, T., Kagiyama, T. (2007) ACTIVE system for monitoring volcanic activity: A case study of the Izu-Oshima Volcano, Central Japan, J. Volcanol. Geotherm. Res., 164, 217-243.
- Yamada, M., Ohsawa, S., Matsuoka, H., Watanabe, Y., Brahmantyo, B., Maryunani, K. A., Tagami, T., Kitaoka, K., Takemura, K., Yoden, S. (2008) Derivation of travel time of limestone cave drip water using tritium/helium 3 dating method, Geophys. Res. Lett., 35, L08405, doi:10.1029/2008GL033237
- Yamamoto, J., Ando, J., Kagi, H., Inoue, T., Yamada, A., Yamazaki, D., Irifune, T. (2008) In situ strength measurements on natural upper-mantle minerals. Physics and Chemistry of Minerals, 35, 249-257.
- Yamamoto, J., Kagi, H. (2008) Application of micro-Raman densimeter for CO<sub>2</sub> fluid inclusions: a probe for elastic strengths of mantle minerals. European Journal of Mineralogy, 20, 529-535.
- Yamamoto, J., Nakai, S., Nishimura, K., Kaneoka, I., Kagi, H., Sato, K., Okumura, T., Prikhod'ko, V.S., Arai, S. (2009) Intergranular trace elements in mantle xenoliths from



Russian Far East: An example for mantle metasomatism by hydrous melt. *Island Arc*, 18, 225-241.

Yamamoto, J., Nishimura, K., Sugimoto, T., Takemura, K., Takahata, N., Sano, Y. (2009) Diffusive fractionation of noble gases in mantle with magma channels: origin of low He/Ar in mantle-derived rocks. *Earth Planet. Sci. Lett.* 280, 167-174.

Yoshikawa, M., Kawamoto, T., Shibata, T., Yamamoto, J. (in press) Geochemical and Sr-Nd isotopic characteristics and P-T estimates of mantle xenoliths from the French Massif Central: evidence for melting and multiple metasomatism by silicate-rich carbonatite and asthenospheric melts. *Geol. Soc. London. Spec. Issue*.

#### < 報告書等 >

後藤章夫, 鍵山恒臣, 宮本毅, 横尾亮彦, 谷口宏充 (2007) 放熱率測定に基づいた有珠 2000 年噴火の活動推移長期予測, 北海道大学地球物理学研究報告, 70, 137-144.

鍵山恒臣 (2009) 霧島火山群－火山群における災害の視点－, 震災予防, 224, 7-10.

鍵山恒臣, 森田裕一 (2008) カルデラ生成噴火の準備過程の理解に向けて, 月刊地球, 号外 60, 5-7.

鍵山恒臣 (2008) カルデラ生成噴火の準備過程－解明のための作業仮説の提案, 月刊地球, 号外 60, 10-20.

鍵山恒臣, 宇津木充, 吉川慎, 寺田暁彦 (2008) 伽藍岳・塚原の地熱活動の周辺域への広がりに関する調査, 大分県温泉調査研究会報告, 59, 35-39.

鍵山恒臣, 寺田暁彦, 吉川慎 (2007) 塚原噴気地帯における噴気活動の短周期時間変動特性, 大分県温泉調査研究会報告, 58, 69-86.

鍵山恒臣 (2007) マグマからの脱ガスと電磁気観測－休止期の長い噴火を考える, *Conductivity Anomaly* 研究会 2007 年論文集, 67-74.

川本竜彦, 高松尚久, 黒岩健一, 高圧下の氷の分子模型をつくる－水の構造を理解するために－現代化学, 444, 51-54, 2008.

小森省吾, 鍵山恒臣, 宇津木充, 寺田暁彦, 井上寛之, スリグトモ ワヒュー, 田中良和, 星住英夫 (2007) 火山体浅部における比抵抗構造と熱水, *Conductivity Anomaly* 研究会 2007 年論文集, 79-80.

中西利典, 竹村恵二, 斉藤武士, 松山尚典, 柴田康行 (2008) 朝見川断層付近のボーリングコアの堆積環境と堆積年代の対比. 大分県温泉調査研究会報告, 59, 3-11.

大久保綾子, 中塚正, 宇津木充, 田中良和, 井上寛之, 神田径, 為栗健, 石原和弘, 高山鐵朗, 小山崇夫, Hurst, A.W., 桜島電磁気構造探査グループ, 桜島火山 2007 年-2005 年空中磁気データから検出された磁気異常変化, 第 10 回桜島火山の集中総合観測報告書, 83-87, 2008.

大沢信二, 渡邊康平, 高松信樹, 加藤尚之 (2008) 未利用温泉資源量に関する基礎調査と研究 (II) -温泉から河川への有用金属元素の流出量-. 大分県温泉調査研究会報告, 59, 13-19.

寺田暁彦, 鍵山恒臣 (2009) 活動的の火口湖からの湖面蒸発量測定の新手法開発－ライダー技術の「安全・安心」への応用－, 平成 20 年度生存圏萌芽・融合ミッションシンポジウム講演要旨集, 83-89.

寺田暁彦 (2009) 阿蘇火山中岳第一火口の熱活動－2008 年度の位置付け－, 阿蘇火山集中総合観測成果報告書, 105-117.

寺田暁彦, 鍵山恒臣, 中村卓司, 太田修史, 橋本武志 (2009) 阿蘇火山火口湖からの湖面蒸発量

- 推定高精度化の試みーラマン・ライダーおよび水温観測ブイによる観測ー, 阿蘇火山集中総合観測成果報告書, 138-145.
- 寺田暁彦, 鍵山恒臣, 松島喜雄, 吉川慎, 吉川章文, 小山寛, 山崎伸行, 平松秀行, 大島弘光 (2009) 有珠火山 2000 年新山の総放熱率, 北海道大学地球物理学研究報告, 72, 139-157.
- 寺田暁彦, 鍵山恒臣, 吉川慎, 吉川章文, 小山寛, 山崎伸行, 平松秀行, 大島弘光 (2009) 氷を用いた噴気地からの放熱率評価ー有珠火山 2000 年新山西山噴気地での観測実験ー, 北海道大学地球物理学研究報告, 72, 125-138.
- 寺田暁彦, 橋本武志 (2008) 阿蘇の火口湖「湯だまり」が 1,500 年間も維持されている理由, 地球 号外, 60, 121-132.
- 寺田暁彦, 鍵山恒臣, 吉川慎 (2008) 阿蘇火山・中央火口丘群における熱活動の定量化, 京都大学防災研究所年報, 51, 275-290.
- 後小路義弘, 寺田暁彦 (2009) カラーチャート (色見本) を用いた火口湖表面色の定量的評価, 阿蘇火山集中総合観測成果報告書, 130-137.
- 宇津木充, 井上寛之, 神田径, 石原和弘, 高山鐵朗, 為栗健, 大久保綾子, 小山崇夫, 田中良和, 桜島電磁気構造探査グループ, 桜島火山及び始良カルデラにおける空中磁気観測, 第10回桜島火山の集中総合観測報告書, 75-82, 2008
- 山田誠, 大沢信二, 風早康平, 安原正也, 高橋浩, 網田和宏, 馬渡秀夫, 吉川慎 (2008) 同位体水文学的手法による火山地下水流動系へのマグマ起源 CO<sub>2</sub> の混入過程の研究ー阿蘇火山を例にしてー, 月刊地球, No. 60, 114-120
- 吉川慎, 宇津木充, 阿蘇火山中岳第一火口湖における湖水の採水手法の確立, 平成 20 年度京都大学総合技術研究会報告集第Ⅱ分冊, 312-313

#### < 学会発表 Conference Presentations >

- Abe, Y., Ohkura, T., Hirahara, K., Kato, M., Shibutani, T., Crustal structure beneath Aso caldera, southwest Japan, as derived from receiver functions, ASC Meet. (2008 年 11 月筑波)
- Abe, Y., Ohkura, T., Hirahara, K., Kato, M., Shibutani, T., Crustal structure beneath Aso caldera, southwest Japan, as derived from receiver functions, AGU, Fall Meet. (2008 年 12 月サンフランシスコ U. S. A.)
- Bianchini M., Sapienza, G. T., Yoshikawa, M., The lithospheric mantle beneath the Hyblean area – Insights from mantle xenoliths Goldschmidt Conference (2008 年 7 月バンクーバ Canada)
- 越後智雄, 郡谷順英, 岩崎孝明, 小俣雅志, 岡田篤正, 寒川旭, 竹村恵二, 北田奈緒子, 井上直人. 中央構造線断層帯, 根来断層登尾および枇杷谷地区における活動履歴調査. 地球惑星科学連合大会 (2008 年 5 月幕張).
- 藤井頌子, 石川尚人, 齋藤武士, 杉本健, 竹村恵二. 古地磁気方位と古地球磁場強度による鶴見岳山頂溶岩の年代推定の試み. 地球惑星科学連合大会 (2008 年 5 月幕張).
- 藤井俊行, 福谷哲, 芳川雅子, 柴田知之, 山名元, 固液平衡系でのストロンチウムの同位体分別に関する研究, 同位体科学研究会 (2009 年 3 月 神奈川)
- 浜田盛久, 川本竜彦, 藤井敏嗣. 火山フロントに産する玄武岩質マグマの Ca に富む斜長石斑晶の含水量, 地球惑星科学連合大会 (2008 年 5 月幕張).
- 浜田盛久, Didier Laroche, Nicolas Cluzel, Kenneth Koga, 川本竜彦. 高速減圧実験により得ら

- れる珪長質マグマの気泡数密度，地球惑星科学連合大会（2008年5月幕張）。
- 浜田盛久，川本竜彦，藤井敏嗣．初生的な島弧玄武岩マグマは水に富む—Ca に富む斜長石斑晶の水素含有量からの制約—，2008年度日本地球化学会第55回年会（2008年9月東京大学）
- 浜田盛久，川本竜彦，藤井敏嗣．初生的な島弧玄武岩マグマは水に富む—Ca に富む斜長石斑晶の水素含有量からの制約—，日本火山学会2008年度秋季大会（2008年10月岩手大学）
- 林田明，安田雅彦，宮島有梨，竹村恵二，原口強．琵琶湖のピストン・コア試料の磁気特性 - 初期磁化率による堆積物の対比．地球惑星科学連合大会（2008年5月幕張）。
- 原口強，奥元かおり，竹村恵二，林田明．琵琶湖湖底高分解能音響反射断面アーカイブ計画．地球惑星科学連合大会（2008年5月幕張）。
- Inoue, N., Kitada, N., Takemura, K., Tabata, T. and Emura, T. Image processing for continuous digital borehole core images from KIX18-1, Japan. 33<sup>rd</sup> IGC, Oslo( Norway), Aug 2008.
- Inoue, N., Kitada, N. and Takemura, K. Neotectonic basement and stratigraphic characteristics around Kansai International airport (KIX), Osaka sedimentary basin, Japan based on integrated analysis of geophysical survey data. 33<sup>rd</sup> IGC, Oslo( Norway), Aug 2008.
- Inoue, N., Kitada, N., Takemura, K. Relationship between earthquake source faults and 3D density structures derived by gravity anomaly inversion in Japan. AGU Fall meeting, San Francisco, Dec. 2008.
- 石橋秀巳，荒川雅，大井修吾，山本順司，三宅亮，鍵裕之．Fo<sub>89</sub>Fa<sub>11</sub> オリビンのラマンスペクトルの結晶方位依存性．日本鉱物科学会（2008年9月，秋田大学）。
- 石橋秀巳，荒川雅，山本順司，鍵裕之．顕微ラマン分光法によるオリビンの Fo#の決定．地球惑星科学連合大会（2008年5月幕張）。
- 石橋秀巳，荒川雅，大井修吾，山本順司，三宅亮，鍵裕之；Fo<sub>89</sub>Fa<sub>11</sub> オリビンのラマンスペクトルパターンと結晶方位の関係．地球惑星科学連合大会（2008年5月幕張）。
- 岩部智紗，竹村恵二，林田明，原口強，檀原徹．マルチサイトピストンコアによる過去5万年の琵琶湖堆積物層序．地球惑星科学連合大会（2008年5月幕張）。
- 泉谷健太郎，渡邊裕美子，松岡廣繁，上田純，一田昌宏，山田誠，太沢信二，中井俊一，BrahmantyoBudi，MaryunaniKhoiril A.，田上高広，竹村恵二，余田成男．インドネシア・ジャワ島、中部および東部石筍試料の年代モデルの構築．地球惑星科学連合大会．地球惑星科学連合大会（2008年5月幕張）。
- 鍵山恒臣．カルデラ生成噴火の準備過程解明のための作業仮説の提案，地球惑星科学連合大会（2008年5月幕張）。
- 鍵山恒臣，宇津木充，吉川慎，寺田暁彦．伽藍岳火山周辺の表層比抵抗分布，日本火山学会秋季大会（盛岡市，2008年10月11-13日）
- 川本竜彦，神崎正美，三部賢治，松影香子，小野重明，臨界終端点を探す：ミベセルを用いたX線ラジオグラフィーは不当に低い圧力を提案しているのか？地球惑星科学連合大会（2008年5月幕張）。
- 川本竜彦，高松尚久，黒岩健一，モル・タロウで高压の氷の分子模型を作る．地球惑星科学連合大会（2008年5月幕張）。
- 川本竜彦，熊谷仁孝，中越邁，佐藤良祐，黒岩健一，高松尚久，高压条件における水と氷6と氷12のその場観察とラマン分光．地球惑星科学連合大会（2008年5月幕張）。

川本竜彦, 沈み込むスラブ由来の水流体を高温高压実験で観察する. 神戸大学地球惑星談話会  
2008 年 7 月 25 日

川本竜彦, 沈み込み帯でのマグマ作りに二酸化炭素は重要か? 地球化学会年会, 2008 年 9 月, 東京大学教養学部

川本竜彦, 神崎正美, 三部賢治, 松影香子, 小野重明, スラブ由来流体相が超臨界流体であることの意義, 日本地質学会, 日本鉱物科学会, 2008 年 9 月, 秋田大学

Kawamoto, T. Fluids in subduction zone 1: significance of elemental partitioning between aqueous fluids and silicate melts. 1st TANDEM Workshop 2008, 2008 年 11 月, GRC, Ehime University

Kitada, N., Inoue, N., Takemura, K., Mitamura, M., Oshima, A. Subsurface Geology in Osaka plain using Borehole database and its application. 33<sup>rd</sup> IGC, Oslo( Norway), Aug 2008.

Kitada, N., Inoue, N., Takemura, K., Masuda, F., Hayashida, A., Tabata, T., Emura, T. Stratigraphy around Kansai Airport and its properties (Reconstruction of the Osaka Group (Pliocene to Pleistocene) in the southern Osaka Basin, Japan. 33<sup>rd</sup> IGC, Oslo( Norway), Aug 2008.

Kitada, N., Inoue, N., Takemura, K. Relationship between Bouguer anomaly and active fault ( source fault) - For the purpose of estimate of source fault -. AGU Fall meeting, San Francisco, Dec. 2008.

北田奈緒子, 井上直人, 竹村恵二, 三田村宗樹, 大島昭彦. 関西圏における表層地質の分布状況～西大阪平野と東大阪平野地域～. 地球惑星科学連合大会 (2008 年 5 月幕張).

北田奈緒子, 井上直人, 竹村恵二, 岡田篤正, 金谷賢生, 岩森暁如, 福本彦吉. 丹後半島地域の重力異常と北丹後地震について. 地球惑星科学連合大会 (2008 年 5 月幕張).

北田奈緒子, 井上直人, 竹村恵二, 三田村宗樹, 大島昭彦. 大阪平野の表層地盤構造～ボーリングデータベースから見えてくること～. 地球惑星科学連合大会. (2008 年 5 月幕張).

小森省吾, 鍵山恒臣 火山体浅部における熱水と比抵抗構造との関係, 平成 20 年度京都大学防災研究所研究発表講演会 (京都市, 2009 年 2 月)

小森省吾, 鍵山恒臣 火山周辺の電気伝導度分布への火山ガス散逸の寄与, 日本火山学会秋季大会 (盛岡市, 2008 年 10 月 11-13 日)

小森省吾, 鍵山恒臣, 宇津木充, 寺田暁彦, 井上寛之, スリグトモ ワヒュー, 田中良和, 星住英夫 火山体浅部における比抵抗構造と熱水流動との関係, 地球惑星科学連合大会 (2008 年 5 月幕張).

小山崇夫, 宗包浩志, 鍵山恒臣, 歌田久司 九州中部比抵抗構造の再解析, 地球惑星科学連合大会 (2008 年 5 月幕張).

Meyers, P.A., Takemura, K. 38 ky East Asian monsoon record from sediments of Lake Biwa JAPAN. 33<sup>rd</sup> IGC, Oslo( Norway), Aug 2008.

三浦勉, 飯尾能久, 片尾浩, 澁谷拓郎, 宮澤理稔, 井口正人, 平野憲雄, 西村和浩, 大見士朗, 平原和朗, 大倉敬宏, 松本聡, 高畠一徳, 大橋善和, 古屋和男, 満点 (万点) 計画-次世代型地震計の開発-, 地球惑星科学連合大会

水上知行, 荒川雅, 山本順司, 鍵裕之, 榎並正樹, 川本竜彦, 小林記之, 平島崇男, 小山内康人, 石橋秀巳, Madhusoodhan Satish-Kumar, ラマン密度計のための二酸化炭素標準試料. 日本地球惑星科学連合大会, 2008 年 5 月, 幕張メッセ

宮縁育夫, 寺田暁彦, 阿蘇火山中岳第 1 火口で採取された湖底堆積物 (予報), 日本火山学会秋季

大会, 盛岡市, 2008 年 10 月.

大久保寛, 竹内昭洋, 渡辺峻, 中村教博, 長濱裕幸, 中村行信, 竹内伸直, 宇津木充, 笹井洋一, 平成 20 年岩手・宮城内陸地震の発振時刻からの地磁気変動信号の観測, 地球電磁気学会, 2008 年 10 月

大久保寛, 竹内昭洋, 渡辺峻, 中村教博, 長濱裕幸, 中村行信, 竹内伸直, 宇津木充, 笹井洋一, 平成 20 年岩手・宮城内陸地震の発振時刻からの地磁気変動信号の観測, 日本地震学会, 2008 年 11 月

大倉敬宏, 及川純, 阿蘇火山における GPS 観測, 火山学会秋季大会 (2008 年 10 月盛岡)

大倉敬宏, 吉川慎, 井上寛之, 宇津木充, 山本圭吾, 高山鐵朗, 松島健, 山崎友也, 多田光宏, 内田和也, 平岡喜文, 三森庸里江, 根本盛行, 加納将行, 由井智志, 中元真美, 山下裕亮, 立尾有騎, 寺田暁彦, 鍵山恒臣, 阿蘇カルデラにおける水準測量 (2008 年 9 月-10 月), 2008 年度京都大学防災研究所研究発表講演会 (2009 年 2 月 京都).

大沢信二, 鍾乳洞の気象と鍾乳石の成長, 平成 20 年度大分地質学会, 特別講演 (2009 年 1 月大分大学)

奥元かおり, 原口強, 西川泰平, 吉永佑一, 垣内佑哉, 石村大輔, 北川浩之, 竹村恵二, 林田明, 横川美和, 琵琶湖北湖湖底表層の高分解能音波探査, 地球惑星科学連合大会 (2008 年 5 月幕張).

Python, M., Arai, S., Interactions between high-T hydrothermal fluids and mantle lithologies: evidence from the Oman fossilised spreading centre, EGU meeting 2009 (April 19-24, 2009, Vienna, Austria).

Shibata, T., Kobayashi, T., Sugimoto, T., Ujike, O., Itoh, J., Takemura, K. (2008) The lateral variations of Sr, Nd and Pb isotopic and trace element compositions for Quaternary volcanics from Kyushu, Japan, Asia Oceania Geosciences Society, 2008 年 6 月 16 日, 韓国・釜山

柴田知之, 芳川雅子, 奥水達司 (2008) 甲府盆地北縁に分布する火山岩類の地球化学的時間変化に対するフィリピン海プレートの役割, 日本鉱物科学会, 2008 年 9 月 20 日、秋田.

田部井隆雄, 木股文昭, 大倉敬宏, フィリピン-インドネシア東部変動帯におけるプレート収束速度の推定, 地球惑星科学連合大会 (2008 年 5 月幕張).

Takemura, K., Okuda, M., Nakagawa, T., Hayashida, A., Meyers, P. A., Horie, S. Lake Biwa drilling project: Providing improved paleoclimate variations and Island Arc tectonics during the past 1 Ma. 33<sup>rd</sup> IGC, Oslo (Norway), Aug 2008.

Takemura, K., Kitada, N., Furudoi, T., Nakaseko, K. Subsurface geology of Kansai International Airport: Sequence related to global glacial -- interglacial cycles. 33<sup>rd</sup> IGC, Oslo (Norway), Aug 2008.

Takemura, K., Hayashida, A., Haraguchi, T. 60 ky high resolution record of the environmental change from Sediments of Lake Biwa, Japan. AGU Fall meeting, San Francisco, Dec. 2008.

竹村恵二, 林田明, 原口強, 北川浩之, 鳥居雅之, 石川尚人, 豊田和弘, 琵琶湖掘削計画の進展—2007 年調査成果の概要. 地球惑星科学連合大会 (2008 年 5 月幕張).

寺田暁彦, 大島弘光, 吉川慎, 鍵山恒臣, 氷を用いた噴気地からの熱および水放出量測定—室内実験および野外観測による検証—, 日本地熱学会平成 20 年金沢大会, 金沢市, 2008 年 11 月

寺田暁彦, 吉川慎, 大島弘光, 松島喜雄, 鍵山恒臣, 氷箱熱流計測(IBC)による有珠 2000 年新山の放熱率評価—1977 年噴火後のマグマ冷却過程との比較—, 日本火山学会秋季大会, 盛岡市,

2008 年 10 月

寺田暁彦, 吉川慎, 橋本武志, 鍵山恒臣, 佐々木寿, 阿蘇火山中岳火口湖（湯だまり）における水温・溶存成分濃度の変動解析, 日本火山学会秋季大会, 盛岡市, 2008 年 10 月

寺田暁彦, 火口湖「湯だまり」を道具として阿蘇火山内部を診る, 阿蘇火山博物館セミナー, 2008 年 7 月.

寺田暁彦, 大島弘光, 鍵山恒臣, 噴気地から放出される熱・水量の新しい測定手法—室内実験による検証—, 地球惑星科学連合大会 (2008 年 5 月幕張).

寺田暁彦, 鍵山恒臣, 橋本武志, 佐々木寿, 阿蘇火山における火口湖を通じた熱活動, 地球惑星科学連合大会 (2008 年 5 月幕張).

寺田暁彦, 橋本武志, 鍵山恒臣, 佐々木寿, 阿蘇火山火口湖周辺の火山性流体輸送モデル, 地球惑星科学連合大会 (2008 年 5 月幕張).

上田純, 渡邊裕美子, 野本哲也, 小林記之, 山田誠, 松岡廣繁, 下林典正, 平島崇男, BrahmantyoBudi, MaryunaniKhoiril A., 大沢信二, 田上高広, 竹村恵二, 余田成男. A high-resolution age model from annual bandings in a stalagmite collected in Java, Indonesia. 地球惑星科学連合大会 (2008 年 5 月幕張).

宇内克成, 鍵山恒臣, 宇津木充, 神田径, 吉川慎, 寺田暁彦, 小森省吾, 霧島火山群・硫黄山周辺における浅部比抵抗構造, 地球惑星科学連合大会 (2008 年 5 月幕張).

宇津木充, 桜島構造探査空中磁気探査グループ, 桜島・始良カルデラに於ける空中磁気探査, 京都大学防災研究所年会, 2008 年 2 月

宇津木充, 桜島構造探査空中磁気探査グループ, 桜島火山及び始良カルデラに於ける空中磁気探査, 地球惑星科学連合大会 (2008 年 5 月幕張).

宇津木充, 繰り返し空中磁気観測による火山地磁気効果検出の試み, 地球惑星科学連合大会 (2008 年 5 月幕張).

宇津木充, 地震地磁気効果における動的シミュレーションについて, 地球電磁気学会, 2008 年 10 月

宇津木充, 地震波伝播に伴う動的地震地磁気効果の定式化, CA 研究集会, 2008 年 2 月

渡邊裕美子, 松岡廣繁, 坂井三郎, 上田純, 山田誠, 大沢信二, 木口雅司, 里村雄彦, 中井俊一, BrahmantyoBudi・MaryunaniKhoiril A., 田上高広, 竹村恵二, 余田成男. Rainfall fluctuation recorded in a stalagmite from West Java, Indonesia. 地球惑星科学連合大会 (2008 年 5 月幕張).

渡邊裕美子, 松岡廣繁, 坂井三郎, 上田純, 山田誠, 大沢信二, 木口雅司, 里村雄彦, 中井俊一, BrahmantyoBudi, MaryunaniKhoiril A., 田上高広, 竹村恵二, 余田成男. Paleoclimatic Reconstruction Using Indonesian Stalagmites: an Overview. 地球惑星科学連合大会 (2008 年 5 月幕張).

山田誠, 大沢信二, 松岡廣繁, 渡邊裕美子, BrahmantyoBudi, MaryunaniKhoiril A., 田上高広, 北岡豪一, 竹村恵二, 余田成男. Derivation of travel time of limestone cave drip water using tritium/helium-3 dating method. 地球惑星科学連合大会 (2008 年 5 月幕張).

Yamada, M., Ohsawa, S., Matsuoka, H., Watanabe, Y., Brahmantyo, B., Maryunani, K. A., Tagami, T., Kitaoka, K., Takemura, K., and Yoden, S. Derivation of travel time of limestone cave drip water using tritium/helium-3 dating method. 地球惑星科学連合大会 (2008 年 5 月幕張)

Yamamoto J., Kurz M.D. Estimates of noble gas contents of pre-degassed oceanic

basalts: implications for undegassed mantle sources, AGU, Fall Meet. (2008 年 12 月サンフランシスコ U. S. A.)

安田雅彦, 宮島有梨, 林田明, 竹村恵二, 原口強. 琵琶湖のピストン・コア堆積物から得られた古地磁気永年変化の記録. 地球惑星科学連合大会 (2008 年 5 月幕張).

Yoshikawa, M., Niida, K. Rb-Sr isotopic systematics of two-pyroxenes and olivines in the dunnite channel from the Horoman peridotite complex, Japan, Goldschmidt Conference (2008 年 7 月バンクーバ Canada)

芳川雅子, 新井田清信, 幌満かんらん岩体ダナイトチャネルの Rb-Sr 年代, 日本鉱物科学会 (2008 年 9 月, 秋田)

芳川雅子, 川本竜彦, 山本順司, フランス中央山塊マントル捕獲岩のSr-Nd 同位体・岩石学的特徴, 日本地球化学会 (2008年9月, 東京)

吉川慎, 大学の技術職員のお仕事, 阿蘇火山博物館セミナー (2009年3月, 阿蘇火山博物館)

吉川慎, 宇津木充, 阿蘇火山中岳第一火口湖における湖水の採水手法の確立, 平成20年度京都大学総合技術研究会 (2009年3月, 京都)



## 共同研究一覧 List of Collaborations

### 国内

鍵山恒臣, 小森省吾, 歌田久司, 東京大学地震研究所一般共同研究 2008-G-16 雲仙火山における  
比抵抗の微視的構造と岩石物性との対応関係  
鍵山恒臣, 京都大学生存圏研究所 研究担当  
鍵山恒臣, 京都大学防災研究所 研究担当  
川本竜彦, 愛媛大学地球深部ダイナミクス研究センター 客員研究員  
大倉敬宏, 東京大学地震研究所特定共同研究(B) 衛星リモートセンシングによる地震・火山活動  
の解析  
大倉敬宏, 東京大学地震研究所特定共同研究(B) フロンティア観測地球科学の推進  
大倉敬宏, 東京大学地震研究所客員教員  
大沢信二, 産業技術総合研究所深部地質環境研究コア深部流体研究グループ 客員研究員  
Marie Python, 金沢大学理工学域自然システム学系(地球科学教室) 自然科学研究科環境科学専攻  
荒井章司と共同研究  
竹村恵二, 京都大学防災研究所一般共同研究(19G-09) 代表: 山本浩司(財団法人地域地盤環  
境研究所主席研究員) (分担): 電子地盤図の作製と地盤防災アセスメントへの有効活用  
に関する研究  
竹村恵二, 京都大学防災研究所特別研究経費 代表: 関口秀雄(分担): 津波堆積物に着目した災  
害環境の復原に関する研究—田辺湾ジオアーカイブズの展開  
竹村恵二, 経済産業省原子力保安院 活断層地下構造高精度化  
竹村恵二, 独立行政法人産業技術総合研究所併任 (図幅担当)  
竹村恵二, 京都大学防災研究所 研究担当(地盤災害研究部門)  
吉川慎, 産業技術総合研究所 協力研究員

### 国際

Marie Python, Georges Ceuleneer, Observatoire Midi-Pyrénées, C.N.R.S.-Université de  
Toulouse, France.  
竹村恵二, ICDP Project, Lake Biwa and Lake Suigetsu: Records of Global  
Paleoenvironments and Island Arc Tectonics.

## 研究費 Funding

### 科学研究費補助金

石橋秀巳(分担), 基盤研究(C) (代表: 神戸大学教授 佐藤博明) 火山噴火様式の予測に関する基  
礎的研究. 3640 千円.  
鍵山恒臣(代表), 基盤研究(B) カルデラ噴火準備過程解明のための火山地域地下構造とマグマ活  
動の研究 4700 千円  
川本竜彦(代表), 基盤研究(C) 高温高压実験による沈み込むスラブ由来流体の化学組成の理解,  
1000 千円  
川本竜彦(分担), (代表: 愛媛大学准教授 井上徹) 新学術領域研究(研究領域提案型) 高压下におけ  
るマグマの物性と構造, 及びその水の影響, 500 千円



大沢信二(代表), 基盤研究(C)一般 鍾乳石の茶色い縞々に着目した古気候変動復元技術構築に関する基礎的研究, 2600 千円

柴田知之(代表), 基盤研究(C) 沈み込むスラブが部分熔融する物理条件の推定, 800 千円

竹村恵二(代表), 基盤研究(A) 琵琶湖堆積物の高精度マルチタイムスケール解析ー過去15万年間の気候・地殻変動, 19400 千円

竹村恵二(分担), 基盤研究(B) (代表: 奈良女子大学教授 高田将志) 琵琶湖周辺域における土砂供給源の時代変化: 気候変化で土砂供給源地は変わるか? 695 千円

竹村恵二(分担), 基盤研究(B) (代表: 名古屋大学教授 北川浩之) 天池堆積物の高分解能解析による過去5万年間の大気中の炭素14濃度変化の解明, 500 千円

寺田暁彦(分担), (代表: 北海道大学准教授 橋本武志), 萌芽研究, 火山噴煙のリモートセンシングに関する新手法の開発, 3300 千円

山本順司(代表), 若手研究(B) 超高精度地質圧力計の開発とマントル流体の四次元精査, 500 千円

芳川雅子(代表), 基盤研究(C) 上部マントルでのマグマ移動の解明: 鉱物の同位体組成を用いた新たな試み, 700 千円

吉川慎 (代表), 奨励研究 阿蘇中岳第一火口湯だまりの採水手法の確立, 580千円

#### 受託研究, 奨学寄付金, 企業との共同研究

鍵山恒臣, 大分県温泉調査研究会, 平成20年度調査研究事業(研究課題: 鶴見・伽藍岳周辺の噴気活動の調査, 70 千円)

鍵山恒臣, 寺田暁彦, 中村卓司, 橋本武志, 京都大学生存圏研究所 平成20年度萌芽ミッションプロジェクト, 活動的火口湖からの湖面蒸発量測定の新手法開発ーライダー技術の「安全・安心」への応用ー, 600千円.

大沢信二, 産業総合技術研究所地質環境研究コア深部流体研究グループ研究費 1000 千円

柴田知之, 九電産業, 「熱水のストロンチウム同位体組成の測定」に対する研究助成, 400 千円

柴田知之, 日鉱探開, 「熱水のストロンチウム同位体組成の測定」に対する研究助成, 380 千円

柴田知之, 芳川雅子, 伊藤勇二, 服部良太, キリンホールディングス, 「重金属の同位体分析技術の開発」, 4050 千円 (継続)

柴田知之, 芳川雅子, 杉本健, 赤塚貴史, 地熱エンジニアリング, 「松川地熱地帯に分布する貫入岩の化学的特徴と変質との関係」, 357 千円

竹村恵二, 地域地盤環境研究所, 近畿地域の活断層の研究, 1000千円

寺田暁彦, 財団法人防災研究協会若手研究者研究助成, 阿蘇火山・火口湖水の連続水温観測ー火山爆発シナリオの作成に向けてー 500 千円.

山田誠, 笹川科学研究助成金, 鍾乳洞地下水の滞留時間の研究ー古気候変動解明への水文学的アプローチー 680 千円

芳川雅子, 九電産業株式会社, 地球化学的手法を用いた地球熱学プロセスの解明 553 千円

## 教育活動 Education

### 学位, 授業 Academics

#### 学位審査

鍵山恒臣：	(審査員)	Nurlia Sadikin (博士 京都大学大学院理学研究科)
	(審査員)	立尾有騎 (修士 京都大学大学院理学研究科)
	(審査員)	岩部智紗 (修士 京都大学大学院理学研究科)
	(審査員)	高木 悠 (修士 京都大学大学院理学研究科)
大倉敬宏：	(審査員)	Nurlia Sadikin (博士 京都大学大学院理学研究科)
	(主査)	安部祐希 (修士 京都大学大学院理学研究科)
	(審査員)	北脇裕太 (修士 京都大学大学院理学研究科)
	(審査員)	立尾有騎 (修士 京都大学大学院理学研究科)
大沢信二：	(審査員)	秋山裕二 (修士 京都大学大学院理学研究科)
	(審査員)	岡野和行 (修士 京都大学大学院理学研究科)
	(審査員)	中屋志郎 (修士 京都大学大学院理学研究科)
竹村恵二：	(主査)	岩部智紗 (修士 京都大学大学院理学研究科)
	(副査)	垣内佑也 (修士 京都大学大学院理学研究科)
	(副査)	石村大輔 (修士 京都大学大学院理学研究科)
	(副査)	西川泰平 (修士 京都大学大学院理学研究科)
	(審査員)	安部祐希 (修士 京都大学大学院理学研究科)
	(審査員)	樋口衡平 (修士 京都大学大学院理学研究科)
	(審査員)	高橋優子 (修士 京都大学大学院理学研究科)

### 講義, ゼミナール

#### (学部)

地球科学実験 B	川本竜彦ほか
ポケットゼミ：火山の噴火を見てみよう Introductory Seminar on Observation in Volcanoes	
	鍵山恒臣, 大倉敬宏, 宇津木充
地球惑星科学入門 II	中西一郎, 福田洋一, 竹村恵二
観測地球物理学演習 A	鍵山恒臣, 大倉敬宏, 宇津木充, 里村雄彦, 宮崎真一, 西憲敬, 斉藤昭則
観測地球物理学演習 B	竹村恵二, 大沢信二, 柴田知之, 川本竜彦, 堤浩之
グローバルテクニクス	田上高広, 古川善紹
地球熱学	竹村恵二, 鍵山恒臣, 大沢信二, 川本竜彦, 柴田知之
火山物理学 I	古川善紹
火山物理学 II	鍵山恒臣, 大倉敬宏, 石原和弘, 井口正人, 宇津木充
陸水学	大沢信二, 諏訪浩
課題演習 DA 固体地球系	古川善紹ほか
課題演習 DC (マグマの発生から噴火まで)	鍵山恒臣, 大沢信二, 柴田知之, 川本竜彦, 宇津木充
課題演習 DC (地球のパターン)	古川善紹
課題演習 DC (活構造)	堤浩之, 岩田知孝, 竹村恵二
課題演習 DC (地震学)	平原和朗, 久家慶子, 大倉敬宏
課題研究 DD：気象学総合演習	余田成男, 石岡圭一, 内藤陽子, 石川裕彦, 林泰一, 大沢信二

課題研究 T8：地表変動，固体地球物理，火山物理 堤浩之，竹村恵二，鍵山恒臣

(大学院，修士課程)

地球熱学，地熱流体学 IA 竹村恵二，大沢信二

地球熱学，地熱流体学 IB 竹村恵二，大沢信二

地球熱学，地熱流体学 IIA 鍵山恒臣，古川善紹，大倉敬宏

地球熱学，地熱流体学 IIB 鍵山恒臣，古川善紹，大倉敬宏

第四紀地質学 竹村恵二

多階層地球変動科学特論：地球生物圏史科学 田上高広，福田洋一，竹村恵二，堤浩之，酒井治孝

多階層地球変動科学特論：地球物質科学 平島崇男，小畑正明，中西一郎，大沢信二，柴田知之

水圏地球物理学 IIA 大沢信二，Sidle, Roy C., 諏訪浩

水圏地球物理学 IIB 大沢信二，Sidle, Roy C., 諏訪浩

応用地球電磁気学 A 大志万直人，鍵山恒臣

応用地球電磁気学 B 大志万直人，鍵山恒臣

地球惑星科学特殊研究(修士論文) 全教員

(大学院修士課程および博士後期課程)

地球物質科学セミナー 小畑正明，平島崇男，柴田知之

地球生物圏史セミナー 増田富士雄，前田晴良，竹村恵二，大野照文

固体地球物理学ゼミナール IV 中西一郎，久家慶子，大倉敬宏

水圏地球物理学ゼミナール III 大沢信二，Sidle, Roy C., 諏訪浩，斉藤隆志

活構造論ゼミナール I 竹村恵二，堤浩之

活構造論ゼミナール II 竹村恵二，堤浩之

地球熱学，地熱流体学ゼミナール I 竹村恵二，大沢信二，川本竜彦，柴田知之

地球熱学，地熱流体学ゼミナール II 鍵山恒臣，古川善紹，大倉敬宏，宇津木充

応用地球電磁気学ゼミナール 大志万直人，鍵山恒臣，神田径，吉村令慧

野外実習

観測地球物理学演習 B (別府，7 月 30 日～8 月 1 日) 教員多数

観測地球物理学演習 A (阿蘇，8 月 1 日～4 日) 教員多数

課題演習 DC (地球の鼓動を探る) 阿蘇実習 (阿蘇，9 月 5 日～9 日) 大倉敬宏，吉川慎，井上寛之

課題演習 DD 別府実習 (別府，11 月 21 日～23 日) 大沢信二

多階層地球変動科学実習 (大学院) 余田成男，他 (随時の実習で，大沢は多階層地球変動科学実習結合系を実施した．11 月 21 日～23 日)

その他

大倉敬宏，熊本大学理学部 非常勤講師 2008 年度後期

鍵山恒臣，熊本大学理学部 非常勤講師 2008 年度前期

鍵山恒臣，京都大学ジュニアキャンパスセミナー「火山の噴火を見てみよう」

## セミナー Seminars

### 地球熱学, 地熱流体学ゼミナールⅠ(別府) (芳川雅子担当)

テレビ会議システムを用い阿蘇・京都に配信

平成 20 年(2008 年)

4 月 9 日 所内共同研究成果報告 山田 誠, 鍾乳洞滴下水の研究

4 月 30 日 所内共同研究成果報告 竹村恵二, 鶴見・由布火山群の活動史とテフラ層序 寺田暁彦,  
火口湖の地球科学的研究

5 月 21 日 所内共同研究成果報告 柴田知之, 九州弧火成岩類の地球化学的特長の時空変化  
芳川雅子, 化学組成とタイミングから見たアルカリマグマと交代佐用の関係

6 月 11 日 所内共同研究成果報告 大倉敬宏, 別府地域の最近の地震活動 西村光史, 斑晶鉱物  
の LA-ICP-MS 分析

7 月 2 日 柴田知之, 甲府盆地北縁周辺に分布する火山岩類の地球化学的特徴の時間変化と沈み込  
み帯の構造との関係

10 月 8 日 Marie Python, 海洋底上部マントルでの高温熱水循環作用: オマーンオフィオライト  
のマントル部分での蛇紋岩化作用と透輝石岩脈発生

10 月 29 日 竹村恵二, 九州の第四紀テクトニクス

11 月 12 日 浜田盛久, 初生的な島弧玄武岩マグマは水に富む--Ca に富む斜長石斑晶の水素含有  
量からの制約--

11 月 26 日 柴田知之, 総長裁量経費・滞在型フィールド実習用地球観測・分析システムの四重極  
誘導結合発光プラズマ質量分析計: 溶液法・レーザーアブレーション法を用いた微量元素測  
定

12 月 24 日 三島崇宏, 少量の試料水を用いる環境水中の炭酸水素イオンの新たな定量分析法

### 特別セミナー(別府) (芳川雅子記録)

平成 20 年(2008 年)

8 月 25 日 薬師寺亜衣, 島根大学, 山陰地域における火成活動とモリブデン鉱化作用に関する研  
究 三谷明日華, 島根大学, 山陰帯横田地域に分布する深成岩類の火成作用とモリブデン鉱  
化作用の成因的關係

11 月 20 日 土谷信高, 岩手大学, スラブの部分溶融についての主に深成岩・実験岩石学からの研  
究

11 月 25 日 横山正敬, 高知大学, 石英のカソードルミネッセンス像に記録されたマグマ混交・混  
合: 足摺岬花崗岩体の例

平成 21 年(2009 年)

3 月 10 日 佐藤大介, 島根大学, アダカイトとしての和久羅山デイサイトの岩石学的研究

3 月 18 日 Ewa Slaby, University of Warsaw, (1) Progress in magma mixing recorded in  
mineral composition and growth textures: a case study of Late Archaean Closepet  
granite (India) (2) Mafic and felsic magma interaction in Karkonosze pluton (SW  
Poland) from macro to micro scale

3 月 24 日 柵山徹也, 東京大学, マントルダイアピルの上昇と累進的融解の証拠: 九州北西部、背  
弧域火成活動からの制約

3 月 30 日 土谷信高, 岩手大学, オフィオライト中の斜長花崗岩の成因: オマーンオフィオライ  
ト北部の珪長質岩の例

阿蘇 <セミナーリスト> (宇津木充, 寺田暁彦担当)

テレビ会議システムを用い別府・京都に配信

平成 20 年(2008 年)

4 月 23 日 鍵山恒臣, 噴火卓越型火山活動と地熱活動卓越型火山活動

—新しい視点で見る火山活動—

5 月 7 日 宇津木充, 繰り返し空中磁気観測による磁場時間変化検出の試み〜その 2〜

6 月 4 日 Nagendra Pratap Singh(外国人客員), Effective skin depth of EM fields due to a large loop source and its application to survey design and data interpretation.

6 月 25 日 寺田暁彦, 氷を用いた火山観測—貫入マグマ冷却過程の観測的研究—

7 月 9 日 大倉敬宏, GPS による阿蘇カルデラの地殻変動観測

12 月 3 日 Chang-Hwa Chen, Y. P.(陳中華 客員教授), The volcanic ash dispersion at the upper wind direction: the ~29 ka Aira super-eruption, southwestern Japan

12 月 17 日 大倉敬宏, InSAR 解析ことはじめ

特別セミナー(阿蘇) (宇津木充記録)

平成 20 年(2008 年)

7 月 22 日 Martha Savage (Victoria Univ. New Zealand), Seismic Anisotropy and Stress Changes on Volcanoes.

地球熱学セミナー(京都) (宇内克成担当)

テレビ会議システムを用い別府・阿蘇に配信

平成 20 年(2008 年) 毎週金曜日 10 時 30 分〜12 時に実施

※ 前期(4 月 18 日〜7 月 11 日) 後期(10 月 3 日〜1 月 16 日)

4 月 18 日 卒業研究発表

安藤隆志 『三宅島 2000 年噴火に伴う火山性地震の研究』

5 月 2 日 研究発表

小森省吾 『雲仙火山における比抵抗構造と熱水流動の関係に関する研究』

5 月 9 日 研究発表(2 名)

岩部智紗 『マルチサイトピストンコアによる琵琶湖の過去 5 万年の琵琶湖堆積物層序』

山本友里恵 『考古地磁気永年変化を用いた古窯跡の年代推定〜福岡県大野城市牛頸本堂遺跡群〜』

5 月 16 日 研究発表(2 名)

熊谷仁孝 『純水と NaCl 水溶液の高圧下での分子シミュレーション』

宇内克成 『霧島火山群・硫黄山周辺における浅部比抵抗構造』

5 月 23 日 研究発表

立尾有騎 『B 型地震群発地震活動及び火山性微動に伴う地盤変動について』

6 月 6 日 研究発表

安部祐希 『レシーバ関数による阿蘇火山の地殻構造の解析』

6 月 13 日 研究発表

安藤隆志 『桜島火山・姶良カルデラの構造と火山体構造調査』

6 月 20 日 研究発表

佐藤智之 『1 次記載で見えたもの：2008 年度琵琶湖掘削調査』

6月27日 研究発表

小森省吾 『火山周辺の比抵抗分布への火山ガス散逸の寄与に関する考察』

7月4日 論文紹介

三井雄太 『“Deep structure of the northeastern Japan arc and its implications for crustal deformation and shallow seismic activity”, Akira Hasegawa, Junichi Nakajima, Norihito Umino, Satoshi Miura, Tectonophysics, 403, 59-75, 2005』

7月11日 研究発表

山本友里恵 『琵琶湖湖底堆積物を用いた環境情報の抽出のために』

10月3日 研究発表(2名)

小森省吾 『火山周辺の電気伝導度分布への火山ガス散逸の寄与に関する研究』

安部祐希 『レシーバ関数による阿蘇カルデラの地殻構造解析』

10月17日 研究発表

宇内克成 『霧島火山群・硫黄山周辺における浅部比抵抗構造』

10月24日 研究発表

岩部智紗 『BIW07 ピストンコアの岩相・層序—堆積環境の推定にむけて』

10月31日 研究発表

熊谷仁孝 『密度汎関数法による水と氷のシミュレーション』

11月7日 研究発表

佐藤智之 『2つの泥と浸食と：潮汐堆積物の水路実験』

11月14日

黒岩健一 『地震発生と水(東京大学出版)を読んで』

11月28日 研究発表

小森省吾 『雲仙火山 USDP-1 コアサンプルを用いた岩石比抵抗測定～熱水流動と比抵抗構造との関係の解明にむけて～』

12月5日 研究発表

安部祐希 『レシーバ関数による阿蘇火山の地殻構造解析』

12月12日 研究発表(2名)

岩部智紗 『BIW07 マルチサイトピストンコアによる琵琶湖の堆積環境と気候変動にむけて』

安部祐希 『Crustal structure beneath Aso caldera, southwest Japan, as derived from receiver functions』

12月19日 研究発表(2名)

熊谷仁孝 『分子動力学法を用いた氷 VI の観察』

宇内克成 『霧島火山群・硫黄山周辺における浅部比抵抗構造』

平成 21 年 2009 年

1月16日 研究発表

黒岩健一 『大気圧におけるゾイサイトの脱水分解反応のその場観察』

## 学会活動 Activities in Scientific Societies

鍵山恒臣

日本火山学会各賞選考委員，国際委員  
Indonesian Journal of Physics 誌 Editor

竹村恵二

日本地質学会地方地質誌九州地方編集委員会委員  
日本地質学会地方地質誌近畿地方編集委員会委員  
日本第四紀学会論文賞受賞候補者選考委員

大沢信二

日本温泉科学会広報・交流委員  
日本水文科学会評議員  
地球惑星科学委員会国際対応分科会 IAHS（国際水文科学協会）委員

## 社会活動 Public Relations

鍵山恒臣

文部科学省科学技術・学術審議会測地学分科会火山部会，臨時委員  
火山噴火予知連絡会，委員  
火山活動評価検討委員会，委員  
霧島火山防災検討委員会および霧島火山緊急減災砂防計画検討分科会，委員  
地震・火山噴火予知研究協議会，委員  
JICA 研修「火山学，総合土砂災害対策コース」，カリキュラム委員および講師  
NPO 法人アソミュージアム「阿蘇人ツーリズム」講師

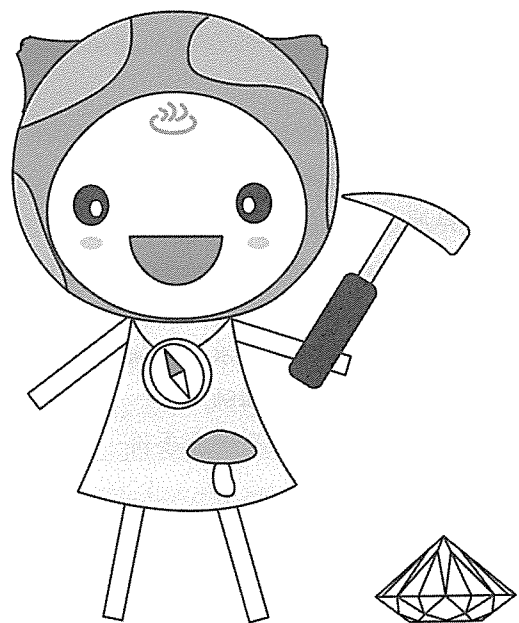
大沢信二

大分県温泉調査研究会理事  
大分県温泉監視調査委員会委員  
大分舞鶴高校スーパーサイエンスハイスクール指導教官  
別府鶴見丘高校『模擬講義』講師  
大分市廻栖野地区地下水調査検討委員会委員  
別府八湯語り部の会講師  
大分県環境審議会温泉部会委員

竹村恵二

京都府環境影響評価専門委員会委員  
海域活断層調査検討会委員（地球科学総合研究所）

KG-R (KG-NET・関西圏地盤研究会) 第2期研究 副委員長  
ひずみ集中帯委託研究プロジェクト運営委員会 委員  
堺市地震被害想定委員会 委員  
三重県防災会議活断層部会委員会 委員  
大分県天然記念物緊急調査(地質・鉱物・自然現象)指導委員  
大分県環境影響評価技術審査会員  
福井県原子力安全専門委員会 臨時委員  
独立行政法人産業技術総合研究所 「地層処分にかかる地質情報データの整備に関する  
評価委員会」 委員  
大分市横尾遺跡指導者会 委員  
琵琶湖博物館総合研究・共同研究審査委員会委員  
地震調査研究推進本部ニュース サイスマ サイスマスコープ執筆委員  
『関西国際空港(二期地区)地盤挙動調査委員会』委員  
石川県能登町真脇遺跡調査指導委員会』委員  
深田研談話会(大阪開催)講師:「上町断層ーどこまで判っているのかー」  
ふるさと地盤診断ウォーク(生駒)講師, 地盤工学会関西支部.  
防災講演会講師:「北部九州での地震予想及び埋立地の地震被害について」, 北九州 LNG.  
地球熱学研究施設(別府)施設公開 「夏休み地獄ハイキング」(浜脇・東別府)講師  
香川県理数系教員指導力向上研修講師「教師のための地球熱学: 別府ー島原地溝  
帯における活火山と活構造」, JST 事業

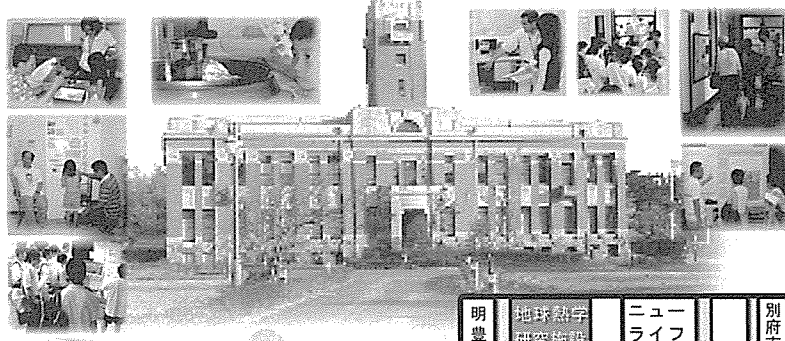




# 一般公開報告 Openhouse

## オープンハウス報告書(別府)

### 別府で感じる地球の息吹 8月22日(金) 研究施設一般公開 AM 10:00 ~ PM 4:00 建物内部と研究内容を公開します。



#### アクセス

亀の井バス「ビーコンプラザ」下車  
徒歩2分

研究施設内に駐車場あり (20 台分)

#### なつやす

### 夏休み地獄ハイキング

別府朝見川断層と温泉湧水地帯を歩く

#### 案内者

竹村恵二 京都大学教授

浜田盛久・山田 誠・西村光史 研究員

PM 1:30 JR 東別府駅集合 / PM 2:00 出発

参加費 一人 300 円



お問い合わせ

〒874-0903 別府市野口原 3088-176 京都大学地球熱学研究施設  
電話: 0977-22-0713 (担当: 川本・浜田・山田)  
電子メール: koukai2008@bep.vgs.kyoto-u.ac.jp

京都大学地球熱学研究施設  
<http://www.vgs.kyoto-u.ac.jp>



京都大学大学院理学研究科附属地球熱学研究施設では、平成20年8月22日(金)午前10時～午後4時まで研究施設の一般公開を行った。また8月23日(土)午後1時～午後4時に別府市朝見川断層沿いを対象とした夏休み地獄ハイキングを行った。一般公開には149名(前年度は317名)にお越しいただき、ハイキングには20名(前年度は46名)の市民に参加していただいた。

広報活動には昨年同様、別府市教育委員会、別府市役所記者クラブ、新聞各紙、テレビやラジオ各局の協力をいただいた。施設の公開翌日には読売新聞に公開の様子を紹介していただいた。平成21年度は土曜日開催とし、隔年で平日と土曜日の開催を計画する予定である。

平成20年度研究施設一般公開担当 川本竜彦、山田誠、浜田盛久

あらゆる人に満足してもらえる説明ができると良いんですが、難しいです。

## マグマの水 浜田 盛久

場所 電子顕微鏡室（地下）

島弧火山フロントの玄武岩マグマは水に富んでいる  
——伊豆大島火山の斜長石に含まれる微量の含水量からの推定——

日本列島では、太平洋プレート、フィリピン海プレートといった海洋プレートが沈み込んでくることによって、火山活動が生じています（図1）。このような場所は、「島弧」と呼ばれています。海洋プレートはたっぷりと水を含んでいて、沈み込みの過程で脱水します。島弧の火山活動の特徴の一つは、この脱水した水が、マグマ中に多く溶け込んでいることです。

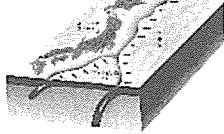


図1 日本列島の下に沈み込む海洋プレート

マグマの水の量について知ることは、マグマの成り立ちを知る上で重要な手がかりを与えます。また、マグマ中の水は、火山噴火の際の原動力としても作用します。それはちょうど、炭酸飲料水の栓を抜くと、炭酸水が泡となった炭酸ガスとともにあふれてくることに似ています（図2）。防災の観点からも、マグマの水の量について知ることは重要なことです。

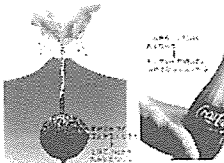


図2 噴火の際のマグマ中の水が泡となってあふれる様子

私は、火山フロント（火山弧の海側側の境界線）上に位置する伊豆大島火山（東京都）を例として、島弧の玄武岩マグマの含水量を調べる研究を行っています。最近、斜長石という鉱物に含まれる微量の含水量を調べる仕事に取り組んでいます。その結果、島弧の火山フロントの玄武岩マグマは、水に富んでいることが分かってきました。この研究のために、走査電子顕微鏡（岩石試料の観察・化学組成の分析ができる）や、フーリエ変換赤外線分光光度計（図3 岩石試料の含水量を調べる装置）という機械を使っています。今日は、この研究の一部をご紹介しますとともに、研究に使っている電子顕微鏡をお見せします。

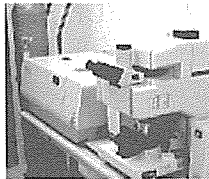


図3 フーリエ変換赤外線分光光度計

## ・地球の鼓動を捉える・地震計

火山噴火の時には、地下の岩層が割れをこわしながら上昇して地面にあられれます。ですから、噴火の前には火山の周りで多くの地震が発生したり、地面が傾いたり変形したりします。地面の傾きや変形などは傾斜計（地面のかたまりをばかる機械）や伸縮計（地面のひらちみをばかる機械）で観測していますが、地面のゆれである地震は地震計ではかります。

現在、世界で使われている地震計の基本形が考案されたのは、今から120年前の日本です。明治維新のあと、当時の日本政府は、ヨーロッパの国々に追いつくため、多くはイギリスやドイツから研究家を依頼して地震計を輸入しました。その中に、そのころをコーンという人が、日本にやってきて、初めて地震計のゆれを記録し、地震に研究をもちました。2人はたがいにいいあい、それぞれ異なる式で地震計、コーン式地震計を作ったのです。これらの地震計は、水平に動くふり子を使っていて、現在の地震計とほとんど同じ構造をもち、ふり子の小さな動きをてこの原理で拡大し、てこの先に取り付けられたペンで地面の動きを記録する「機械式地震計」です。

バネとおもりによるふり子を用いた地震計では、地震のゆれをうまく記録するよう、ふり子のゆれる速度をゆっくりにするためにはおもりを重くしなければならず、ウィーバート式という地震計では、約1トンのおもりが使われています。この地震計はたいへん精度が高かったため、日本にも多く輸入され、当施設でも地震活動の観測に役立てられ、昨年度で設置されていました。

20世紀の初頭に考案されたガリフィン式地震計は、機械式地震計のふり子の部分にコイルを付け、地震計の本体に磁石を取り付けた物です。ふり子の動きによってコイルが動き、発電機と同じ原理でコイルの両端に電圧（電圧）が生じます。そのため「電磁式地震計」ともよばれています。電磁式地震計は、現在でも体に感じないような小さなゆれの地震を正確に記録するのに使われています。

## ・地震データを伝送するIP（インターネット プロトコル）

地震観測データは、各観測点から、IPという通信手順を使って伝送されてきます。

### ・IPとは？

IPの歴史は比較的長く、1960年代後半、アメリカ国防総省軍事研究計画（ARPA）により、ある程度の軍事に必要とする通信網を構築するという目標のもと開発されました。これは、有事における核戦争で発生する大量のプラズマによる電磁波の影響による、電子機器の破壊・動作が原因の通信障害を軽減するのが目的であるとの地味ななされた。IPの作りの重要な部分は、それまでの回線交換（通話）を止め、情報をパケット（小荷物）と着う小さな単位に分けて交換（通話）する方式を採用したことです。これは、回線交換（通話）は途道のみでの転送、パケット交換（通話）は途道やトワック（素）など、小荷物さえ運べれば何でも使って転送する、と考えると良いかも知れませんが、途道は線路が整備でどこにもは敷設できないこと、線路や架線の障害による影響が大きいこと、他の転送手段と線路を併用できないこと等が問題点となります。

回線交換（通話）も同じような問題点を持っています。そしてパケット交換（通話）は、小荷物にあるため先きえ判ってれば、色々な手段、経路を使うことが出来るため、あて先に到着できる可能性が高くなる、という特徴を持っています。

その後、アメリカの大学で開発されたBSD-UNIXと着うOSにIPが搭載され、各国の学術情報ネットワークで普及する事になります。そして、アメリカの学術情報ネットワークであるNSF-NETが民間に開放され、また、情報通信・教育の手段であるWWW（ワールドワイドウェブ）がIPの上で開発、利用される事により世界中にIP通信網が広がることになりました。

そして現在では、さまざまな情報通信がIPを使って行われるようになっていて、見えない所で大活躍しています。

展示されているパソコンでは、IPによる通信の様子が分かるようになっていきますので、ご自由に御覧になって下さい。

## 来場者よりの要望と感想

### 要望

イベントの表示に工夫がほしい。一般人に理解できるイラスト・マンガ形式がほしい。説明が難しい様な気がしました。特に子供にはもっとくだけてほしいと思いました。もっと子ども向けの体験コーナーを増やしてほしい。週末も含めて3日間位公開して下さい。1日かけてじっくり見たいです。休日だとさらによかった。子供を連れての見学でした。もっと地元の子にも見学する機会を作してほしい。夏休みののに小中学生が少ない。もっと関心がほしい。一般の市民向けにメールマガジンを作って楽しい研究内容や活動等教えてください。この研究所で取り組んでいる内容を知りたい。もし地震が起きた場合地盤にどのような変化があるのか興味があります。建物の外側の雑草はなんとかならないのか。

### 感想

地震計を見て私が感じなかった小さな揺れを実感することができました。月も揺れていることがわかりました。またこの体験を受けたいです。私は地震計が一番好きです。顕微鏡やプラズマの装置など普段触れることのない装置を、子どもが見ることができるので毎回楽しみにしています。5才の息子でも十分楽しんでいました。今までより出し物は少なかったが、じっくり話を伺うことができてよかった。いろいろな（本など）情報もいただけてありがとうございました。とても分かり易く説明してくださって勉強になりました。



新層によって出来た地形を遠望しながらハイキングをする様子。

丁寧な質問に答えてもらえた。科学を知らない者にも分かり易い説明でした。  
 水の分子の模型作りがおもしろい。  
 初めて見学しましたが、幼稚園年中と、小二の子どもも興味深く見させていただきました。今はよくわからなくても、よい経験をさせていただきました。  
 建物がとっても素敵ですね。  
 帰省中に来ました。子どもが小二と年長で「わからないことが多かったけど楽しかった」と。  
 水や氷の構造を作ろうでブロックみたいなのをもらってうれしかった。  
 初めて見学しました。来年は是非孫といっしょに来ます。小さい子どもにはきっと夢が持てそうな所だと思います。  
 初めてきました偶然通りかかってよかったです。プラズマは雷かと思った。マグマの水＝温泉かと思ったら石の水分だった。地震計絶えず頑張って。石の輪廻転生おもしろい。  
 自分の暮らしている地域の火山の事をよく知る事ができて勉強になりました。地球ってすごい！とも改めて感じました。子供が小さいのでまたわかる年になった頃連れてきたいです。  
 文系の脳みその私にもわかりやすく説明して下さい、鍾乳洞のことがとてもよくわかりました。この催しは本当に良いと思います。建物内を見るのも楽しかったです。  
 京都大学は日本一の研究の進んでいる大学。別府の一角に立派な建物、温泉を化学的に分析して観光客に話したいと思います。ぜひ静かな研究所でなく、はばたく京都大学に変身して下さい。もっと市民の中に存在感を見せてください。別府温泉観光士より  
 地球のこと、別府のこと、宇宙の不思議を知るのに大変役立ちました。  
 難しかったけど面白かったです。来年もまた来たらいいなと思います。  
 とても親切に説明して頂きました。ありがとうございました。来年もまた来ます。  
 勉強になりました。  
 天井が高いですね。  
 皆さんの対応がとっても親切でありがとうございました。各分野で難しいかな？と思いましたが、分かりやすく説明をうけよかったです。  
 別府に住んで地震を身近にしたとき気になりまして、今回見学に来ました。とてもよかった。  
 我々にわかる様説明するのも大変だったと思う。ありがとう。  
 お茶のサービスがあつてよかった。  
 職員の方の説明が丁寧で分かりやすかったです。混み過ぎずゆっくり見学できよかったです。  
 また来年も来たいです。  
 小さい子供に分かりやすく説明してもらえると興味をもっと持つと思います。宜しくお願いします。ありがとうございました。  
 楽しかった。  
 「水や氷の構造を知ろう」が楽しかった。夏休みの自由研究に出来る！  
 とても興味深くおもしろかったです。各コーナーで実際に色々な体験ができ、楽しく見てまわることができました。  
 水の模型が楽しかった。  
 自然といえば山を頭にうかべますが別府、九州、日本列島では日々変化を遂げている事を教わりました。  
 永遠の姿は中々お目にかかれなことも知りました。  
 日ごろ考えない事なので解らない事だらけだが面白い。めずらしいという感じが強かった。  
 面白かったしわかりやすかった。  
 スタッフの教え方がわかりやすかった。  
 子供が柴田さんの説明が毎年好きらしくいろいろと興味を持って聞いています。ありがとうございます。  
 もっと詳しく知りたい。丁寧と話してくれた。



目的地別府。こちらでも竹村教授、断層運動でのずれを説明しています。

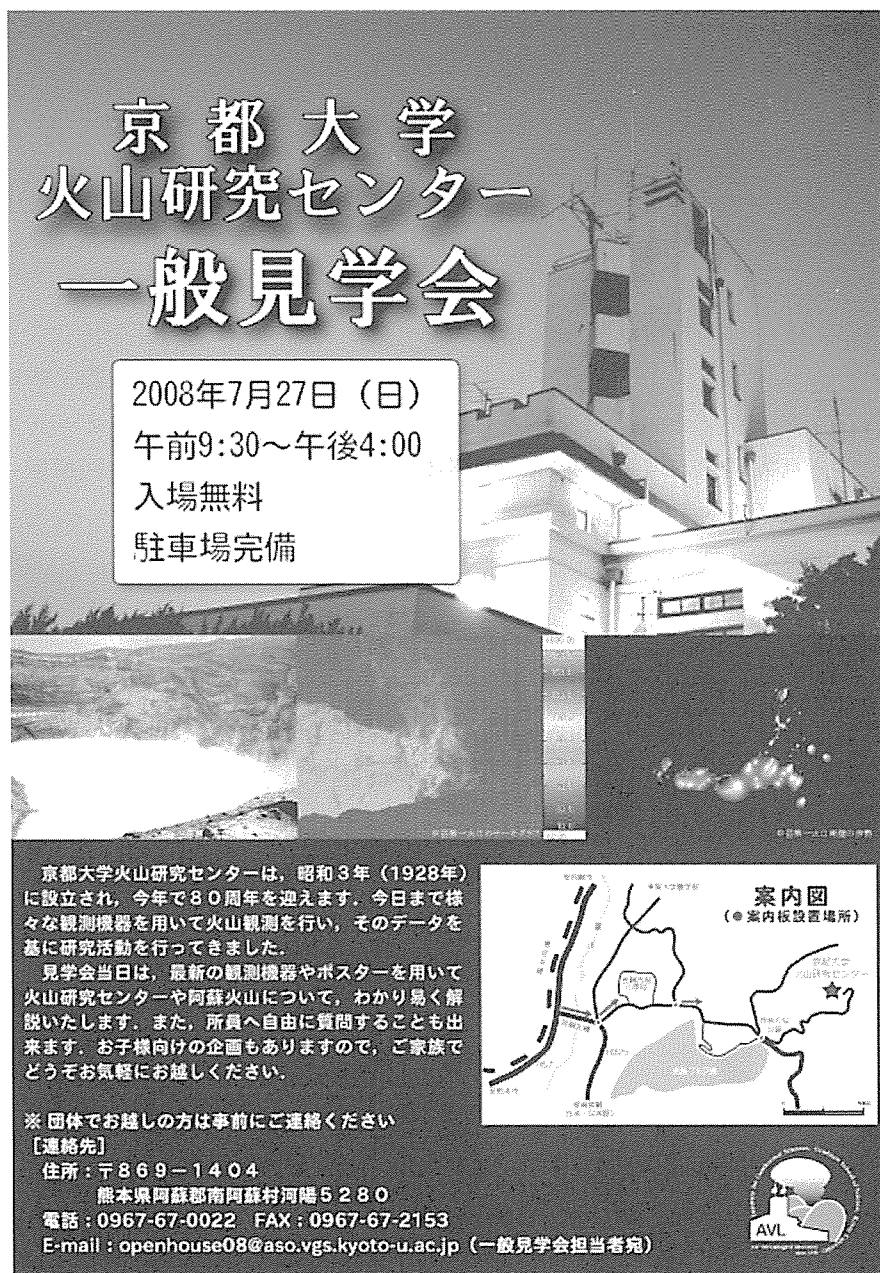
## 一般見学会報告書（阿蘇）

### 1. 目的

一般市民，特に地域住民・関係機関に，当センターの活動内容を広く知ってもらうことで，センターに対する関心・理解を得る．また，社会への学術的知識の還元・啓蒙をはかる．

### 2. 開催日時

平成20年 7月27日（日） 9：30～16：00



# 京 都 大 学 火山研究センター 一般見学会


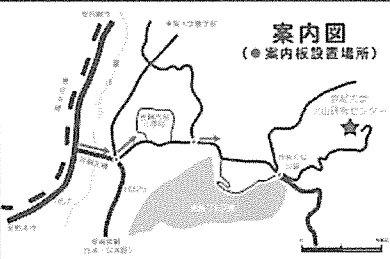
2008年7月27日（日）  
午前9:30～午後4:00  
入場無料  
駐車場完備

京都大学火山研究センターは，昭和3年（1928年）に設立され，今年で80周年を迎えます．今日まで様々な観測機器を用いて火山観測を行い，そのデータを基に研究活動を行ってきました．

見学会当日は，最新の観測機器やポスターを用いて火山研究センターや阿蘇火山について，わかり易く解説いたします．また，所員へ自由に質問することも出来ます．お子様向けの企画もありますので，ご家族でどうぞお気軽にお越しください．

※ 団体でお越しの方は事前にご連絡ください  
【連絡先】  
住所：〒869-1404 熊本県阿蘇郡南阿蘇村河陽5280  
電話：0967-67-0022 FAX：0967-67-2153  
E-mail：openhouse08@aso.vgs.kyoto-u.ac.jp（一般見学会担当者宛）

案内図  
（●案内板設置場所）



### 3. 内容

特別講演「阿蘇火山の生い立ち～火山を作った噴火活動の歴史～」 森林総合研究所 宮縁育夫氏 午前10:00～11:00， 午後 2:00～3:00 （計2回）

世界最大級のカルデラで知られる阿蘇火山がいつ誕生し，これまでどのような噴火を起こしてきたのか？阿蘇火山の歴史を解説するとともに，最近の火山活動や火山研究者が取り組んでいる最新の研究についての紹介．

ポスター展示（約30点）による研究内容の紹介・火山学の一般向け解説

公開実験・工作・体験

・「立体震源模型を作ろう」・「サーモトレーサーで記念撮影」・「磁力計で宝探し」・「湧水の違いを調べてみよう」・「EDMで距離を測ろう」

視覚的展示物

・「地震計のデモンストレーション」・「九州の地震活動リアルタイムモニター」・「阿蘇火山の微動振幅レベルモニター」・「ウィヘルト地震計の再起動」

施設備品展示（新旧地震計等各種観測装置の展示・解説）

火山に関するビデオの上映

火山に関する書籍の閲覧供与

見学者パンフレット（大人用，子供用）を配布

お年寄りの来場者を考慮し休憩室を設置

#### 4. 社会告知の方法

A4・A3版ポスター・チラシを配布・掲示

赤水郵便局・アゼリア21・あぜり庵・阿蘇火山博物館・阿蘇市営運動公園・阿蘇市役所・大津町役場・温泉センターウィナス・火山研究センター入口・カドリードミニオン・九州東海大学・熊本大学・京大理学部4号館・京大理学部事務室・高原の宿・JR阿蘇駅・立野病院・原水公民館・古木常七商店・森山石油店・ヤマサキビューティ（50音順）

イベント案内レター（13件）

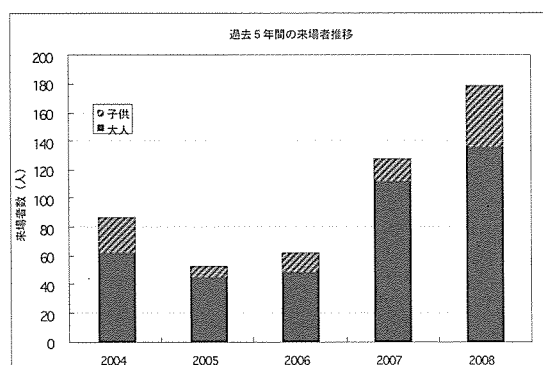
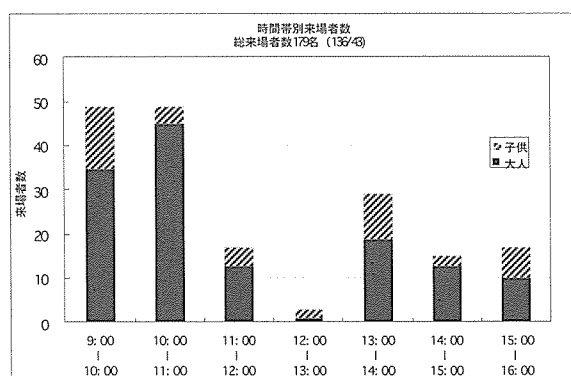
熊本日日新聞・朝日新聞イベント情報掲載

市町村広報（阿蘇市・大津町・高森町・南阿蘇村）

火山研究センターWebページによる公示

#### 5. 見学者に関する集計

来場者数：179名（大人136名，子供（高校生以下）43名）



#### 6. アンケート集計結果

Q1. どちらからお越しになりましたか？

	阿蘇郡市内	熊本県内 阿蘇郡市以外	熊本県外	合計
回答数	21	52	7	80
百分率	26.25%	65.0%	8.75%	100%



Q 2. 年代を教えてください

	10代	20代	30代	40代	50代	60代以上	合計
回答数	7	5	5	20	20	23	80
百分率	8.75%	6.25%	6.25%	25.0%	25.0%	28.75%	100%

Q 3. どのようにして今回の一般公開を知りましたか？

	友人・知人	インターネット	新聞・雑誌	ポスター	その他	合計
回答数	21	5	33	4	9	72
百分率	29.17%	6.94%	45.83%	5.56%	12.5%	100%

Q 4. 来年も来たいと思いましたか？

	はい	いいえ	わからない	合計
回答数	69	2	9	80
百分率	86.25%	2.5%	11.25%	100%

## 6. まとめ

今年度は昨年度より2週間早い7月27日に行った。夏休みに入ったばかりということもあり、たくさんの子供連れの方々に来場していただいた。さらに今回は、来場者数がこれまでの最高を記録したことから、一般見学会の目的のひとつである「センターの活動内容を広く知ってもらおう」という点において成功を収めたと言える。この事の要因として以下の点が挙げられる。

### ・広報について

今回の一般見学会の告知は、従来から行ってきたポスター掲示・Webにおける情報掲載等にくわえて、新聞の「週末のイベント」欄への掲載を各新聞社へ依頼した。アンケート結果からもわかるように、今回のイベントを新聞で知ったという方が約半数にのぼる。一般の記事ではなく、イベント欄ということがこれまでと違う点である。この違いは大変重要なポイントである。

### ・開催時期について

先に述べたとおり、今年度の一般見学会は昨年度より2週間早く行った。この結果、子供を伴った家族の方々に多く来場していただき、来場者数増加につながった。小学生の夏休み自由研究の課題の参考にするため、子供を伴って参加される方が増えたことが推察される。

### ・一般見学会の世間への浸透

過去5年間の来場者推移グラフからわかるとおり、一番少なかった2005年と比較すると前年度で2倍、今年度にいたっては3倍の来場者が火山研究センターを訪れている。立地上、公共交通機関ではアクセスできない場所において、この数字は大変素晴らしいことである。これまで一般見学会に携わった職員、大学院生等の地道な努力の結果である。

最後に、今年度の成功に甘んじることなく、これからも同様に一般の方々に我々の活動、火山の素晴らしさを伝えていかなければならないと考えている。

火山研究センター 吉川 慎

## 来訪者 Visitors

### 【阿蘇】

平成20年（2008年）

6月10日 後小路 他1名 （気象庁阿蘇防災連絡事務所）

7月21-23日 Dr. Martha Savage

7月24日 平野丈夫（理学研究科）

8月1日-4日 西憲敬,宮崎真一,松本全史（京大理）

9月5日-10日 才ノ木順太（京大理）

9月15日-17日 立尾有騎（京大防災研）

9月15日-23日 高山鐵朗,山崎友也,多田光宏（京大防災研）

9月17日-23日 山本圭吾（京大防災研）

9月22-27日 松島健,内田和也（九大理）

9月23日 飯野英樹 他6名 （気象庁）

9月24-27日 中元真美,山下裕亮（九大理）

9月30日 後小路義弘 他1名 （気象庁阿蘇防災連絡事務所）

10月2日 長崎県長崎市立小江原小学校児童13名ほか

10月30日 長崎県長与町立長与小学校児童16名ほか

平成21年（2009年）

1月6日 松島健（九大理）

2月13日 後小路 他1名 （気象庁阿蘇防災連絡事務所）

3月18日 飯尾能久 （防災研究所）

3月18日 余田成男 （理学研究科地球物理教室）

3月18日 藤浩明 他2名 （理学研究科地磁気世界資料センター）

3月23日 橋本武志 （北海道大学理学研究院）

3月23日-26日 及川純 （東京大学地震研究所）

3月23日 京都大学財務部 3名

### 【別府】

平成20年（2008年）

4月7～8日 森下 他2名 （金沢大学・Pavia 大学）

4月8日 小野 （大分地方气象台）

4月8日 亀井 他1名 （島根大学）

4月16～5月5日 下田 （産業技術総合研究所）

4月23～24日 鍵裕之・荒川雅 （東京大学地殻化学実験施設）

4月30日 伊勢戸 他3名 （大分県治山植林）

5月2～5日 松岡 他学生引率 （京大地質鉱物教室）

5月14日 別府市環境部

5月14～15日 大倉 （阿蘇火山研）



5月21～22日 藤井・福谷・太田 （京都大学・原子炉実験所）  
 5月24日 大塚 他30名ほど （大分舞鶴高校SSH・他）  
 6月7日 大塚 他30名ほど （大分舞鶴高校SSH・他）  
 6月11日 田村・中澤 （京大本部事務・情報）  
 6月15～17日 石川尚人・藤井 （京大人間・環境）  
 6月18日 友永・油布・西村 他23名 （明星小学校3年生）  
 7月14～16日 北川 （名古屋大学環境学研究科）  
 7月15日 立石 （大分地方気象台）  
 7月16日 中学生7名（連絡担当足立先生） （別府市鶴見台中2年生）  
 7月23～24日 平野 （理学研究科）  
 7月24日 大上 他30名 （大分県私立高校多数）  
 7月17日 斉藤 （愛媛大学）  
 7月28日 桧垣 他2名 （別府市教育委員会）  
 7月29～8月2日 観測地球物理演習 堤 他学生20名（京都大学）  
 8月6～11日 杉本健 （地熱エンジニアリング）  
 8月8日 小林 他20名ほど （大阪教育大学）  
 8月18～31日 河内 （京大・理学研究科）  
 8月19～21日 塩田 他12名ほど （香川県高校理科教員）  
 8月18～30日 亀井 他2名 （島根大学教員及び学生）  
 8月22～23日 大倉 （阿蘇火山研）  
 8月22日 施設一般公開 一般市民149名 （大分・別府市民ほか）  
 8月23日 一般市民21名  
 8月23～27日 石川・藤井 （京大人間・環境）  
 8月27日 黒澤 他2名 （自衛隊別府病院）  
 8月30日 川野 他17名 （全国大学高専教職員組合九州支部）  
 9月1～ 日 マリ・ピトン （金沢大）  
 9月9～10月8日 米村 （京都大学生）  
 9月11日 本部財務3名，理学部財務等4名 （京大）  
 9月12～13日 鈴木勝彦 （JAMSTEC）  
 9月17日 山添 （別府史談会）  
 10月1～3日 マリ・ピトン （地球熱学）  
 10月26～31日 Alex Nichols （海洋研究開発機構地球内部変動研究センター）  
 11月7～20日 米村 （京都大学生）  
 11月15～18日 網田和宏 （秋田大学）  
 11月20日 本部総務広報1名、出版社1名 （京大及び契約出版社）  
 11月20～21日 松岡廣繁 （地質鉱物）  
 11月21～23日 余田 他13名 （地球物理，地質鉱物）  
 11月21～22日 磯部博志・吉朝朗・学部3回生3名 （熊本大学）  
 11月23日 木戸道男 他5名 （福岡県地学(研究会)）  
 11月25～12月4日 横山正敬 （高知大学修士2年）  
 11月26～27日 大倉 （阿蘇）  
 12月9日 古川 （別府市民）

12月9～11日 藤井・福谷 (京都大学原子炉)

12月12～13日 小林哲夫 (鹿児島大学)

12月21～26日 網田和宏 (秋田大学)

平成21年(2009年)

1月15～18日 黒岩健一 (京都大学 地球熱学)

1月24日 サンガ・小林 他11名 (APU)

2月6～7日 新村・三好 (熊本学園大・熊大)

2月12～13日 京都大学情報環境部長 他3名 (京都大学)

3月2日 北島 (九州大学地球惑星科学)

3月4～13日 苗村 (京都大学)

3月7～9日 松本 (島根)

3月7～13日 佐藤 (島根)

3月9～10日 磯部ほか (熊本大学)

3月13～16日 平島・山路 他11名 (京大地鉦)

3月13～16日 黒岩健一 (京都大学理学部4回生)

3月14～31日 土谷 (岩手大)

3月16～18日 余田 他研究科メンバー等30名 (京大関係者および九州内大学教員)

3月17～30日 Ewa Slaby (ワルシャワ大学)

3月24日 中尾 他5名 (京大本部財務・理学財務・理学施設)

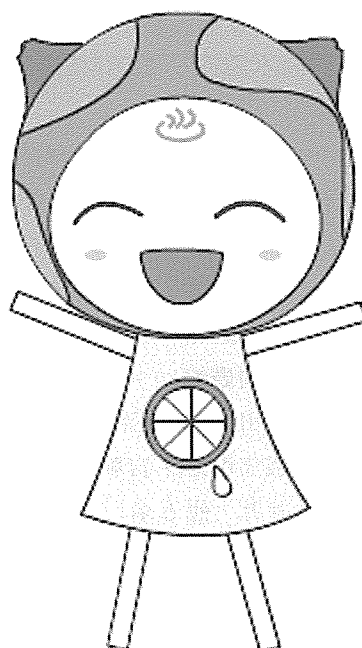
3月24～25日 小澤 (東京大学)

3月24～26日 柵山 (東京大学)

3月27～28日 中西 (産業技術総合研究所)

3月28～4月2日 鈴木 (京大・学部生)

3月30～31日 下山・上原・北島ほか (九州大学)



定 常 観 測 Routine Observations

## Geophysical Monitoring Under Operation at AVL

### Aso Volcanological Laboratory

#### Permanent Stations

##### Nakadake monitoring network

Seismic Stations: HNT, PEL, KSM, SUN, KAE, KAE, KAN, UMA, TAK (microwave telemetry)

Tiltmeters: HNT (water tilt 3-comp.), SUN, KAE, NAR, UMA, KAK (on-site logging)

Extensometers: HNT (invar 3-comp.)

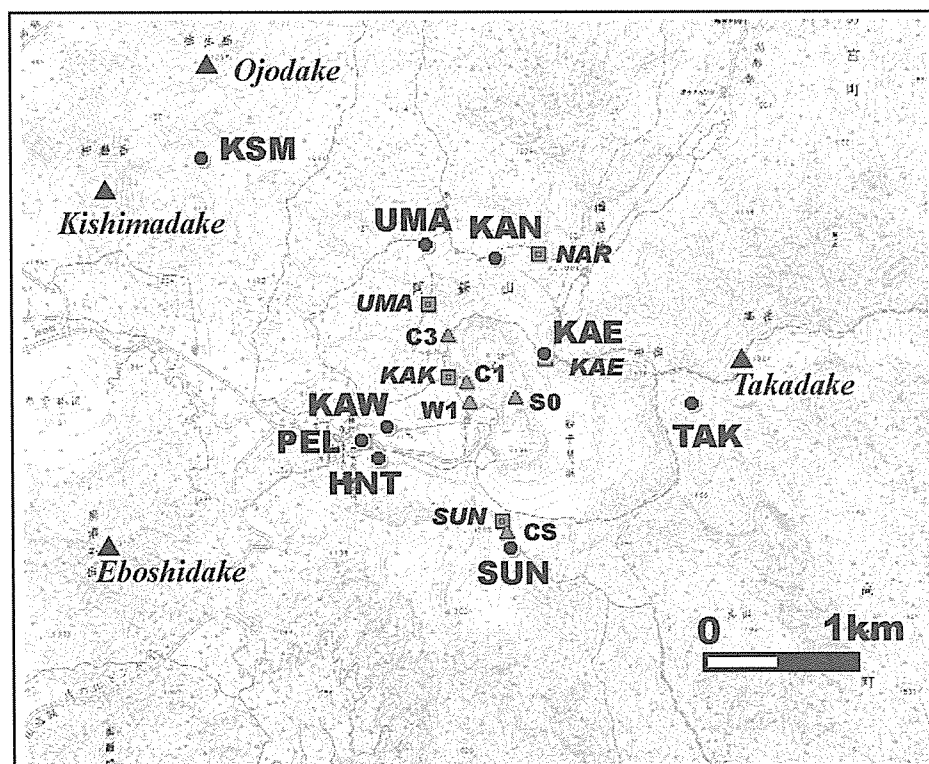
Microphone: HND (microwave telemetry)

Geomagnetic Stations: C1, C3, S0, W1, CS, NGD, FF1 (proton; on-site logging)

C223 (fluxgate 3-comp.; on-site), newC223 (fluxgate 3-comp.; online)

FF2 (proton; online)

Ground Temperature: KAK (boreholes of 70 and 150 m deep; microwave telemetry)



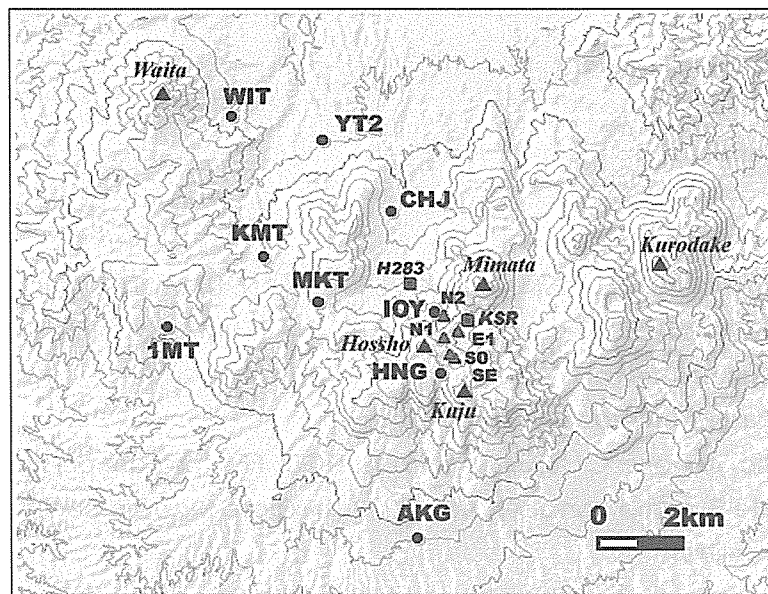
Seismic, geodetic and geomagnetic stations in the central part of Aso.

### Kuju monitoring network

Seismic Stations: HNG (radio-telemetry), AKG, CJB, IOY (on-site logging)

Tiltmeters: H283, KSR (on-site logging)

Geomagnetic Stations: N2, E1, S0, SE (proton; on-site logging)

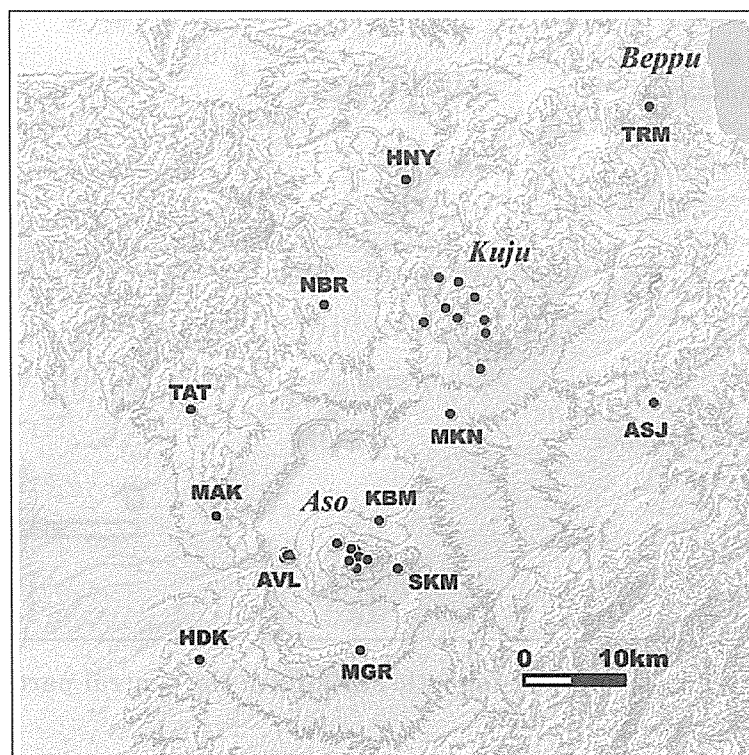


Seismic, geodetic and geomagnetic stations in Kuju area.

### Central Kyushu regional network

Seismic Stations: AVL(6), MAK, NBR, MKN, HDK, TAT, MGR (online telemetry)

ASJ, HNY, SKM, KBM (dial-up)



Seismic network in the central Kyushu.

## 装置, 設備 Instruments and Facilities

### 装置 Instruments

#### 【別府】

ICP 発光分光分析装置  
波長分散型電子プローブマイクロアナライザー(海洋科学技術センターに貸し出し中)  
エネルギー分散型電子プローブマイクロアナライザー  
波長分散型蛍光 X 線分析装置  
エネルギー分散型蛍光 X 線分析装置  
粉末 X 線回折装置  
液体シンチレーションシステム  
イオンクロマトグラフ  
ガスクロマトグラフ

#### 【阿蘇】

阿蘇, 九重火山連続地震観測システム  
地殻変動観測坑道  
孔中温度観測システム  
ビデオ映像監視システム  
プロトン磁力計  
フラックスゲート磁力計  
地磁気絶対測定システム

#### 【Beppu】

ICP emission Spectrometer  
Wavelength dispersive electron microprobe  
(lent to JAMSTEC)  
Energy dispersive electron microprobe analyzer  
Wavelength dispersion type X-ray Fluorescence analyzer  
Energy dispersion type X-ray Fluorescence analyzer  
Powder X-ray diffractometer  
Liquids scintillation system  
Ion chromatography  
Gas chromatography

#### 【Aso】

Continuous seismic monitoring system for Aso and Kuju Volcanoes  
Observation tunnel for ground deformation  
Borehole temperature monitoring system for Aso  
Video monitoring system of Aso and Kuju Volcanoes  
Proton and fluxgate magnetometers  
Geomagnetic absolute measurement system  
Tiltmeters

自動滴定装置  
ピストンシリンダー型高圧発生装置  
ICP-MS 用レーザーアブレーション装置  
四重極型 ICP-MS 装置  
表面電離型質量分析装置  
外熱式ダイヤモンドアンビル (京都実験室)  
ラマン顕微鏡 (京都実験室)  
フーリエ変換型近赤外分光光度計  
赤外顕微鏡  
加熱ステージ (京都実験室)

傾斜計  
可搬型地震計(広帯域, 短周期)  
人工震源車  
重力計  
地磁気地電流測定装置(広帯域型 ULF, ELF, VLF 型)  
光波測距儀  
水準測量システム(自動読み)

Automatic titration system  
Piston cylinder type high pressure apparatus  
Laser ablation system  
Inductively coupled plasma mass spectrometer(ICP-MS)  
Thermal ionization mass spectrometer(TIMs)  
Externally heated diamond anvil cell (at Kyoto)  
Raman microscope (at Kyoto)  
FT-NIR spectrometer  
IR microscope  
Heatings stage (at Kyoto)

Portable seismometers (broadband short period)  
Car-mounted seismic source  
Gravimeters  
Magnetotelluric measurement system(broad-band type, ULF, ELF, VLF-band)  
Electronic distance measurement system  
Leveling survey system (automatic reading)

## 設備 Facilities

### 【別府】

#### 岩石粉碎, 鉍物分離室

パックミル, ディスクミルによる岩石粉碎やアイソダイナミックセパレータによる鉍物分離を行う。

#### 器具洗浄室

実験に用いる器具の洗浄を行う。クリーンドラフト1台, ドラフト1台, イオン交換筒, Milli-Q が設置されている。

#### クリーンルーム

ニューロファインフィルターを設置し極力金属使用を控えた設計で, クラス 100 のクリーン度を達成している。Sr, Nd, Pb 同位体比分析のための化学処理(試料の分解, イオン交換クロマトグラフィーによる目的元素の抽出)を行っている。

### 【阿蘇】

#### 地下観測坑道(阿蘇火山地殻変動観測坑道)

阿蘇中岳第一火口から南西 1km の, 地下 30m に設けられた, 直角三角形の水平坑道で, 1987 年度に竣工した。現在は, 水管傾斜計(25m), 伸縮計(20, 25m), 短周期地震計, 長周期地震計, 広帯域, 地震計, および強震計が設置されている。

#### 火山研究センター構内地震観測システム

火山研究センター構内では, 従来からトリパタイトによる地震観測を行ってきたが, 平成 13 年度に, ノイズ低減の為, 約 200m のボーリング孔を 4 本掘削し, 孔底に地震計を導入した。これにより, S/N 比は大幅に改善され, 従来識別できなかった中岳の長周期微動が検出されるようになった。また, ボーリングコアを採取したことにより, 研究センターの丘, 高野尾羽根(たかのおばね)火山について地質学的に新たな知見が得られつつある。これは, 阿蘇中央火口丘の噴火史を研究する上でも貴重な資料である。

### 【Beppu】

#### An analysing system of trace element and isotopic compositions

Radiogenic isotope and trace element compositions of natural samples (e.g. rock and water, etc.) provide us important information about source materials of a sample, generating processes from the sources and age of the sample formation. Therefore isotope and trace element compositions of natural samples are important for investigating the phenomena accompanied with material transfer, such as magma genesis and mantle-crust recycling. Hence, we established an analytical method for determining trace elements by using an inductively coupled plasma mass spectrometer (Fig. 1) and for isotopic ratios of Sr, Nd and Pb: employing a thermal ionization mass spectrometer (Fig. 2) at Beppu Geothermal Research Laboratory (BGRL). The system presented here is made from collaboration with Institute for Frontier Research on Earth Evolution. The methods of chemical preparation for the each analysis were also established. All our chemical procedures are performed under a clean environment, which is basically handmade with our original design (eg. Fig. 3). The analytical methods established at BGRL realize the precise analyses of trace and isotopic compositions of ultra trace amounts of the samples (Fig. 4). Furthermore, we are developing methods to realize the mass production of the assay tests. By employing the described analytical methods, we are progressing with the study of magma genesis and material transfer in the mantle, etc.



Fig. 1. Inductively coupled plasma mass spectrometer



Fig. 2. Thermal ionization mass spectrometer



Fig. 3. Sample evaporation system under the ultra clean environment

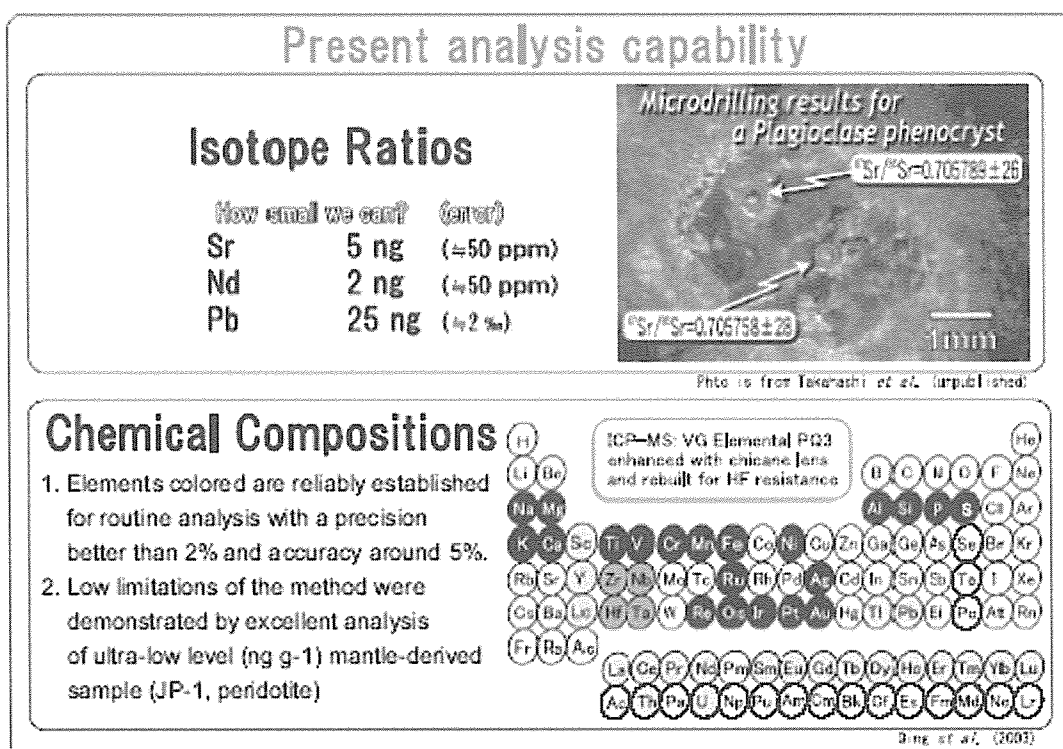


Fig. 4. Analytical method for isotopic and trace element compositions established at BGRL

